COMPARATIVE BIOCHEMICAL CHARACTERIZATION OF *DROSOPHILA MELANOGASTER* EPSILON CLASS GLUTATHIONE S-TRANSFERASE, DmGSTE6 AND DmGSTE7

VENNOBAAHSHINI A/P VENU

DISSERTATION SUBMITTED IN FULFILMENT OF THE REQUIREMENT FOR THE DEGREE OF MASTER OF SCIENCE

INSTITUTE OF BIOLOGICAL SCIENCES
FACULTY OF SCIENCE
UNIVERSITY OF MALAYA
KUALA LUMPUR

2015

ORIGINAL LITERARY WORK DECLARATION

Name of Candidate: **VENNOBAAHSHINI A/P VENU** I.C/Passport No: **860608-43-6700**

Registration/Matrix No: **SGR110083**

Name of Degree: **MASTER OF SCIENCE**

Title of Project Paper/Research Report/Dissertation/Thesis **"COMPARATIVE BIOCHEMICAL CHARACTERIZATION OF *DROSOPHILA MELANOGASTER* EPSILON CLASS GLUTATHIONE S-TRANSFERASE, DmGSTE6 AND DmGSTE7"**

Field of Study: **BIOLOGY & BIOCHEMISTRY**

I do solemnly and sincerely declare that:

1) I am the sole author/writer of this Work;
2) This Work is original;
3) Any use of any work in which copyright exists was done by way of fair dealing and for permitted purposes and any excerpt or extract from, or reference to or reproduction of any copyright work has been disclosed expressly and sufficiently and the title of the Work and its authorship have been acknowledged in this Work;
4) I do not have any actual knowledge nor ought I reasonably to know that the making of this work constitutes an infringement of any copyright work;
5) I hereby assign all and every rights in the copyright to this Work to the University of Malaya ("UM"), who henceforth shall be owner of the copyright in this Work and that any reproduction or use in any form or by any means whatsoever is prohibited without the written consent of UM having been first had and obtained;
6) I am fully aware that if in the course of making this Work I have infringed any copyright whether intentionally or otherwise, I may be subject to legal action or any other action as may be determined by UM.

Candidate's Signature Date

Subscribed and solemnly declared before,

Witness's Signature Date

Name: **DR ZAZALI ALIAS**

Designation:

ABSTRACT

The study compares the biochemical behavior of two epsilon class Glutathione S-Transferase (GSTs) genes from *Drosophila melanogaster*, namely *gste*6 and *gste*7. Both GSTs were cloned, expressed and homogenously purified using a combination of anionic exchange chromatography and GSH-affinity matrix. Bioinformatics analysis indicated that both shared 83% and 69% amino acid sequence similarity and identity respectively. Each GSTE6 shared 79% and 77% similarity and GSTE7 has 77% similarity towards GST6A and GST6B of *Musca domestica*, respectively which are known to participate in resistance towards insecticides. The expressed recombinant proteins were tested for their activity towards 12 model substrates. Based on the pattern of activity toward these substrates, these GST isozymes exhibited overlapping but similar substrate specificities. The isozymes were only active towards 1-chloro-2, 4-dinitrobenzene (CDNB), 1, 2-dichloro-4-nitrobenzene (DCNB) and *p*-nitrobenzyl chloride (*p*-NBC). GSTE6 possesses greater catalytic efficiency (K_{cat}/K_m) towards substrate CDNB but GSTE7 possesses greater catalytic efficiency (K_{cat}/K_m) towards substrate DCNB and *p*-NBC. Thin layer chromatography analysis showed the isozymes were not able to conjugate 13 tested insecticides. The inhibition kinetics of natural products and dyes towards both GSTs *in- vitro* revealed that phenol red dye possessed inhibition effects only on GSTE6 while rose bengal and cardiogreen dye inhibit excellently both GSTE6 and GSTE7. Interestingly, methylene blue dye and *trans*-chalcone have been showed to stimulate GSTE7 activity towards CDNB.

ABSTRAK

Kajian ini membandingkan tingkah-laku biokimia dua kelas epsilon gen Glutathione S-Transferase (GSTs) daripada *Drosophila melanogaster*, iaitu *gste*6 dan *gste*7. Kedua-dua GST ini telah diklon, diexpressi dan ditulenkan menggunakan gabungan kromatografi pertukaran anion dan GSH-affiniti matriks. Analisa bioinformatik menunjukkan bahawa kedua-dua gen masing-masing mempunyai persamaan dan pengenalan dalam urutan asid amino dan identiti sebanyak 83% dan 69 %. GSTE6 masing-masing mempunyai persamaan sebanyak 79% dan 77% manakala GSTE7 masing-masing mempunyai 77 % persamaan dengan GST6A dan GST6B daripada *Musca domestica* yang dikenali terlibat dalam kerintangan terhadap racun serangga. Protein rekombinanasi ini masing-masing telah diuji untuk aktiviti mereka terhadap 13 model substrat. Berdasarkan corak aktiviti ke arah substrat berkenaan, GSTE6 dan GSTE7 ini mempamerkan urutan bertindan tetapi sama spesifikasi substrat. GSTE6 dan GSTE7 aktif ke arah 1-chloro-2, 4-dinitrobenzene (CDNB), 1, 2- dichloro-4-nitrobenzene (DCNB) dan *p*-nitrobenzyl klorida (*p*-NBC). GSTE6 mempunyai kecekapan pemangkin yang lebih besar (K_{cat}/K_m) terhadap CDNB substrat manakala GSTE7 pula mempunyai kecekapan pemangkin yang lebih besar (K_{cat}/K_m) terhadap substrat DCNB dan *p*-NBC. Analisis kromatografi menunjukkan GSTE6 dan GSTE7 tidak dapat mengkonjugasikan 13 racun serangga yang diuji. Analisa kinetik perencatan dengan produk asli dan pewarna terhadap GSTE6 dan GSTE7 menunjukkan bahawa pewarna fenol merah memiliki kesan perencatan yang sangat baik hanya pada GSTE6 manakala pewarna ‘rose bengal’ dan ‘cardiogreen’ berjaya merencat kedua-dua GSTE6 dan GSTE7. Menariknya, pewarna metilena biru dan *trans*-chalcone telah menunjukkan untuk merangsang GSTE7 aktiviti terhadap CDNB.

ACKNOWLEDGEMENTS

I would like to thank all people who have helped and inspired me during my years of MSc.

First and foremost, my utmost gratitude to my supervisor, Dr. Zazali Alias, whose sincerity and encouragement I will never forget. Dr. Zazali helped me as I hurdle all the obstacles in the completion of this research work.

I was delighted to interact with Dr. Normawati Zahari during our meetings. She has shared valuable insights in the relevance of the study.

I am heartily thankful to my lab-mate Tanusya Murali and Kithalakhmi for teaching me all the experimental molecular and proteomic techniques from the start of this project. I would also like to thank other members of the lab for their support and valuable input especially Siti Nasuha, Chin Chee Soon and Tan Yong Hao.

A special thanks to Shevin Rizal for helping and guiding me on performing circular dichrorism analysis.

Thanks to University Malaya for their scholarship and Postgraduate Research Fund (PPP), Grant PV034/2012A for supporting me financially during my research.

Many thanks due to third year lab staffs for technical help during my work there.

Last but not the least, million thanks to my family especially my mum and dad, whose decision to allow me to pursue my dream to complete M.Sc. Thanks to my brother Prem Ganes and my dearest friend, Audra Shaleena for their encouragement during the stumbling phase of my research.

TABLE OF CONTENTS

LIST OF TABLES

LIST OF FIGURES

LIST OF SYMBOLS AND ABBREVIATIONS

APS	Ammonium Persulphate
BSA	Bovine serum albumin
BSP	Sulfobromophthalein
CD	Circular Dichroism
CDNB	1-chloro-2, 4-dinitrobenzene
CuH_2O_2	Cumene Hydroperoxide
DCNB	1, 2-dichloro-4-nitrobenzene
DDT	dichlorodiphenyltrichloroethane
DNA	Deoxyribonucleic acid
EA	Ethacrynic acid
EDTA	Ethylenediaminetetraacetic acid
EPNP	1, 2-epoxy-3-nitrophenoxypropane
G-site	Glutathione binding site
GSH	Reduced glutathione
GSSG	Oxidized glutathione

GST	Glutathione S- transferases
GR	Glutathione reductase
HED	2-hydroxyethyl disulfide
H-site	Hydrophobic binding site
H_2O_2	Hydrogen peroxide
IPTG	Isopropyl β-D-thiogalactopyranoside
Kb	Kilobase
kDA	Kilodalton
k_{cat}	Catalytic constant
k_{cat}/K_m	Catalytic efficiency
K_m	Michaelis-Menten constant
LB	Luria Bertani
MAPEG	Membrane Associated Proteins in Eicosanoid and Glutathione metabolism
$MgCl_2$	Magnesium chloride
MGST	Membrane associated microsomal GSTs
MWCO	Molecular weight cut off

mL	Mililiter
mM	Milimole
NaCl	Sodium hydroxide
NaOH	Sodium hydroxide
ng	Nanogram
PBO	*trans*-4-phenyl-3-buten-2-one
PCR	Polymerase chain reaction
PEITC	Phenethyl isothiocyanate
PGA2	Prostaglandin A2
PhB	Phenobarbital
p-NBC	*p*-Nitrobenzyl chloride
pmol	Picomole
PQ	1, 1-dimethyl-4, 4`-bipyridilium
RNA	Ribonucleic acid
rpm	Revolutions per minute
SDS	Sodium Dodecyl Sulphate

Ser	Serine
SOC	Super optimal broth
TBE	Tris/Borate/EDTA
TEMED	*N*, *N*, *N'*, *N'*-tetramethylenediamine
TLC	Thin Layer Chromatography
Tyr	Tyrosine
V_{max}	Maximum velocity
4-HNE	4-hydroxynonenal
5(S)-HpETE	5 -hydroperoxyeicosatetraenoi
µL	Microliter
µg	Microgram
µM	Micromole

CHAPTER 1

INTRODUCTION

1.1 General Introduction

The introduction to this thesis will review literature concerning glutathione s- transferases (GSTs) from a broad point of view but with an emphasis on their properties, functions, structure and expressions. The focus will be on the occurrence of GSTs in insects and the understanding of their role in insecticide, pesticides, herbicides and other various carcinogen resistances. The intention of this study will be to establish the relationship of particular isoforms of the GSTs namely Epsilon Class GSTs subunits 6-6 and 7-7 to response to toxins and other challenges. *Drosophila melanogaster* has been used as a model to study a number of the expressed products of the GST genes in relation to responses to different environmental conditions. The availability of the entire genome sequence of *Drosophila melanogaster* has made it possible to study the multiple isoforms of GST in the model.

1.2 Introduction

Insect are major vectors of transmissible diseases and pests of major crops. They are perpetually exposed to sundry exogenous compounds such as insecticides, pesticides, herbicides, toxicants, mutagens, carcinogens and other naturally occurring toxics such as plant and fungal toxins and reactive oxygen species, such as the hydrogen peroxide (H_2O_2) and superoxide radical. Thus, it is vital to develop an efficacious insecticide as insecticides resistance becoming persisting quandary around the world. Insecticide resistance across sundry species has been attributed to up regulation of enzymes associated with xenobiotic

detoxification and metabolism. For example in *Drosophila melanogaster*, up regulation of several different cytochrome P-450s and glutathione s-transferases has been associated with diverse xenobiotic detoxification and metabolism.

The glutathione s-transferases (GSTs: E.C. 2.5.1.18) are a super-family of enzymes with a broad range of substrates and catalytic activities. They emanate from a diverse family of enzymes that is found ubiquitously in virtually all living things such as mammals, yeast, insects, plants, helminthes and bacteria (Sheehan *et al*., 2001). GSTs play roles in metabolism, conveyance, cell mediation against oxidative stress and most importantly xenobiotic compounds detoxification (Enayati *et al*., 2005).

CHAPTER 2

LITERATURE REVIEW

2.1 Glutathione-Dependent Enzymes

A non-protein thiol and most plenteous low relative molecular mass sulfhydryl compound which found intra-cellularly in all mammalian tissue is commonly referred as Glutathione (GSH, γ- glutamylcysteinylglycine), largely occurring at high (0.1 to 10 mM) concentrations. Figure 2.1 shows the tripeptide conferring the sequence of glutamic acid; cysteine and glycine. GSH is a crystalline solid with a melting point of 192-195 °C and relative molecular mass of 307.33. It dissolves promptly in water. It's composed of two peptide bonds, two carboxylic acid groups (pK_{COOH} = 3.53 and 2.12), one amino group (pK_{NHE+} = 8.66) and a thiol group (pH_{SH} = 9.66). At the time of evolution, glutathione has become adapted to perform numerous functions. Glutathione alone ready to give a first line of defense against varied reactive oxygen species, it detoxifies xenobiotics, synthesize leukotrienes and prostaglandin, maintain proteins and membrane structures and regulates numerous enzyme activities. Additionally, glutathione act as a cofactor or a substrate for various enzymes. This functional diversity is due to the properties of the thiol group. In order to keep relatively constant and stable intracellular condition, glutathione supplies thiol groups to stop protein thiols from oxidizing into disulfides. It is involved in reactions such as protein and nucleic acids synthesis, free radicals and peroxides detoxification. The ionized (thiolate) act as nucleophile to respond towards electrophilic compounds and to avert them from reacting with biomolecules such as proteins and DNA (Meister, 1988).

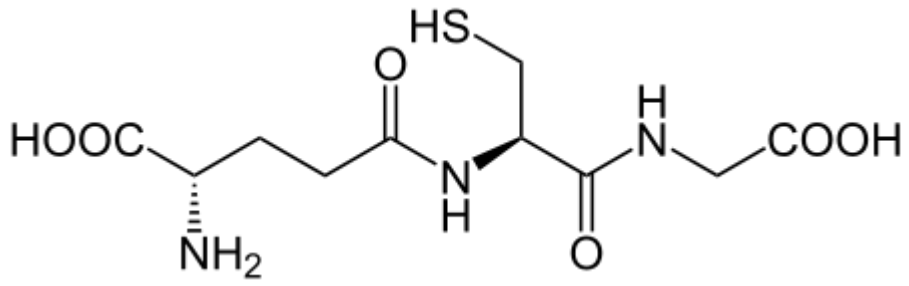

Figure 2.1: Chemical structure of glutathione (Adapted from Anne, 2013)

A variety of enzymes utilize glutathione during a variety of biotransformation (Fukami, 1984). Glutathione reductase (GR) promotes the reduction of GSSG (oxidized glutathione) utilizing NADPH as a reductant. GR is very consequential in maintaining the highest cellular reduction potential. Selenium-dependent glutathione peroxidase is another type of GSH-requiring enzyme that initiates the reduction of peroxides exploiting GSH as the reducing agent (Krohne-Ehrich *et al.*, 1977).

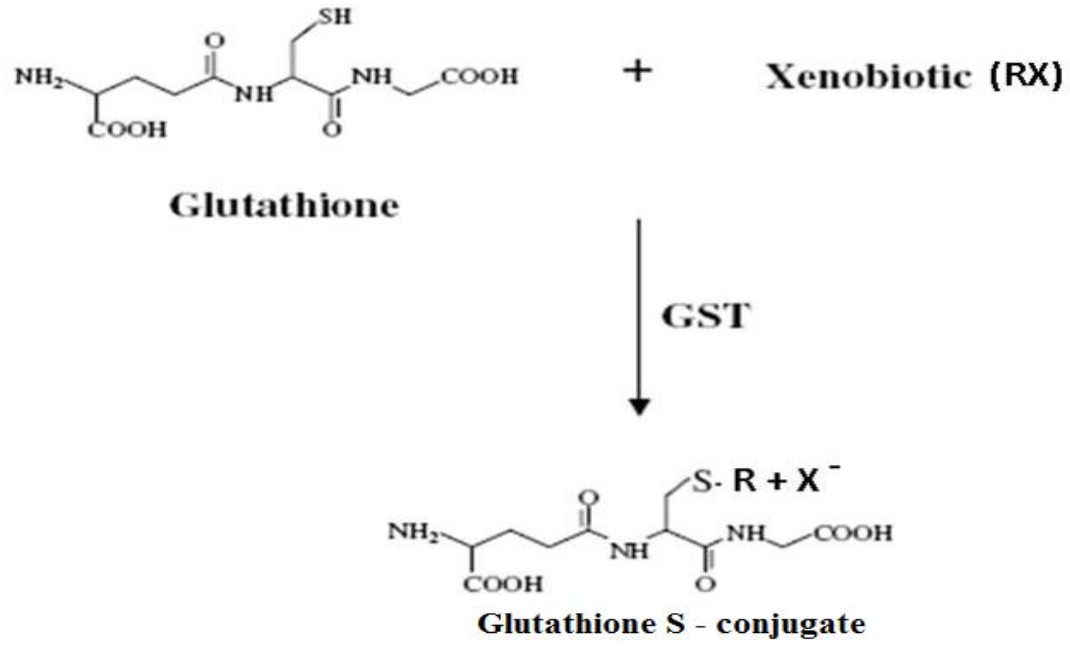

Figure 2.2: Glutathione conjugation to a generic electrophilic xenobiotic (RX) by GST (Adapted from Townsend and Tew, 2003)

2.2 Glutathione S- Transferases (GSTs, E.C.2.5.1.18)

One of the most popular classes of detoxification enzymes that constitute randomly in all living organisms are the glutathione s-transferases (GSTs). GSTs conjugate the thiol groups of reduced glutathione (GSH) towards the negative charge center of lipid soluble compounds (xenobiotics) to make it water soluble and excrete out easily. The breakthrough of GSTs dated as early 1960s, bearing on the revelation of cytosolic extracts of rat liver catalyzes the conjugation of glutathione to arylhalides (Booth *et al.*, 1961; Combes and Stakelum, 1961). These enzymes have extensive distribution in nature and are found rampantly in almost all living things including plants, animals and even bacteria (Hayes and Pulford, 1995). These renowned GSTs in animals are often divided into two defined super families: the membrane-bound microsomal GSTs and the cytosolic or soluble GSTs.

2.2.1 Membrane Associated Microsomal GSTs (MGST)

The microsomal GSTs belong to the family of membrane-bound enzymes or MAPEG (Membrane Associated Proteins in Eicosanoid and Glutathione metabolism). Microsomal GSTs are structurally different from the soluble cytosolic GSTs (Jakobsson *et al.*, 1999). To date, six members of the family are identified that includes: prostaglandin E synthase, 5-lipoxygnase-activating protein, microsomal GST1, 2, and 3 and leukotriene C4 synthase (Jakobsson *et al.*, 1999). Microsomal GST1, microsomal GST2 and 3, are familiar to be detoxification enzymes, (Morgenstern *et al.*, 1982) due to their GST activity which helps to conjugate glutathione to 1-chloro-2, 4-dinitrobenzene (CDNB). The MAPEG enzyme family thus participates both in the endogenous metabolism of physiologically important leukotrienes and prostaglandins besides concerned in the detoxification of extremely active lipophilic compounds of exogenous and endogenous origin (Jakobsson *et al.*, 1999).

2.2.2 Cytosolic GSTs

The soluble GSTs or conjointly referred as cytosolic GSTs. They are subdivided into categories based upon sequence identity where the identities at certain intervals for a category are more than 50% (Mannervik *et al.*, 1985). The soluble GSTs exist as either homodimeric or heterodimeric proteins. They are shaped by two polypeptide chains or subunits of approximately 25 kDa in size respectively (Armstrong, 1997). Each subunit can be folded into two domains. They are known as the N-terminal (extreme 5´) and C-terminal (extreme 3´) joined by a variable linker region. The N-terminal domain (1 – 80 residues) looks alike as thioredoxin domain (arranged in βαβαββα motifs) which found in all GST structures (Sheehan *et al.*, 2001). This domain consists mostly of active or G-sites, which is the specific binding site of endogenous tripeptide GSH (g-L-glutamyl-L-cysteinylglycine) widely known as glutathione (Che-Mendoza *et al.*, 2009). The larger C-terminal domain consists of a variable number of alpha helices, and includes largely the electrophile-binding site and it is the residues of the hydrophobic H-site or the substrate binding site. It's less specific, thus enables GSTs to react to a wide range of xenobiotics (Dirr *et al.*, 1994). The abundant level of diversity towards this region confers partly the specificity of the GSTs for a broad range of electrophilic substrates (Mannervik and Danielson, 1988).

Cytosolic GSTs are found ubiquitously in all aerobic organisms with almost 10 members in each species. This number includes 15-20 different mammalian GSTs, 40-60 GSTs in plants, 10 -15 GSTs in bacteria and over 10 in insects (Frova, 2006). The GSTs are grouped into different classes based on several criteria including amino acid/ nucleotide sequence identity, physical structure of the gene (example intron number and position) and immunoreactivity properties as they are widely distributed throughout taxa, kingdom with same organism specific (Frova, 2006). Complete genome sequence data for some species

with over 40 GST genes has been discovered. To date, there are seven mammalian classes of cytosolic GSTs namely Alpha, Mu, Pi, Kappa, Theta, Omega, Sigma and Zeta, and a microsomal class, Delta and Epsilon classes in insects, Sigma class in arthropods, cephalopods and human, Phi and Tau classes in plants, Zeta and Theta classes in plants, insects and bacteria as well as animals.

The nomenclature for GST had been designed with the name of the Greek letters; Alpha, Mu, Phi, Theta, etc., abbreviated in Roman capitals; A, M, P, and T and so on. Class members are represented by Arabic numerals and native dimeric protein structures are named according to their subunit composition (Mannervik *et al.*, 2005). For example, GSTE6-6 is a homodimer of *Drosophila melanogaster* GST which consist of two sub-units 6 in the Epsilon class.

GSTs are expressed in sex, age, tissue, organ, species, and tumor-specific patterns of expression and their composition differ significantly (Hayes and Pulford, 1995). For an example the Alpha class is plentiful in human liver, kidney and testis, while the Pi class is predominant in lung, brain, erythrocytes and skin (Sherratt and Hayes, 2002). Besides that, the regulation of each individual isoenzyme expression seems to be different in every tissue and cell type. GSTs have a broad and overlapping specificity. Among the reactions catalyzed by GSTs are substitutions of halogens in halogenohydrocarbon, addition to double bonds, cleavage of epoxides and reduction of organic peroxides. 1-chloro-2,4-dinitrobenzene (CDNB) is the most typical substrate used to assay GSTs besides 1,2-dichloro-4-nitrobenzene (DCNB), ethacrynic acid (EA), 1,2-epoxy-3-nitrophenoxypropane (EPNP) and sulfobromophthalein (BSP).

Insect cytosolic GSTs were initially assigned to a particular class based on their amino acid sequence homology and immunological properties (Beall *et al.*, 1992; Fournier *et al.*, 1992; Toung *et al.*, 1990). Classes that possess GST include of having an identity of over 40% of the amino acid sequence and other properties such as immunological character, tertiary structure, their ability to form heterodimers and chromosomal location (Ding *et al*., 2003; Hemingway *et al*., 2004; Ranson and Hemingway, 2005).

GSTs plays important roles in the development of resistance to a variety of exogenous xenobiotics, such as chemotherapeutic drugs (Hayes and Pulford, 1995), chemical carcinogens (Coles and Ketterer, 1990), herbicides (Edwards *et al.*, 2000) and insecticides (Clark, 1989; Yu, 1996).

2.3 Structure of GSTs

2.3.1 General Structure of GSTs

Each monomer of GST comprise of two definite domains that is N-terminal sub-domain, which uses the thioredoxin fold, and a C-terminal all-helical sub-domain connected by a variable linker region. The N-terminal domain encompass four beta sheets and three flanking alpha helices which adopts a conformation like thioredoxin domain found in many proteins binds GSH or cysteine (Sheehan *et al*., 2001). The glutathione molecule binds in a cleft between N and C-terminal zone. The catalytically vital residues are proposed to reside within the N-terminal domain. Although each subunit has a kinetically independent active site, their quaternary structure is important for their functional activity (Danielson and Mannervik, 1985). Cytosolic GST super-family members can be divided into two prominent sub-groups based on identifiable sequence or structural elements and active site architecture (Atkinson and Babbit, 2009; Armstrong, 2012). These sub-groups are

classified as Y-type and S/C-type based on conservation of a key active site residue. The S/C-type sub-group includes the beta, omega, phi, tau, theta, and zeta classes which utilize a serine residue to activate GSH while the Y-type sub-group includes the alpha, mu, pi, and sigma classes utilize tyrosine residue in interaction with GSH.

2.3.2 Structure of Epsilon Class GSTs

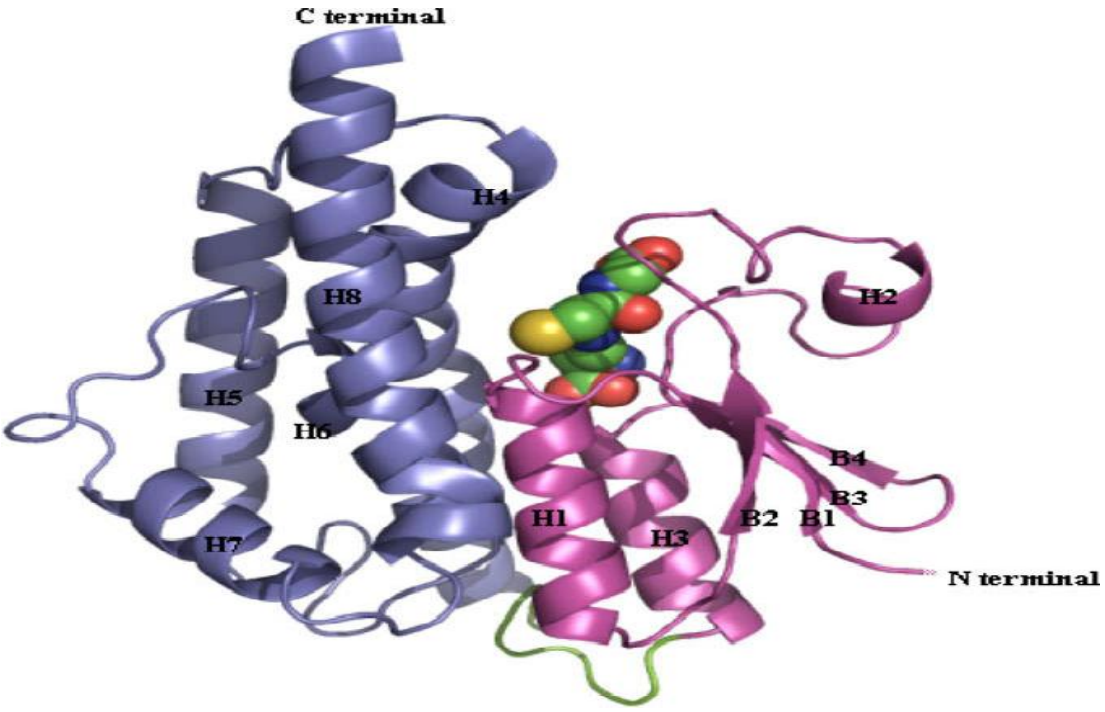

The N-domain is colored in magenta and C-domain in blue. The linker between two domains is colored in green. The bound GSH molecule from agGSTE2-GSH complex is shown in spheres with carbon atoms in green, oxygen atoms in red, nitrogen atoms in blue, and sulfur atom in gold. All secondary-structure elements are labeled with H for α-helix and B for β-strand

Figure 2.3: Ribbon diagram of *Anopheles gambiae* GST Epsilon-2 structure (Adapted from Wang *et al.*, 2008)

2.4 Mechanism of Action of GSTs

2.4.1 Conjugation of Exogenous Toxins

GSTs play important roles in the protection of macromolecules from attack by reactive electrophiles. While retaining a high specificity toward the thiol substrate glutathione, each class of GSTs exhibit overlapping but defined hydrophobic substrate and ligand binding specificities (Winayanuwattikun and Albert, 2005). Danielson and Mannervik, (1985) reported that, the cytosolic isoenzymes have two active sites per dimer and it behaves independently of one another. A review by Chasseaud, (1979) listed xenobiotics that could be conjugated by GSTs includes halogenonitrobenzenes, organophosphorous compounds, steroids, α-β-unsaturated carbonyl compounds, aryl halides epoxides, quinines, isothiocynates and arylnitro compounds.

The catalytic strategy of GST are divided into few steps, which involve binding of substrates to the enzyme active site in the beginning followed by activation of GSH, by thiol deprotonation and nucleophilic attack by the thiolate at the electrophilic center, finally product formation and product release (Winayanuwattikun and Albert, 2005). The conjugations catalyzed by the GSTs occur between the nucleophilic GST and the compounds possessing a sufficiently electrophilic centre. The GSTs function by decreasing the pKa of GSH from 9.0 to between 6.0 and 6.9, thereby allowing its deportation and the formation of a more reactive thiolate anion (active site residue). This thiolate anion stabilized by interaction between mammalian GSH classes (Phi, Mu, Alpha and Sigma) and a tyrosine residue in the N-terminal, serine and cysteine residue respectively in Theta and Omega classes in mammals and serine residue in insects Delta and Epsilon classes (Tyr-8 for Pi, Tyr-9 for Alpha, Tyr-6 for Mu, and Ser-9 for Delta class) (Sheehan *et al.*, 2001;

Winayanuwattikun and Albert, 2005). This active site residue proposed to be highly conserved within GST classes but differs between classes (Che Mendoza *et al.,* 2009). This GSH conjugation happens in mammals, birds, reptiles, amphibians, fish, insects and other vertebrates (Boyland and Chasseaud, 1969) and it is the first step of mercapturic acid formation that is one of the metabolic pathways for detoxification of xenobiotics *in vivo.* The glutathione conjugates which are water soluble and generally non-toxic may be converted to the corresponding cysteine conjugate following sequential removal of glutamate and glycine. The cysteine conjugate is either N-acetylated to be excreted as a mercapturic acid or cleaved to a mercaptan which can be further metabolized to be excreted as a glucuronide (Boyland and Chasseaud, 1969).

2.5 GSTs in Insects

In insects, GSTs genes were classified into two groups, class I and class II GSTs (Fournier *et al.*, 1992). According to Chelvanayagam *et al.*, (2001), an insect-specific Class I GST is now referred as a Delta class GST. This includes those from *Drosophila melanogaster*; *gstd*1 to *gstd*10 (Chelvanayagam *et al.*, 2001), *Musca Domestica*; *mdgstd*1 to *mdgstd*5 (Zhou *et al.*, 2007), *Anopheles gambie*; *aggstd*1 to *aggstd*6 (Ranson *et al.*, 1997) and *Lucilia cuprina*; *lcgstd*1 (Wilce *et al.*, 1995). Class II is now defined to consist primarily of Sigma class GSTs as identified in *Drosophila melanogaster*, *gsts*1, *Anopheles gambie*; *aggsts*1 and *Manduca sexta*; *msgsts1* (Che Mendoza *et al*., 2009). Ranson *et al*., (2001) proposed a third class of insect's GST (Class III) that comprised GSTs now classified as the Epsilon class in *Drosophila melanogaster*; *gste*1 to *gste*10 and the *aggst*3-1 and *aggst*3-2 of *Anopheles gambie*. In most of the species, the Omega GSTs including *A. gambiae* appear to be enciphering by a single gene; however five putative Omega GSTs have been identified in *D. melanogaster* (Ding *et al.*, 2003). Omega GSTs has also been identified in the Silk

Moth, *Bombyx mori* (Yamamoto *et al.*, 2009a). Two Theta GST genes have been identified in *A. gambiae* (Ding *et al.*, 2003) and five putative Theta GSTs have been identified in *A. aegypti* (Lumjuan *et al.*, 2007). The Zeta GSTs has been identified in Silk Moth, *Bombyx mori* (Yamamoto *et al.*, 2009b) and a single Zeta GST gene was found in *A. gambiae* (Ding *et al.*, 2003). The Xi and Iota GSTs have so far been found uniquely in mosquitoes of *A. aegypti* and clear orthologs of these GSTs were found in *A. gambiae* (Lumjuan *et al.*, 2007).

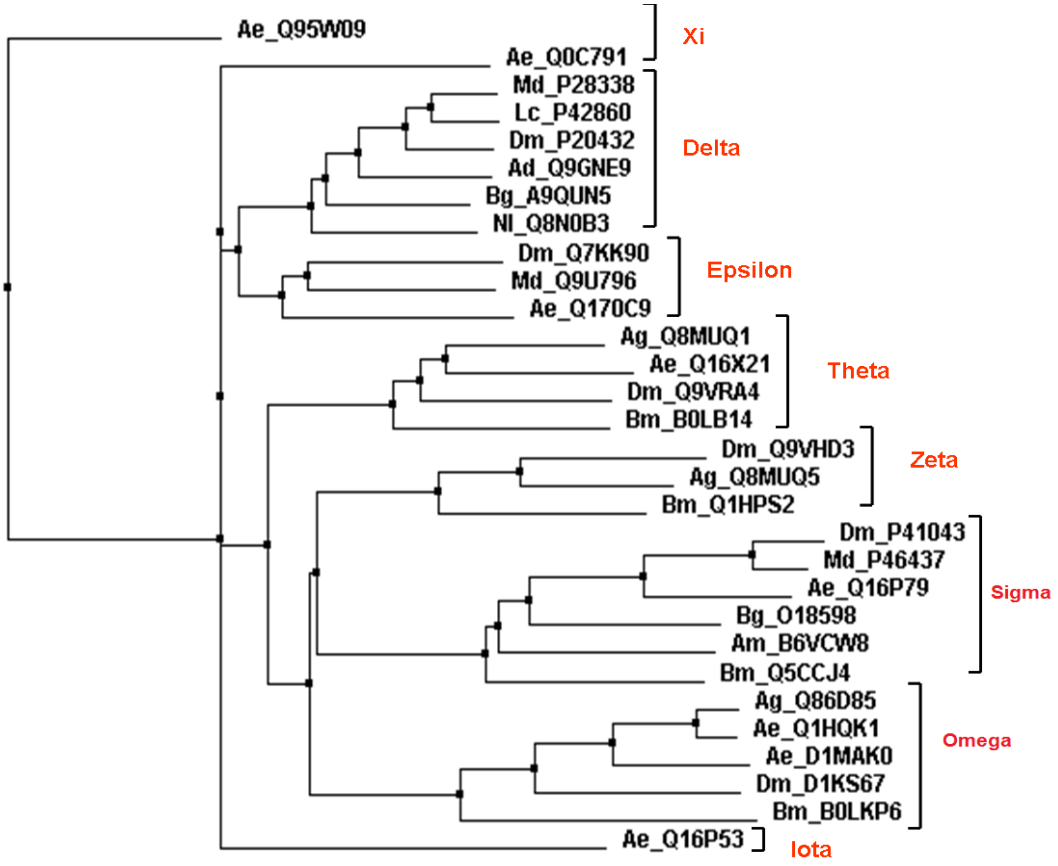

Ag = *Anopheles gambiae*, Ad = *Anopheles dirus*, Ae = *Aedes aegypti*, Dm = *Drosophila melanogaster*, Bm = *Bombyx mori*, Md = *Musca domestica*, Bg = *Blattella germanica*, Lc = *Lucilia cuprina*, Nl = *Nilaparvata lugens*.

Figure 2.4: Phylogenetics tree of insect GST classes. Phylogenetic tree of different GST classes demonstrating the relationships of the various insect GSTs to one another (Adapted from Ramavati, 2010)

2.5.1 GSTs and Insecticides Resistance

The majority of studies on insects GSTs have been focused on their role in conferring insecticides resistance. Wilson, (2001) pointed out the importance of genetic and biochemical mechanisms in *Drosophila* in encountering toxins and thus developing resistance. Elevated GSTs activity has been linked with resistance towards all major classes of insecticides (Enayati *et al.*, 2005). Che-Mendoza *et al*., (2009) demonstrated that, resistance are described by increase in the amount of one or more GST enzymes, either due to outcome of gene amplification or mainly through increases in transcriptional rate, instead of qualitative changes in individual enzymes.

2.5.2 Epsilon Class GSTs

Insect GSTs can be categorized into six classes but it is the Delta and Epsilon class that is most commonly associated with resistance (Tang and Tu, 1994; Ranson *et al.*, 2001; Ding *et al.*, 2003). An aggregate of GST expansions mainly resides in the Delta and Epsilon subclasses which are insect specific (Friedman, 2011). Figure 2.5 shows a close relationship between the Delta and Epsilon class GST as evidence as they share a common branch not shared with other subclasses. According to Friedman, (2011), Epsilon class GSTs are said to be evolved from the Delta subclass between times when Hymenoptera and Coleoptera originated as a lineage and only confined to the dipterans (*Culex, Drosophila, Aedes, Anopheles*), a coleopteran, and a lepidopteran through recent species event of tandem and segmental gene duplication. Niranjan *et al.*, (2011) reported that an intron at position 218 (tyrosine (y)/phenylalanine (f)) is highly conserved between Delta-and Epsilon-members which also supports the evidence of Delta and Epsilon classes could have shared a common ancestor during their evolution. Several studies also reported that,

Epsilon classes in *Dipteran* organisms, is to confer insecticide resistance and their catalytic diversity would likely promote their role in detoxification (Enayati *et al.*, 2005; Ketterman, *et al.*, 2011 and Saisawang, *et al.*, 2011). It has been reported that, homo-dimers of one *Ae. aegypti* epsilon class GST enzyme, GSTE2 is very efficient at metabolizing DDT. The enzyme expression was elevated in a DDT and pyrethroid resistant population from Thailand (Lumjuan *et al.*, 2005). Lumjuan *et al.*, (2011) provide evidence that the epsilon class GSTs enzyme, GSTE2 and GSTE7 are involved in conferring resistance to the pyrethroid deltamethrin in the *Ae. Aegypti* strain. The expression of the epsilon class GSTs, *slgste2* and *slgste3* genes in *Spodoptera litura* a Lepidoptera detoxifies carbaryl, DDT, RH5992, malathion and deltamethrin which is a synthetic chemical insecticides (Deng *et al*., 2009). DDT is likely to be converted to DDE [1,1-dichloro-2,2-bis-(p-chlorophenyl) ethylene] which is break down product through an elimination reaction triggered by the nucleophilic attack of the thiolate group of GS^- on the β-hydrogen of DDT through molecular modeling (Wang *et al*., 2008). Moreover, Wei *et al.*, (2001) demonstrated that housefly isozymes (MdGST6A and MdGST6B) belonging to the epsilon class function as key enzymes in the detoxification of insecticides such as methyl parathion and lindane. In addition, a quantitative PCR assay showed five of the eight Epsilon GSTs enzyme (namely GSTE1, GSTE2, GSTE3, GSTE4, and GSTE7) expressed at significantly greater levels in the DDT resistant strain of *Anopheles dirus* (Charoensilp *et al*., 2006).

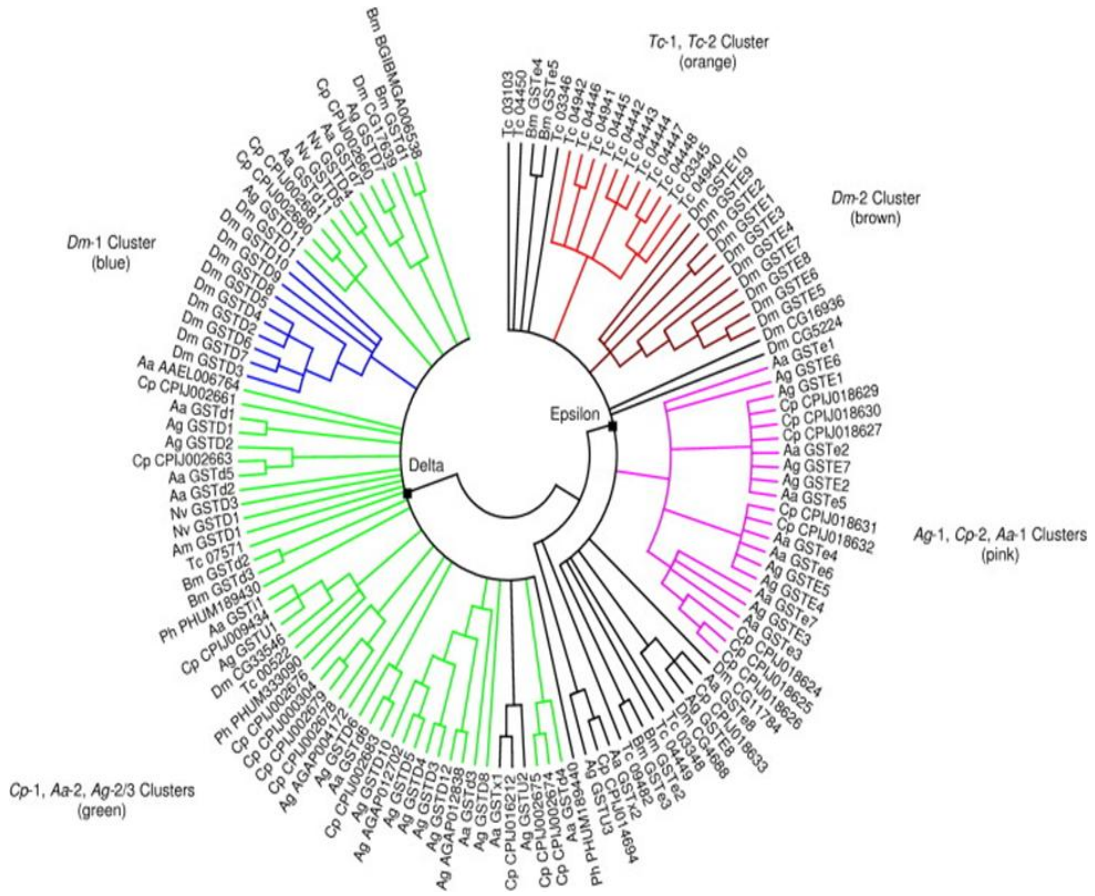

The topology is based on a 75% condensed tree obtained by bootstrap analysis. The branches are colored by "Cluster". Species abbreviations occur before the gene name and the cluster names are as follows: Aa = *Aedes aegypti*, Ag = *Anopheles gambiae*, Cp = *Culex quinquefasciatus*, Dm = *Drosophila melanogaster*, Bm = *Bombyx mori*, Tc = *Tribolium castaneum*, Am = *Apis mellifera*, Nv = *Nasonia vitripennis*, Ap = *Acyrthosiphon pisum*, Ph = *Pediculus humanus*

Figure 2.5: Unrooted cladogram of the Delta/Epsilon-GST superclass (Adapted from Friedman, 2011)

2.5.2.1 *gste*6 *and gste*7

A recent study on the *Drosophila* systems approach to xenobiotic metabolism revealed that the *gste*6 is found most abundant in the hindgut of the adult and larvae whereas *gste*7 mostly found abundant in the tubule of the adult and larvae (Yang *et al.*, 2007). A comprehensive microarray-based atlas of adult gene expression in multiple *Drosophila* tissues available (http://flyatlas.org) reported that, *gste*6 expressed in adult crop, midgut, tubule, hindgut, ovary and larval hindgut while *gste*7 expressed in adult crop, midgut, tubule, hindgut, virgin spermatheca and larval midgut, hindgut and fat body. Several lines of evidence have also suggested that the tubule may be the dominant tissue for xenobiotic mechanism in adult *Drosophila.* According to Alias and Clark, (2007), the protein expression of GSTE6 and GSTE7 significantly increased by more than 50% upon exposure to PQ (1, 1-dimethyl-4, 4`-bipyridilium) and PhB (Phenobarbital). Besides that, acute insecticides exposure of methyl parathion results in significant increase in protein expressions; GSTE6 (100%) and GSTE7 (72%) (Alias and Clark, 2010).

2.6 *Drosophila melanogaster*

Drosophila melanogaster is a small, ordinary insect that colonize unripe and rotted fruit. It has been in use to study genetics and behavioral studies for over a century. Geneticists have been using *Drosophila* ever since due to its short generation time, small size, and ease of culture. It has been widely used for various types of study because of its known genome and many genes have been identified found from gene bank and flybase since its first publication in year 2000. Classification of *Drosophila melanogaster* as below;

Kingdom: Animalia

Phylum: Arthropoda

Class: Insecta

Order: Diptera

Family: Drosophilidae

Genus: *Drosophila*

Subgenus: Sophophora

Species group: melanogaster group

Species subgroup: melanogaster subgroup

Species complex: melanogaster complex

Species: *Drosophila melanogaster*

(Geiger, 2002)

2.6.1 Characterization and Classification of GSTs of *Drosophila melanogaster*

Difference in age profiles, subcellular distribution and substrate selectivity, lead to the presence of multiple forms of GSTs in *Drosophila melanogaster*. Some isoforms of Delta, Epsilon, Sigma and Omega *Drosophila* GSTs have been reported previously for various aspects. Delta and Epsilon classes have more than ten members each respectively. Omega class has four genes one of which is alternatively spliced so Omega class yields five proteins. Theta class has four genes that encode five proteins. Zeta class has two genes one of which encodes three spliced products for a total of four Zeta enzymes (Saisawang *et al.*, 2011).

The *Drosophila* GST genes are located on chromosomes 2, 3 and X. Sawicki *et al.*, (2003) has previously reported that the Delta class cluster contained ten genes, *gstd*1 to *gstd*10. Recently, a newly identified Delta GST has been reported, *gstd*11 (CG17639). The *gstd*11 gene has 2 annotated transcripts which referred to as variant a and b. Phylogenetic analysis also supports inclusion of this gene in Delta class. In addition the *gstd*11 gene is only 2.5 kb from the Delta cluster of 7 genes. All eleven Delta GST genes span approximately 20 kb on chromosome arm 3R as the Zeta genes are approximately 3000 kb away from the Delta cluster. There are two Zeta GST genes sequentially located with a 1 kb distance (Saisawang *et al.*, 2011).

Four proteins previously identified as unknown Epsilon class proteins are also classified in addition to the ten Epsilon members that have been previously reported by Sawicki *et al* ., (2003). These new proteins are denoted as GSTE11-11 to GSTE14-14; CG5224, CG16936, CG11784 and CG4688, respectively. *gste*1 to *gste*10 genes form a tight cluster whereas the remaining Epsilon genes are dispersed along the chromosome (Saisawang *et al.*, 2011).

This suggests that these paralogous GSTs initially originated from a series of tandem duplication events. The gene duplication events in the *Drosophila* lineage gave rise to differentially expressed GST isoforms and generated diverse members with differing functionality.

Table 2.1: A summary of *Drosophila melanogaster* Epsilon class GSTs from Flybase and Genbank databases (Adapted from Saisawang *et al.*, 2011)

GSTs	**Fly base No.**	**Genebank accession No.**			
		Nucleotide	**Base pairs**	**Protein**	**Amino acid**
Epsilon class					
GSTE1-1	CG5164	NM_137479.2	675	NP_611323	224
GSTE2-2	CG17523	NM_137480.2	666	NP_611324	221
GSTE3-3	CG17524	NM_137481.2	663	NP_611325	220
GSTE4-4	CG17525	NM_137482.1	669	NP_611326	222
GSTE5-5	CG17527	NM_137483.1	669	NP_611327.1	222
GSTE6-6	CG17530	NM_137484.2	669	NP_611328.1	222
GSTE7-7	CG17531	NM_137485.2	672	NP_611329.1	223
GSTE8-8	CG17533	NM_137486.3	669	NP_611330.2	222
GSTE9-9	CG17534	NM_166279.2	666	NP_725784.1	221
GSTE10-10	CG17522	NM_137478.1	723	NP_611322.1	240
GSTE11-11	CG5224	NM_137495.2	678	NP_611339.1	225
GSTE12-12	CG16936	NM_138120.1	672	NP_611964.1	223
GSTE13-13	CG11784	NM_136613.2	681	NP_610457.1	226
GSTE14-14	CG4688	NM_137011.2	699	NP_610855.1	232

2.6.2 Expression of GSTs in *Drosophila melanogaster*

The most commonly used substrate to study GSTs is 1-chloro-2, 4-dinitrobenzene (CDNB). CDNB conjugates with GSH and gives S-(2, 4-dinitrophenyl) glutathione, which possesses an absorbance spectrum sufficiently different from that of CDNB to allow a simple spectrophotometric assay at 340 nm (Clark *et al.*, 1973). For some years, the efficiency of cytosolic GSTs in using certain substrates and their sensitivity to some inhibitors were parameters for determining the class of GSTs. For examples, ethacrynic acid (EA, Pi class), cumene hydroperoxides (CuH_2O_2, Alpha class), 1,2-epoxy-3-(*p*-nitrophenoxy) propane (EPNP, Theta class), dehydro ascorbic acid (DHA, Omega class) *trans*-4-phenyl-3-buten-2-one (PBO, Mu class), and 1,2-dichloro-4-nitrobenzene (DCNB, Mu and Epsilon classes) are still used as class markers (Hayes *et al*., 2005; Ketterer, 1986; Kim *et al*., 2006; Danielson and Mannervik, 1985; Wang *et al*., 1991). Some of the substrates used for the study of GSTs are shown in Figure 2.6. All Delta-class GSTs except for GSTD3-3 isolated from adult *Drosophila*, conferred CDNB conjugating activity on lysates of bacterial cells in which they were expressed. In contrast, GSTD3-3 and GSTE1-1 had no activity with CDNB but were able to conjugate 4-HNE in crude bacterial lysates (Sawacki *et al.*, 2003). GSTS1-1 isolated from adult *Drosophila* or expressed in *Escherichia coli* is essentially inactive toward the commonly used synthetic substrate 1-chloro-2, 4-dinitrobenzene (CDNB), but has fairly high glutathione-conjugating activity for 4-hydroxynonenal (4-HNE) (Singh *et al.*, 2001). According to Saisawang *et al.*, (2011) GSTs enzymes isolated from *Drosophila* S2 embryonic cell line; GSTD3-3, GSTT4-4 and four Zeta GSTs displayed no activity toward GSH and CDNB substrate. Theta class is known to have negligible or no activity against CDNB substrate but GSTT2-2, unlike the other *Drosophila* Theta class GSTs indicating a lower affinity for GSH substrate. Apart from that, GSTE4-4

and GSTE11-11 showed very low affinity for GSH, in contrast to the high affinity for CDNB. Nevertheless GSTE11-11 was appeared to possess the highest catalytic efficiency to CDNB. Omega and Zeta class GSTs seems to be unable to conjugate CDNB substrate. In *Drosophila*, Delta and Epsilon classes are mostly able to conjugate 4-hydroxynonenal (4-HNE), adrenochrome, phenethyl isothiocyanate (PEITC), prostaglandin A2 (PGA2), and 5-hydroperoxyeicosatetraenoic acid (5(S)-HpETE). 2-hydroxyethyl disulfide (HED) is a synthetic compound thought to be a specific substrate for Omega class. Omega class and several members of Delta and Epsilon class GSTs also show activity for HED. GSTO2a-2a is the only enzyme in the class that has activity for adrenochrome whereas GSTO2b-2b was the only Omega enzyme to show activity for PEITC. *Drosophila melanogaster* GSTs shows that these proteins possess broad overlapping substrate specificity which also implies functional redundancy. However, Saisawang *et al*., (2011) suggested that the enzymatic function of a GST does not correlate with the criteria for classification. A study done by Alias and Clark, (2010), an acute exposure of insecticide methyl parathion to adult *Drosophila* resulted in a significant increase in GSTD1, GSTE6 and GSTE7 expression. Reaction between GSTs and 1-chloro-2, 4-dinitrobenzene (CDNB) was observed in many kinds of developmental stages of *Drosophila melanogaster*. Studies have demonstrated for the first time the induction of glutathione transferases by oxadiazolone and detected kinetic heterogeneity among the enzyme from different stages (Hunaiti *et al*., 1995). GSTs ability to detoxify pesticides and herbicides such as DDT, chlorpyrifos, atrazine, lindane, tetrachlorvinphos, alachlor, diazinon, and methyl parathion shown in Figure 2.7.

1

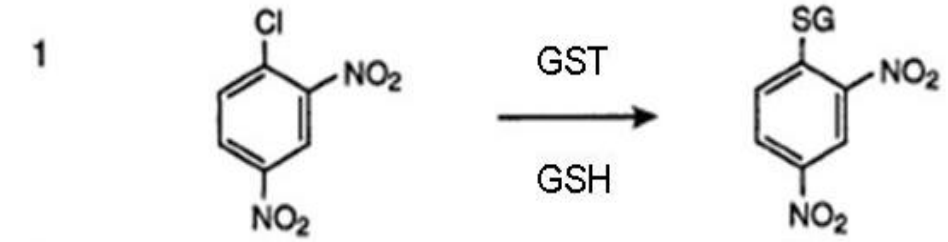
Cl
NO2
NO2
GST
GSH
SG
NO2
NO2

2

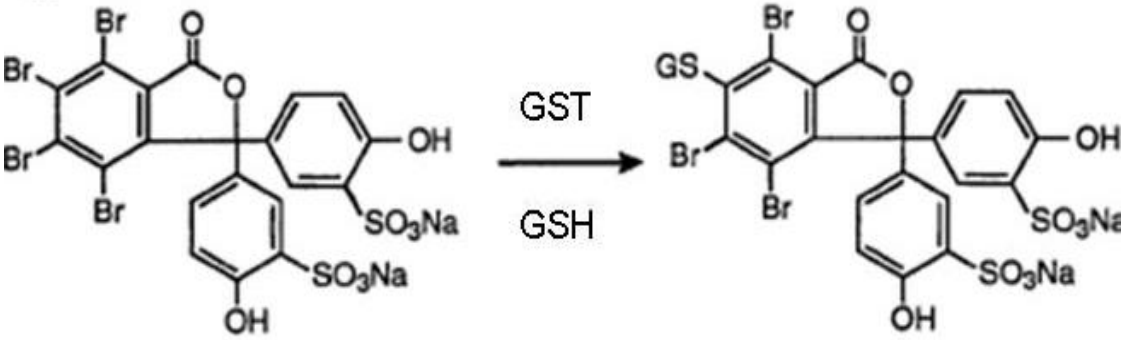
Br
O
Br
Br
Br
O
OH
SO3Na
SO3Na
OH
GST
GSH
Br
O
GS
Br
Br
O
OH
SO3Na
SO3Na
OH

3

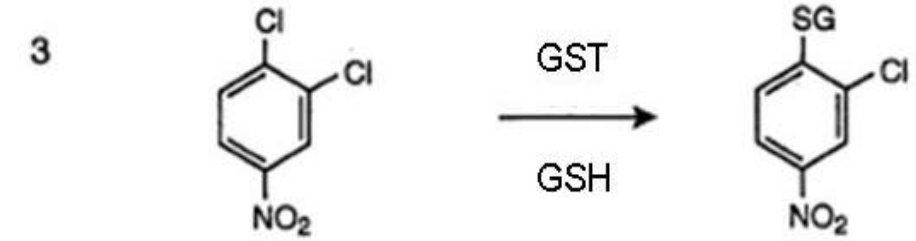
Cl
Cl
NO2
GST
GSH
SG
Cl
NO2

4

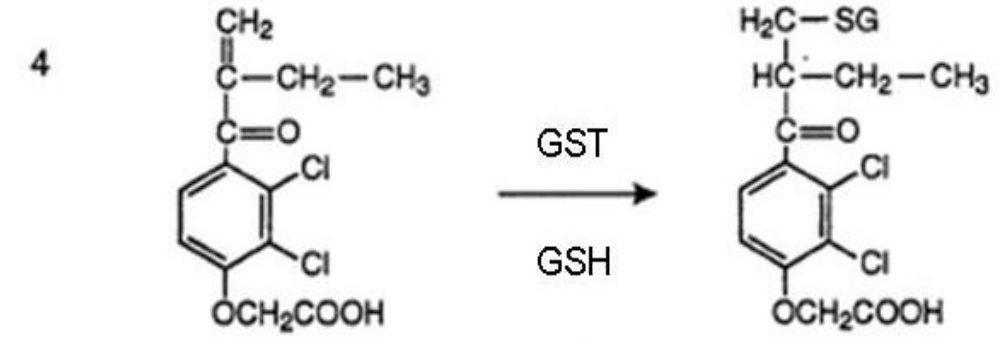
CH2
C—CH2—CH3
C=O
Cl
Cl
OCH2COOH
GST
GSH
H2C—SG
HC—CH2—CH3
C=O
Cl
Cl
OCH2COOH

5

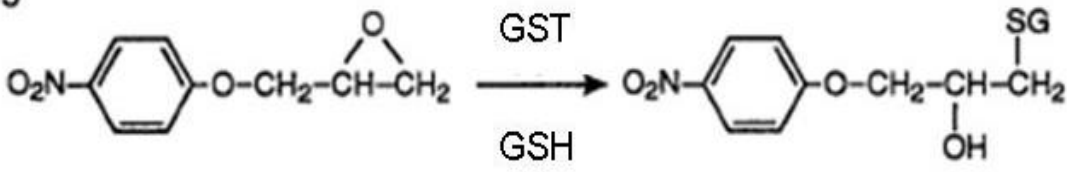
O2N
O
O—CH2—CH—CH2
GST
GSH
O2N
SG
O—CH2—CH—CH2
OH

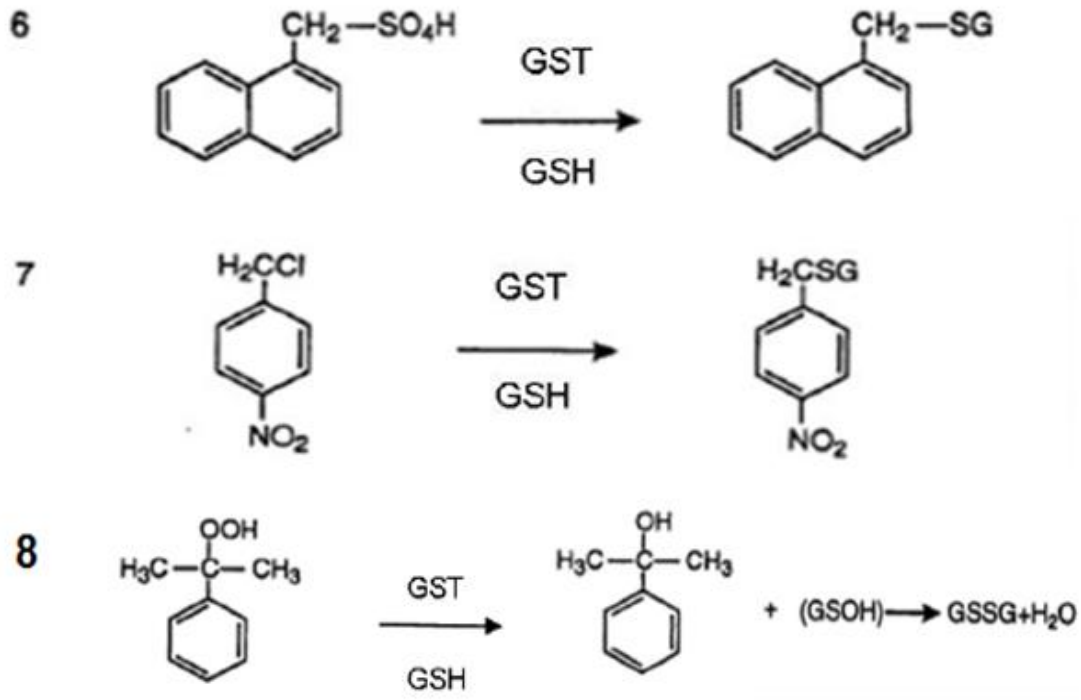

(1) 1-chloro-2, 4-dinitrobenzene; (2) Bromosulfophthalein; (3) 1, 2-dichloro-4-nitrobenzene; (4) Ethacrynic acid; (5) 1, 2-epoxy-3-(p-nitrophenoxy) propane; (6) 1-menaphthyl sulphate; (7) *p*-nitrobenzyl chloride (8) cumene hydroperoxide.

Figure 2.6: Model substrates used in the study of GSTs (Hayes and Pulford, 1995)

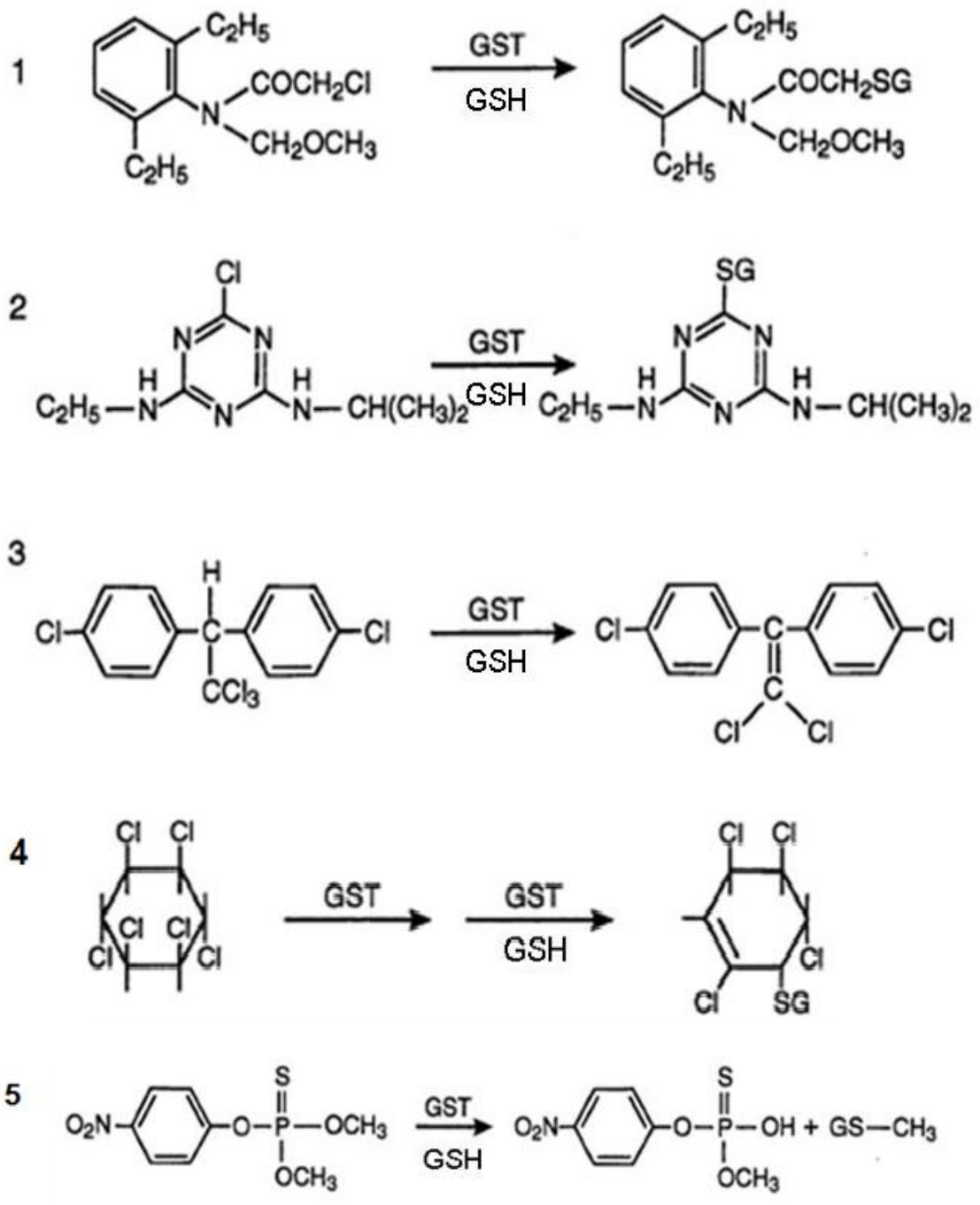

(1) alachlor; (2) atrazine; (3) DDT; (4) lindane; (5) methyl parathion.

Figure 2.7: Detoxification of Herbicides and Insecticides (Hayes and Pulford, 1995; Wilson and Clark, 1996; Alias and Clark, 2010)

2.7 Research Statement

The GST super-family has diverse paramount roles in the mundane functions of cells in additament to the pristinely toxicological roles as described above. This suggests that, being as its role in defense mechanisms and because of their critical metabolic role, some GSTs being constitutes sites of susceptibility to chemical attack and might represent incipient targets for chemical control. Hence, the detailed study of GSTs is very utilizable to determine their role in development, physiology and insecticide resistance in any pest species. In the present investigation, gene cloning, protein expression coupled with purification methods has been applied to study species *D. melanogaster* gene, *dmgste*6 and *dmgste*7. The underlying aim of this research is to undertake the first molecular study of *D. melanogaster* gene, *dmgste*6 and *dmgste*7 GSTs, their preliminary expression and purification, their possible paramount in insecticide metabolism and therefore to investigate its potential role in *D. melanogaster* metabolism. This can be broken down to three major objectives as follows;

2.8 Objectives

1. To isolate, clone, and express GSTs E6 and E7
2. To purify recombinant protein GSTE6 and GSTE7
3. To characterize recombinant protein GSTE6 and GSTE7

CHAPTER 3

MATERIALS AND METHODS

3.1 Materials

3.1.1 Insects

The adult flies of *D. melanogaster*, laboratory strain were obtained from Genetic department, University Malaya in the year 2012. The adult flies were reared on oats and glucose based diet as described in Appendix A at room temperature. Only 5 days post emerged flies were used for the experiments. All were stored at -20°C.

All reagents were of analytical grade purity or equivalent unless otherwise stated.

3.1.2 Chemicals and Disposables

SYSTERM CHEM AR

Chloroform, Methanol, Ortho-Phosphoric acid, Ethanol, Ammonium Sulphate, Sodium dihydrogen phosphate, Sodium Chloride, Potassium Chloride, Sodium hydroxide, Acetone, Acetic acid, 1-Chloro-2,4-dinitrobenzene (CDNB),1,2-Dichloro-4-nitrobenzene (DCNB), Ethylenediaminetetraacetic acid (EDTA), glycerol, sodium hydroxide (NaOH) and butan-1-ol

PROMEGA

Agarose L.E analytical grade, Blue/Orange Loading Dye 6X and Tris-base

GENET BIO

HS Prime Taq Premix (2X)

MAESTROGEN

AccuRuler 1 kb DNA RTU Ladder

COSMO GENETECH

SP-Taq DNA Polymerase, *EcoR1* enzyme, *Nde1* enzyme, *Xho1* enzyme and T4 Ligase Kit

BIORON

Sets of dNTPs

SIGMA ALRICH

Ethidium bromide, Commassie Brilliant Blue G-250, Sodium Dodesyl Sulphate (SDS), Propionic acid, *p*-nitrobenzyl chloride (*p*-NBC), ethacrynic acid, *trans*-4-phenyl-3-buten-2-one, Sulfobromophthalein (BSP), *trans*,*trans*-Hepta-2,4-dienal, Hexa-2,4-dienal, *trans*-Oct-2-enal, *trans*-Hex-2-enal, Triphenyltin acetate, Tetradecanedioic acid, Sebacic acid, *trans*-chalcone, Cardiogreen, Crystal Violet, Rose Bengal, Phenol Red, Cibacron blue, L-glutathione reduced (GSH), Lysozyme, Bovine serum albumin (BSA), ninhydrin, Nicotinamide adenine dinucleotide phosphate (NADPH), Glutathione Reductase (GSSR), Cumene hydroperoxide and Methly parathion

RIEDEL-DE HAËN

Clodinafop-propargly and Fenonoxaprop-ethyl

FERMENTAS

Nucleases free water

NOVAGEN

pET-30a (+) plasmid DNA and Competent cell (*E.coli* BL21 (DE3) pLyss; *E. coli* BL21 Star™ (DE3) pLysS)

INVITROGEN

Competent cells (*E.coli* TOP10), Super optimal broth (SOC) medium, pBAD/TOPO® ThioFusion™ Expression Kit and Bench mark protein ladder

CALBIOCHEM

Kanamycin Sulphate

PRODANISA

Luria Bertani Agar and Luria Bertani broth

GOLD BIO.COM

Isopropyl β-D-thiogalactopyranoside (IPTG)

BIORAD LABORATORIES

30% Acrylamide/bis-acrylamide (29:1), 1.5M Tris-HCL pH 8.8, 0.5M Tris-HCL pH 6.8, Ammonium Persulphate (APS), *N, N, N', N'*-tetramethylenediamine (TEMED) and SDS Running buffer

SARTORIUS

Vivaspin 20: 10,000 MWCO

R&M CHEMICALS

Methylene Blue

FLUKA ANALYTICAL

Propoxur and Isoproturon

QIAGEN

DNeasy Blood & Tissue Kit

ANALYTIK JENA BIO SOLUTION

InnuPrep Double Gel Extraction Kit and innuPrep Plasmid Rapid Kit

MERCKS

TLC Silica gel 60 $F_{2s4,}$ Mercaptoethanol and Hydrogen peroxide

FIRST BASE

TBE buffer (10X)

DUCHEFA BIOCHEMIE

Ampicilin sodium

BIO BASIC

TE buffer

WHATMAN

Whatman #1 filter paper

PESTICIDES

(A gift from Professor Dato' Dr. Mohd Sofian Azirun, Faculty of Science, University Malaya)

Temophos, Malathion, DDT, Fenthion, Fenitrothion, Permetrin, Bromophos and Chlopyrifos.

3.1.3 Buffers

- TBE buffer (0.09 M Tris Borate and 2 mM EDTA, pH 8.0)
- TE buffer (Tris Buffer and EDTA disodium salt, pH 8.0)
- Buffer A (0.1 M Sodium Phosphate, pH 6.8)
- Buffer B (0.1 M Tris, pH 9.0)
- Buffer C (0.1 M Sodium Phosphate, pH 7.5)
- Buffer D (0.25 M Sodium Phosphate, pH 7.0)
- SDS reducing buffer [0.5 M Tris-HCl pH 6.8, glycerol, 10% (w/v) SDS and 0.5% (w/v) Bromophenol Blue and β- Mercaptoethanol (prior to use)]
- Tris/Glycine/SDS running buffer (25 mM Tris, 192 mM Glycine and 0.1% (w/v) SDS, pH 8.3)

3.1.4 Instrumentations

- Polymerase Chain Reaction Thermal cycle (Biorad)
- Gel Electrophoresis Tank (Biorad)
- Thermal Mixing Block (Biocher)
- Gel Image UV Transilluminator (Alpha Innotech)
- Thermal Shaking Incubator (Wisebath)
- Sonicator (Roop Ultrasonic Powersonic 603)
- Orbital Shaker (Protech)
- Microwave oven (Pensonic)
- Fume Hood (Sastec)
- PCR work station (ISC Bioexpress)
- Mini Centrifuge (MSC)
- Vortex (Labnet International)
- Hot plate (Heidolph)
- Centrifuge Machine (Eppendoft)
- Amersham Bioscience AKTA FPLC™
- Spectrophotometer (Jusco V630)
- pH Meter (Hanna Instruments)
- Nanodrop 2000 Spectrophotometer (Thermo Scientific)
- CD Spectrometer (J-815 Jasco)
- Freeze Dryer (Labconco)

3.1.5 Plasmid constructs used

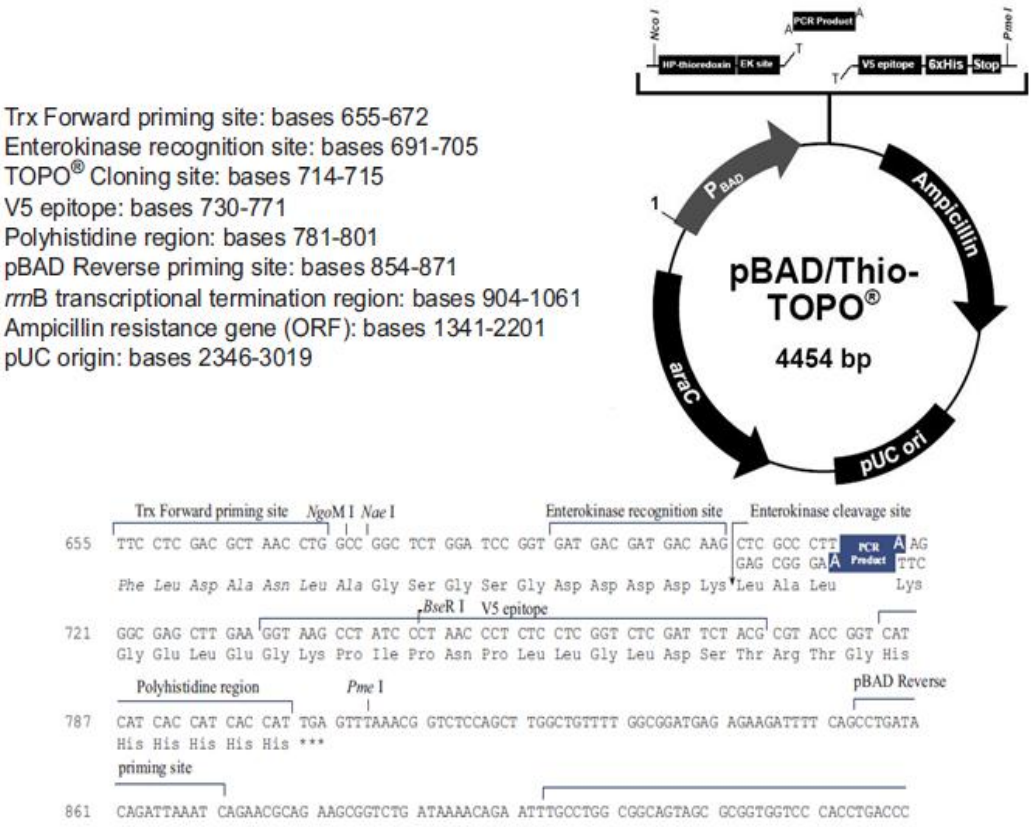

Figure 3.1: A sketch showing the pBAD/Thio-TOPO vector and the multiple cloning site region (Invitrogen)

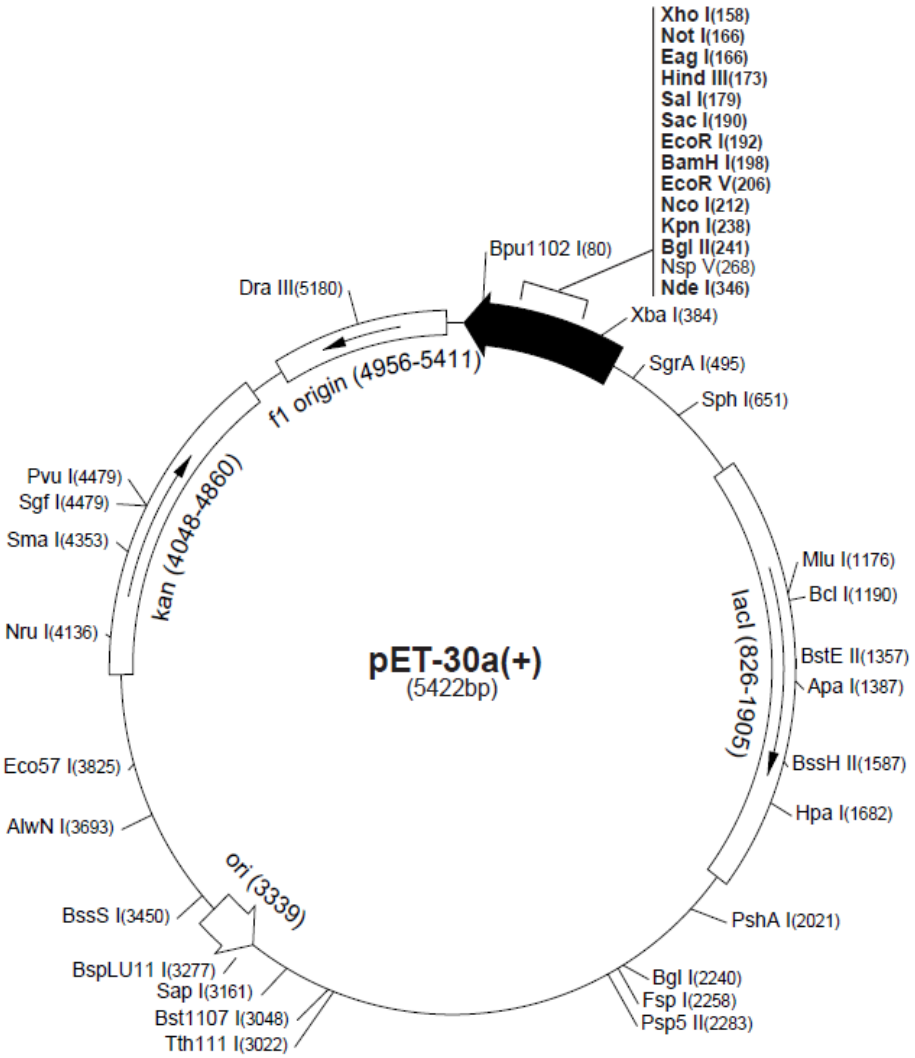

Figure 3.2: A sketch showing the pET-30a (+) vector and the multiple cloning site region (Novagen)

3.2 Methods

3.2.1 Purification of Total DNA from Animal Tissue

Total DNA was purified using DNeasy Blood & Tissue Kit according to the manufacturer's instructions. About 40-50 mg of frozen thawed adult *Drosophila melanogaster* was placed in 1.5 mL microcentrifuge tube. A total of 180 µL Buffer ATL was added. The tissue samples were disrupted using homogenizer or a bead mill. Then, 20 µL Proteinase-K was added and mix thoroughly by vortexing and incubated at 56°C until the tissue samples were completely lysed. The samples were occasionally vortex during incubation to disperse the sample. The samples were vortex for 15 seconds. A total of 200 µL Buffer AL was added and vortex. About 200 µL of ethanol (96%-100%) was added and vortex until white precipitate forms. The mixture was pipette (including any precipitate) into the DNase Mini spin column which was placed in a 2 mL collection tube. The tube was centrifuged at > 6000 x g (8000 rpm) for 1 minute. The flow though and the collection tube was discarded. The DNase Mini spin column which was placed in a new 2 mL collection tube. 500 µL of Buffer AW1 was added. The same steps were repeated with 500 µL Buffer AW2 and followed by 200 µL of Buffer AE. The tube was incubated at room temperature for 1 minute and centrifuged again at > 6000 x g (8000 rpm) for 1 minute to eluted the DNA genomic template. The DNA purity and concentration was quantified using Nanodrop (Thermo Scientific).

3.2.2 Polymerase Chain Reaction (PCR)

3.2.2.1 Oligonucleotide primers of *gste*6 and *gste*7 for TOPO Cloning

Oligonucleotide primers used in this study as tabulated in Table 3.1 below.

Table 3.1: List of primers for *gste*6 and *gste*7 for TOPO cloning

	Forward primer	Reverse Primer
GSTE6	5'-**ATG** GTG AAA TTG ACT TTA TAC G -3'	5'-TGC TTC GAA TGT GAA ATT GGT C- 3'
GSTE7	5'-**ATG** CCC AAA TTG ATA CTG TAC G-3'	5'-ATT CGA TGC GAA AGT GAA ATT A- 3'

The forward primer followed by initiation codon ATG (bold) and reverse primer

3.2.2.2 Oligonucleotide primers of *gste*6 and *gste*7 for Restriction Enzyme Cloning

Oligonucleotide primers used in this study as tabulated in Table 3.2 below.

Table 3.2: List of primers for *gste*6 and *gste*7 for restriction enzyme cloning

	Forward primer	Reverse Primer
GSTE6	5' GGAATTC **CATATG** gtgaaattgactttatac 3'	5' CG <u>GAATTC</u> tcatgcttcgaatgtgaa 3'
GSTE7	5' GGAATTC **CATATG** cccaaattgatactgtac 3'	5' CCG <u>CTCGAG</u> ttaattcgatgcgaaagt 3'

NdeI restriction site (bold) and *EcoRI* for GSTE6 and *XhoI* for GSTE7 restriction site (underlined) respectively

3.2.3 PCR Amplification Product

PCR were carried out to amplify both *gste*6 and *gste*7 genes. For TOPO cloning; 2 µL of 100 ng of DNA template, forward and reverse primer 1 µL each at final concentration of 0.5µM, 10 µL of HS Prime Taq Premix (2X) were added up in total of 20 µL with sterile distilled water. For negative control everything added was similar except 100 ng of DNA template was replaced with distilled water. For restriction enzyme cloning; 1 µL of 100 ng of DNA template, 5 µL of 10X buffer, forward and reverse primer 1 µL each at final concentration of 100 pmol, 5 µL of dNTPs, 0.5 µL of SP-Taq DNA Polymerase were added up in total of 50 µL with nuclease free water. For negative control everything added was similar except 100 ng of DNA template was replaced with nucleases free water. The PCR mixture was placed in a thermal cycle as and the DNA was amplified with hot start using the following cycling parameters respectively as tabulated in Table 3.3 and Table 3.4 below. The PCR components and cycling parameters was optimized few times for optimized band and without primer-dimer.

Table 3.3: Parameter set for TOPO cloning PCR reaction

Steps	Time	Temperature	Cycles
Initial Denaturation	3 minutes	95°C	1 X
Denaturation	30 seconds	95°C	32 X
Annealing	30 seconds	60°C	
Extension	1 minutes	72°C	
Final Extension	7 minutes	72°C	1 X
Storage	Infinite	4°C	1 X

Table 3.4: Parameter set for restriction enzyme cloning PCR reaction

Steps	Time	Temperature	Cycles
Initial Denaturation	5 minutes	95°C	1 X
Denaturation	60 seconds	95°C	25 X
Annealing	60 seconds	55°C	
Extension	90 seconds	72°C	
Final Extension	7 minutes	72°C	1 X
Storage	Infinite	4°C	1 X

3.2.4 Agarose Gel Electrophoresis

The PCR product was analyzed by agarose gel electrophoresis to obtain correct size of amplified PCR product. A total of 1% (w/v) of analytical grade agarose was weighed and dissolved in 100 mL of 50X TBE buffer in a 300 mL schott bottle. The agarose was placed in microwave oven until it completely dissolved. The melted agarose was left for 45 minutes for it to cool down and poured into electrophoresis gel chamber. Gel comb (1.5 mm) were carefully placed into the gel and waited for 30 to 45 minutes until it solidified. The solidified gel was placed inside the gel electrophoresis tank and filled until the gel was completely immersed with 50X TBE buffer. A total of 2 µL of 1 Kb DNA ladder and 20 µL samples (restriction enzyme cloning PCR products) mixed with 4 µL of Blue/Orange Loading Dye 6X loaded into the gel wells respectively. No loading dye used for TOPO cloning PCR product because HS Prime Taq Premix (2X) contains loading dye. Blue/Orange Loading Dye 6X loading dye/buffer gives colour and density to the sample to facilitate loading into the wells. The dye is negatively charged in neutral buffers and thus moves in the same direction as the DNA during electrophoresis. The tank covered and connected to power source. The gel was run at 60 V for 70 minutes. The gel was then stained for ethidium bromide (0.5 mg/mL) for an hour and de-staining for 10 minutes in distilled water. The gel was then viewed under ultraviolet light (302 nm wavelength) inside a gel imager (Alpha Innotech). The gel image were captured and saved.

3.2.5 Agarose DNA Extractions (Gel Purification)

The DNA fragment at correct size were excised from the agarose gel with a sharp knife/ or scalpel which is not more than 300 mg. The DNA was extracted using InnuPrep Double Kit according to the manufacturer's instructions. The gel slice was then transferred into 1.5 mL centrifuge tube and 650 µL of gel solubilizer solution was added. The gel was incubated for 10 minutes at 50°C water bath until the gel fully dissolved. Then, 50 µL of binding optimizer was added and mixed well by vortex. The whole sample was applied into spin filter (green) located inside 2 mL receiver tube. The sample then was centrifuged at 12, 000 rpm for 1 minute. The filtrate was discarded and 700 µL of washing solution LS was added and centrifuged at 12 000 rpm for 1 minute. The filtrate was again discarded. The spin column sample was centrifuged at maximum speed for 2 minutes to remove all the ethanol. The spin filter was then placed into 1.5 mL elution tube. A total of 20 µL of elution buffer (pre-warmed to 50°C) was added. The sample was incubated at room temperature for 1 minute. The sample centrifuged at 8000 rpm for 1 minute. The elution was collected and stored in -20°C freezer.

3.2.6 TOPO Cloning Reaction

TOPO cloning reaction was performed using pBAD/TOPO® ThioFusion™ Expression Kit according to the manufacturer's instructions. Two µL of fresh PCR product of *gste*6 were added into a PCR tube followed by 1µL of salt solution (at final concentration of 200 mM NaCl, 10 mM $MgCl_2$), double sterile water was added to a total volume of 5 µL and finally 1µL of TOPO vector was added. The reaction was mixed gently and incubated for 5 minutes at room temperature. The reaction was placed on ice or kept in -20°C overnight and proceed to One Shot TOP10 Chemical Transformation.

3.2.6.1 TOPO Cloning Reaction Transformation

Two µL of the TOPO® Cloning reaction was added into a vial of One Shot® TOP10 Chemically Competent *E. coli* and mixed gently without pipetting up and down. The vial were incubated on ice for 5 minutes and then heat-shocked the cells for 30 seconds at 42°C without shaking. The vial then was immediately transferred into ice. Two hundred fifty µL of room temperature SOC medium was added. The vial was capped tightly and shaken horizontally (200 rpm) at 37°C for an hour. A total of 25–200 µL from each transformation was spread on a pre-warmed selective ampicillin plate (100 µg/mL) and incubated overnight at 37°C. pBAD/Thio vector was used as a positive control and cells without vector as a negative control.

3.2.6.2 Positive Clone Analysis

The clones were directly analyzed for positive transformants using colony PCR method using the Trx Forward and pBAD Reverse sequencing primers as PCR primers. A PCR cocktail consisting of 10 µL HS Prime Taq Premix (2X) and 1 µL primer each was prepared for a 20 µL reaction volume with distilled water. The reaction multiplied by the number of colonies to be analyzed. Ten colonies were picked and resuspended them individually in 20 µL of the PCR cocktail. The reactions were incubated for 10 minutes at 94°C to lyse the cells and inactivate nucleases. The mixtures was amplified for 30 cycles with following cycling parameters (94°C for 1 minute, 55°C for 1 minute, and 72°C for 1 minute). Finally, the mixtures were incubated at 72°C for 10 minutes for the final extension and hold at 4°C. The clones were then analyzed by 1% (w/v) agarose gel electrophoresis for presence of correct band size. Clones were further analyzed by plasmid DNA analysis as described in **3.2.8**.

3.2.7 Restriction Enzyme Cloning

3.2.7.1 Restriction Enzyme Digestion

Two different restriction enzymes were used which chosen based on the map of the cloning vector. *NdeI*, *EcoRI* and *XhoI* enzyme were chose because it includes 6X Histidine tagging to the gene of interest which will assist with purification procedure later. The following components are added as following schema in ice: For *gste*6; 26 µL of fresh PCR product, 3.5 µL of 10X buffer, 0.5 µL of each *EcoRI* and *NdeI* restriction enzyme and 4.5 µL of nucleases free water which total volume was 35 µL. For *gste*7; 26 µL of fresh PCR product, 3.5 µL of 10X buffer, 3.5 µL of 10X BSA, 0.5 µL of each *NdeI* and *XhoI* restriction enzyme and 1 µL of nucleases free water which total volume was 35 µL. The components

were mixed gently and spun down. The mix then incubated at 37°C in a heat block for overnight.

For digestion of pET 30a(+) the following component were added as following schema in ice: For *gste*6; 26 µL of pET 30a(+), 3.5 µL of 10X buffer, 0.5 µL *EcoRI* restriction enzyme and 1 µL of nucleases free water which total volume was 35 µL. The components were mixed gently and spun down. The mix then incubated at 37°C in a heat block for 2 hours. The mixture is then enzyme inactivated by incubation at 65°C for 20 minutes. The 35 µL mixtures was added with 4 µL of 10X buffer, 0.5 µL of *NdeI* restriction enzyme and 0.5 µL of nuclease free water which total volume was 40 µL. The components were mixed gently and spun down. The mix then incubated at 37°C in a heat block for 2 hours. For *gste7*; 26 µL of fresh PCR product, 3.5 µL of 10X buffer, 3.5 µL of 10X BSA, 0.5 µL of each *NdeI* and *XhoI* restriction enzyme and 1 µL of nucleases free water which total volume was 35 µL. The components were mixed gently and spun down. The mix then incubated at 37°C in a heat block for overnight.

An aliquot of both PCR product and vector of the reaction mixture loaded directly on 1% (w/v) gel. For each 30 µL sample, 6 µL of loading dye (Blue/Orange Loading Dye 6X) were mixed and loaded into gel well to obtain purified product.

3.2.7.2 Ligation

Ligation was done using the T4 DNA Ligase kit. Digested PCR product, pET-30a (+) plasmid DNA, T4 Ligase Kit thawed and placed on ice. The ligation mixture was prepared by following procedure: For GSTE6; 1 µL of 10X T4 Ligase Buffer, 4 µL (38.9 ng/µL) of digested PCR product, 4 µL (21.4 ng/µL) of digested pET-30a (+), 1 µL of T4 Ligase enzyme in total volume of 20 µL. For GSTE7; 1 µL of 10X T4 Ligase Buffer, 5 µL (22.6 ng/µL) of digested PCR product, 3 µL (71.5 ng/µL) of digested pET-30a (+), 1 µL of T4 Ligase enzyme in total volume of 20 µL. The components were mixed gently and spun down. The mix then incubated at room temperature for 3 hours. The ligation mixture mixed with 4 µL loading dye (Blue/Orange Loading Dye 6X) was loaded directly into 1% (w/v) gel well to obtain correct band size and purified ligation product.

3.2.7.3 Transformation with *E.coli* BL21 (DE3) pLysS

A vial of competent cell (50 µL) was thawed on ice. Fifty ng or 5 µL of ligated DNA was added to the transformation reaction and swirled gently. For the control transformation reaction, 1 µL of the pUC18 control plasmid was added to a separate 50 µL aliquot of the competent cells and swirled gently. The reactions were incubated on ice for 30 minutes. Each transformation reaction was heat-pulse in a 42°C water bath for 45 seconds. The reactions were incubated on ice for 2 minute. A total of 250 µL of preheated (42°C) Super Optimal broth with Catabolite repression (SOC) medium were added to each transformation reactions respectively and incubated the reactions at 37°C for 1 hour and 30 minutes with shaking at 225–250 rpm. Using a sterile spreader, 50-100 µL of the cells was spread and transformed with the experimental DNA onto LB agar plates with 30 µg/mL of Kanamycin. For the pUC18 control transformation, 200 µL of the reaction was spread onto

an LB–ampicillin (100 μg/mL) agar plate. The plates were incubated at 37°C for 16-18 hours. The transformants was sub-cloned, streaked on new selective plates and cultured in 5 mL LB broth for plasmid extraction. Some was stored in glycerol stock at -80ºC for long term storage.

3.2.8 Plasmid DNA Extraction

Double Pure Rapid Plasmid extraction kit from Analytikjena Biosolution was used to extract the plasmid DNA according to the manufacturer's instructions to confirm of positive clones. A single colony from a freshly streaked selective plate was picked and inoculated in a starter culture of 5 mL LB medium containing (100 ug/mL Ampicilin for TOPO clones) or (30 μg/mL Kanamycin for restriction enzyme digested clones). The culture incubated for approximately 18 hours at 37°C with vigorous shaking (300 rpm). The bacterial cells were harvested by centrifugation at 13, 000 rpm for 1 minute at room temperature. The pellet stored at -20ºC or suspended in 0.2 mL of resuspension buffer by vortex/ pipetting until no clumps remain. 0.2 mL of lysis buffer was added and mixed by vigorously inverting the sealed tube 4-6 times and incubated at room temp (~15-25°C) for 2 minutes. 0.3 mL of neutralizing buffer was added and mixed by vigorously inverting the sealed tube 4-6 times (~15-25°C) for 5 minutes. The sample was transferred into prefilter (vanilla) spin column located on collection tube and centrifuged at maximum speed (10 000 -13 000 rpm) for 1 minute. The flow-through was transferred into new tube with spin column (Orange) and centrifuged at 13, 000 rpm for 1 minute. The flow through was discarded and 0.65 mL of Washing Solution A was added into the spin column and centrifuged at 13,000 rpm for 1 minute. The flow through was discarded again and 0.7 mL of washing solution B was added. The spin column was centrifuged at 13, 000 rpm for 1 minute and the flow through with the collection tube was discarded. The spin column was

placed into new receiver tube and 10-30 µL of elution buffer P was added directly on the center of the spin column. The spin column was incubated at room temperature for 1 minute before centrifuge at 13,000 rpm for 1 minute to collect the plasmid DNA. The same procedure was repeated for few colonies. The plasmids were then analyzed by 1% (w/v) agarose gel electrophoresis for presence of correct band size. A total of 2 µL of plasmid DNA with 1 µL of loading dye mixed and loaded into gel to check for correct insert with plasmid size.

3.2.8.1 Plasmid DNA Analysis

The plasmid DNA with correct size was used as template in a PCR reaction to check for presence of desired gene inside the plasmid. For TOPO cloning; A PCR consisting of 10 µL HS Prime Taq Premix (2X), 1 µL of each primers was prepared for a 20 µL reaction volume with distilled water. For Restriction enzyme cloning; a PCR consist of component used in PCR reaction described in section **3.2.3** was used. For negative control everything added was similar except plasmid DNA was replaced with distilled water or nucleases free water. The mixtures were amplified for 30 cycles with described PCR cycling parameters as follows; (95°C for 5 minute, 95°C for 30 seconds, 60°C (TOPO cloning reaction) and 55°C (Restriction cloning reaction) for 30 seconds, and 72°C for 60 seconds). Finally, the mixtures incubated at 72°C for 5 minutes for the final extension and hold at 4°C. The PCR of plasmids DNA were then analyzed by 1% (w/v) agarose gel electrophoresis for presence of correct band size. A total of 20 µL of plasmid DNA PCR was loaded into agarose gel electrophoresis gel to check for correct insert with plasmid size. PCR products and plasmid DNA which shows correct insert with plasmid size were sent out for full plasmid sequencing.

3.2.9 Cell Culturing and Lysis

A total of 1g of LB broth powder was dissolved in 50 mL of distilled water in a conical flask and sterilized by autoclaving. The flask was cooled to 37°C and kanamycin was added to a final concentration of 30 µg/mL. Single positive bacteria colony was transferred into the broth flask and placed in a shaking incubator of 200 rpm at 37°C overnight. Ten mL of fresh overnight culture were transferred into new 400 mL LB broth and placed in shaking incubator at 37°C for 5 hours. IPTG was added to the final concentration of 1 mM into the culture flask and continued shaking at 37°C for an additional of 4 hours.

The bacteria culture was then centrifuged at 6,000 rpm for 15 minutes at 4°C. The cell pellet was then resuspended with 5 mL binding buffer. A total of 100 uL of lysozymes (10 mg/mL) was added and the tube was inverted gently for 5-10 minutes. The crude lysate was centrifuged at 10,000 rpm for 1 hour at 4°C to remove the cell debris. The supernatant was transferred to a clean eppendoft tube without disturbing the cell pellet and kept in ice prior to analysis.

3.2.10 Protein Purification

Crude lysate of the bacterial lysis was subjected to ion exchange and affinity chromatography using several columns. Protein purification was carried out using Amersham Bioscience AKTA FPLC™ connected to a fraction collector. Each column was equilibrated with 30 mL of binding buffer to ensure proper column equilibration. Five mL of crude lysate was injected, allowing the sample to flow through the column followed by 20 mL of binding buffer to wash out all the unbound proteins completely. The bound proteins were eluted out using elution buffer as specified. Elute from the low to highest peak were collected to determine absorbance range which the protein in eluted out. For

columns such as bromosulfopthalein (BSP), additional washing with 1 M NaCl was required to remove the non-specific protein binding followed by protein elution using elution buffer as stated below (Table 3:5).

Table 3.5: Summary of columns and buffers used for both GSTE6 and GSTE7

Enzymes	Column	Binding buffer	Elution buffer	Washing buffer
GSTE6	GSTrap™ HP	25 mM Sodium Phosphate buffer, pH 7.4	10 mM GSH, pH 7.4	NIL
	HiTrap™ Q HP	25 mM Sodium Phosphate buffer, pH 7.4	1 M Sodium Chloride, pH 7.4	NIL
	HiTrap™ Q HP followed by BSP-SG and Hi-Trap Desalting(G-25)	25 mM Sodium Phosphate buffer, pH7.4	2 mM BSP, pH 7.4	1 M NaCl, pH 7.4
GSTE7	HiTrap™ Q HP	25 mM Sodium Phosphate buffer, pH 7.4	1 M Sodium Chloride, pH 7.4	NIL
		25 mM Sodium Phosphate buffer, pH 8.0	0.5 M Sodium Chloride, pH 8.0	NIL
		25 mM Sodium Phosphate buffer, pH 8.0	0.3 M Sodium Chloride, pH 8.0	NIL
	HiTrap™CM FF	25 mM Sodium Phosphate buffer, pH 7.4	1 M Sodium Chloride, pH 7.4	NIL
	HiTrap™ Q HP followed by BSP-SG and Hi-Trap Desalting(G-25)	25 mM Sodium Phosphate buffer, pH7.4	2 mM BSP, pH 7.4	1 M NaCl, pH 7.4

3.2.11 SDS- Polyacrylamide Gel (PAGE)

The polyacrylamide gel casting was performed using Bio-Rad Mini PROTEAN II System (Bio-Rad Laboratories, USA) following the manufacturer's instructions. SDS-PAGE gel formulation was as described in the Table 3.6 below. The resolving gel (lower part) was prepared and allowed to polymerize for 30 minutes to an hour before overlaid with distilled water. The overlaid distilled water was poured away and replaced with the stacking gel. A comb was placed on top of the stacking gel to form wells. After polymerization, the comb was removed and the stacking gel was washed with distilled water to remove the un-polymerized acrylamide solution.

Table 3.6: SDS-PAGE gel formulations

Components	Stacking Gel (4%)	Resolving Gel (12%)
Deionized H2O	15 mL	3.4 mL
30% Acrylamide/bis-acrylamide (29:1)	3.3 mL	4.0 mL
1.5 M Tris (pH 8.8)	-	2.5 mL
0.5 M Tris HCl (pH 6.8)	6.3 mL	-
10% (w/v) SDS	0.25 mL	0.1 mL
10% (w/v) Ammonium Persulphate	0.125 mL	0.05 mL
TEMED	0.005 mL	0.005 mL

The electrophoresis apparatus were assembled following the instruction for Bio-Rad Mini PROTEAN ® II System. The collected elute was concentrated for 15-30 minutes using vivaspin 20: 10,000 MWCO (Sartorius). Sample was then diluted with SDS reducing buffer (at least 1:2) and heated at 95°C for 4 minutes. Sample and protein standard marker were loaded into wells. Electrophoresis was performed in descending directions, with running buffer 1X Tris- glycine running buffer (25 mM Tris, 192 mM Glycine and 0.1% (w/v) SDS at pH 8.3) with a constant voltage of 120 volts until the bromophenol marker reaches the bottom edge of the gel tank which will take approximately 60-90 minutes. As soon as it

finished running, the apparatus was disassembled and the gel was stained in Commasie staining solution [(5% (w/v)) Commasie Brilliant Blue, 85% H_2PO_4, Ammonium Sulphate] and left overnight. The gel washed with 20% (v/v) methanol until its clear enough to view the bands. The band viewed under visible white light.

3.2.12 Bradford Assay

A total of 100 mg Coomasie Brilliant Blue G-250 was dissolved in 50 mL 95% ethanol and 100 mL of 85% (w/v) phosphoric acid was added to the mixture. The solution was then diluted by topping up to 1 liter once the dye has completely dissolved. The mixture was filtered using Whatman #1 filter paper (Spector, 1978). The filtrate, Bradford solution was wrapped in aluminum foil and stored in dark as it is light sensitive.

Standard (BSA) ranging from 20-100 µg was prepared in 100 µL volume. Five mL Bradford reagent was added and mixed well using vortex. The mixture was incubated for 30 minutes in the dark. Absorbance was measured at 595 nm (Bradford, 1976).

3.2.13 Assay for GSTs

The substrate specificity kinetics assays for GSTs done according to method of Habig *et al.*, (1974), Brophy *et al.*, (1989) and Paglia and Valentine, (1967).

3.2.13.1 1-Chloro-2, 4-dinitrobenzene (CDNB)

A total of 2.85 mL Buffer A, 0.05 mL 60 mM GSH (freshly prepared) (0.0553g in 3 mL buffer A), 0.05 mL sample were added into a cuvette accordingly .The sample was replaced with buffer A for negative control. At the end, 0.05 mL of 60 mM (0.2430 g in 20 mL ethanol) CDNB was added (which makes the total volume of 3 mL) and mixed well. Enzyme activity conjugating GSH to the CDNB (1-chloro-2, 4-nitrobenzene, a universal GST substrate) was measured by monitoring the increase in absorbance at 340 nm over time using Jasco V630 spectrophotometer. This standard GST assay was performed according to Habig *et al*., (1974) at 25^{o}C and was measured for 10 minutes. Molar absorption coefficient $\xi_{m,}$ is 9600 1.mol^{-1}.cm^{-1}.

3.2.13.2 1, 2-Dichloro-4-nitrobenzene (DCNB)

A total of 2.80 mL Buffer B, 0.05 mL 240 mM GSH (freshly prepared) (0.2212 g in 3 mL buffer B) and 0.10 mL sample were added into a cuvette accordingly. The sample was replaced with buffer B for negative control. Finally, 0.05 mL 24 mM (0.092 g in 20 mL ethanol) DCNB was added (total volume of 3 mL) and mixed well. Enzyme activity conjugating GSH to the DCNB (1, 2-Dichloro-4-nitrobenzene) was measured by monitoring the increase in absorbance at 344 nm over time using Jasco V630 spectrophotometer. This standard GST assay was performed according to Habig *et al.*,

(1974) at 25°C and measured for 20 minutes. Molar absorption coefficient $\xi_{m,}$ is 8400 $1.mol^{-1}.cm^{-1}$.

3.2.13.3 *p*-Nitrobenzyl Chloride (*p*-NBC)

A total of 2.60 mL Buffer A, 0.25 mL 60 mM GSH (freshly prepared) (0.0553g in 3 mL buffer A) and 0.10 mL sample were added into a cuvette accordingly. The sample was replaced with buffer A for negative control. At the end, 0.05 mL 60 mM (0.2058 g in 20 mL ethanol) *p*-NBC was added (total volume of 3 mL) and mixed well. Enzyme activity conjugating GSH to the *p*-NBC was measured by monitoring the increase in absorbance at 310 nm over time using Jasco V630 spectrophotometer. This standard GST assay was performed according to Habig *et al.*, (1974) at 25°C and measured for 10 minutes. Molar absorption coefficient $\xi_{m,}$ is 1900 $1.mol^{-1}.cm^{-1}$.

3.2.13.4 Sulfobromophthalein (BSP)

A total of 2.60 mL Buffer C, 0.25 mL 60 mM GSH (freshly prepared) (0.0553g in 3 mL buffer A) and 0.10 mL sample were added into a cuvette accordingly. The sample was replaced with buffer C for negative control. Finally, 0.05 mL 2 mM (0.0334 g in 20 mL ethanol) BSP was added (total volume of 3 mL) and mixed well. Enzyme activity conjugating GSH to the BSP was measured by monitoring the increase in absorbance at 330 nm over time using Jasco V630 spectrophotometer. This standard GST assay was performed according to Habig *et al.*, (1974) at 25°C and measured for 10 minutes. Molar absorption coefficient $\xi_{m,}$ is 4500 $1.mol^{-1}.cm^{-1}$

3.1.13.5 Ethacrynic acid (EA)

A total of 2.8 mL Buffer A, 0.05 mL 15 mM GSH (freshly prepared) (0.0138 g in 3 mL buffer A) and 0.10 mL sample were added into a cuvette accordingly. The sample was replaced with buffer A for negative control. Finally, 0.05 mL 12 mM (0.0727 g in 20 mL in ethanol) EA was added (total volume of 3 mL) and mixed well. Enzyme activity conjugating GSH to the EA was measured by monitoring the increase in absorbance at 270 nm over time using Jasco V630 spectrophotometer. This standard GST assay was performed according to Habig *et al.*, (1974) at 25^{o}C and measured for 10 minutes. Molar absorption coefficient $\xi_{m,}$ is 5000 1.mol^{-1}.cm^{-1}.

3.2.13.6 *trans*-4-phenyl-3-butene-2-one (PBO)

A total of 2.8 mL Buffer A, 0.05 mL 15 mM GSH (freshly prepared) (0.0138 g in 3 mL buffer A) and 0.10 mL sample were added into a cuvette accordingly. The sample was replaced with buffer A for negative control. Finally, 0.05 mL 3 mM (0.0876 g in 20 mL ethanol) PBO was added (total volume of 3 mL) and mixed well. Enzyme activity conjugating GSH to the PBO was measured by monitoring the increase in absorbance at 290 nm over time using Jasco V630 spectrophotometer. This standard GST assay was performed according to Habig *et al.*, (1974) at 25^{o}C and measured for 10 minutes. Molar absorption coefficient $\xi_{m,}$ is -24800 1.mol^{-1}.cm^{-1}.

3.2.13.7 Hexa-2, 4-dienal

A total of 2.8 mL Buffer A, 0.05 mL 150mM GSH (freshly prepared) (0.0461 g in 1 mL buffer A) and 0.10 mL sample were added into a cuvette accordingly. The sample was replaced with buffer A for negative control. Finally, 0.05 mL 3 mM (34.8 µL in 100 mL buffer A) Hexa-2,4-dienal was added (total volume of 3 mL) and mixed well. Enzyme activity conjugating GSH to the substrate was measured by monitoring the change of absorbance at 280 nm over time using Jasco V630 spectrophotometer. This standard GST assay was performed according to Brophy *et al.*, (1989) at 25^{o}C and measured for 10 minutes. Molar absorption coefficient $\xi_{m,}$ is -34200 1.mol^{-1}.cm^{-1}.

3.2.13.8 *trans, trans* -Hepta-2, 4-dienal.

A total of 2.8 mL Buffer A, 0.05 mL 150 mM GSH (freshly prepared) (0.0461 g in 1 mL buffer A) and 0.10 mL sample were added into a cuvette accordingly. The sample was replaced with buffer A for negative control. Finally, 0.05 mL 3 mM (41.6 µL in 100 mL buffer A) *trans,trans*-Hepta-2,4-dienal was added (total volume of 3 mL) and mixed well. Enzyme activity conjugating GSH to the substrate was measured by monitoring the change in absorbance at 280 nm over time using Jasco V630 spectrophotometer. This standard GST assay was performed according to Brophy *et al.*, (1989) at 25^{o}C and measured for 10 minutes. Molar absorption coefficient $\xi_{m,}$ is -30300 1.mol^{-1}.cm^{-1}.

3.2.13.9 *trans*-Oct-*2*-enal

A total of 2.8 mL Buffer A, 0.05 mL 60 mM GSH (freshly prepared) (0.0553 g in 3 mL buffer A) and 0.10 mL sample were added into a cuvette accordingly. The sample was replaced with buffer A for negative control. Finally, 0.05 mL 3 mM (47.6 µL in 100 mL buffer A) *trans*-Oct-2-enal was added (total volume of 3 mL) and mixed well. Enzyme activity conjugating GSH to the substrate was measured by monitoring the change in absorbance at 225 nm over time using Jasco V630 spectrophotometer. This standard GST assay was performed according to Brophy *et al.*, (1989) at 25^{o}C and measured for 10 minutes. Molar absorption coefficient $\xi_{m,}$ is -22000 1.mol^{-1}.cm^{-1}.

3.2.13.10 *trans*-Hex-2-enal

A total of 2.8 mL Buffer A, 0.05 mL 60 mM GSH (freshly prepared) (0.0553 g in 3 mL buffer A) and 0.10 mL sample were added into a cuvette accordingly. The sample was replaced with buffer A for negative control. Finally, 0.05 mL 3 mM (48.4 µL in 100 mL buffer A) *trans*-Hex-2-enal was added (total volume of 3 mL) and mixed well. Enzyme activity conjugating GSH to the substrate was measured by monitoring the change in absorbance at 225 nm over time using Jasco V630 spectrophotometer. This standard GST assay was performed according to Brophy *et al.*, (1989) at 25^{o}C and measured for 10 minutes. Molar absorption coefficient $\xi_{m,}$ is -24000 1.mol^{-1}.cm^{-1}.

3.2.13.11 Cumene hydroperoxides (CuH_2O_2)

A total of 2.7 mL Buffer D, 0.05 mL 10 mM GSH (freshly prepared), 0.05 mL 6µM Glutathione Reductase, 0.05 mL 2.5 mM NADPH and 0.10 mL sample were added into a cuvette accordingly. The sample was replaced with buffer D for negative control. Finally, 0.05 mL 3 mM cumene hydroperoxide was added (total volume of 3 mL) and mixed well. Enzyme activity conjugating GSH to the substrate was measured by monitoring the change in absorbance at 366 nm over time using Jasco V630 spectrophotometer. This standard GST assay was performed according to Paglia and Valentine, (1967) at 25^{o}C and measured for 20 minutes. Molar absorption coefficient ξm of NADPH is 6220 1.mol-1.cm-1.

3.2.13.12 Hydrogen peroxide (H_2O_2)

A total of 2.7 mL Buffer D, 0.05 mL 10 mM GSH (freshly prepared), 0.05 mL 6µM Glutathione Reductase, 0.05 mL 2.5 mM NADPH and 0.10 mL sample were added into a cuvette accordingly. The sample was replaced with buffer D for negative control. Finally, 0.05 mL 3 mM hydrogen peroxide was added (total volume of 3 mL) and mixed well. Enzyme activity conjugating GSH to the substrate was measured by monitoring the change in absorbance at 366 nm over time using Jasco V630 spectrophotometer. This standard GST assay was performed according to Paglia and Valentine, (1967) at 25^{o}C and measured for 20 minutes. Molar absorption coefficient ξm of NADPH is 6220 1.mol-1.cm-1.

3.2.14 The Effect of Substrate Concentration and Determination of Km and Vmax

The kinetic parameters of K_m and V_{max} values for GSTE6 and GSTE7 were determined by fixing GSH at saturating concentration and changing the concentration of second substrate. An appropriate substrate dilution was chosen that allows the whole set of different substrate concentrations to be measured within the initial rate period showing a linear reaction slope. The K_m value and the maximum reaction velocity V_{max} were calculated by means of the nonlinear least-squares regression and fitting the acquired data to the Michaelis-Menten equation with the program GraphPad Prism version 6.00 for Windows, GraphPad Software, La Jolla California USA, www.graphpad.com. The values obtained were again used to construct Michaelis-Menten and Lineweaver-Burk plot to determine the K_m and V_{max} values. The catalytic constant k_{cat} and the catalytic efficiency (k_{cat}/ K_m) were calculated by using the molecular weight calculated from the amino acid composition.

K_m value for CDNB was determined by using 1-150 mM stock solution of CDNB and 60 mM GSH at which GSTE6 and GSTE7 was saturated under assay conditions as described in 3.2.13.1.

K_m value for DCNB was determined by using 1-100 mM stock solution of DCNB and 24 mM GSH at which GSTE6 and GSTE7 was saturated under assay conditions as described in 3.2.13.2.

K_m value for *p*-NBC was determined by using 1-100 mM stock solution of *p*-NBC and 60 mM GSH at which GSTE6 and GSTE7 was saturated under assay conditions as described in 3.2.13.3.

3.2.15 Secondary Structure Analysis by Circular Dichroism (CD)

The protein concentration of the recombinant GSTs was adjusted to 0.2 mg/mL for GSTE6 and GSTE7 respectively in 0.1 M sodium phosphate buffer at pH 6.5. The recombinant protein of GSTE6 and GSTE7 was filtered before proceeding with circular dichroism (CD) spectra determination. The circular dichroism (CD) spectra were determined at 25 °C on a Jasco J-815 Circular Dichroism Spectrometer using a 1 mm path length Hellma quartz cuvette. The CD spectra were scanned from 250 to 200 nm with the scanning speed 50 nm per minutes. Background CD spectrum of 0.1 M Sodium phosphate buffer was automatically subtracted from each sample analysis.

3.2.16 Thin Layer Chromatography of Pesticides

Thin layer chromatography (TLC) was used to determine the presence of chemically synthesized S-glutathionylated pesticide conjugates. Each assay was prepared according to method described in 3.2.13.1 replacing CDNB (positive control) with pesticides temophos, malathion, DDT, fenthion, fenitrothion, permetrin, bromophos, chlopyrifos, clodinafop-propargyl, fenoxaprop-ethyl, propoxur, isoprofuron and methyl parathion. Control reaction was prepared replacing sample with buffer A. Of each reaction preparation, 8 µL were independently applied to a Merck 10 x 8 cm silica gel 60 F2s4 TLC aluminium sheet with control reaction was run alongside each reaction mix. The TLC plate was developed for 2 hours in butan-1-ol: acetic acid: distilled water (12:3:5). The glutathione-conjugates were visualised with conjugated reaction products staining positive after applied with 0.25% (w/v) ninhydrin in acetone (Rogers et al., 1999).

3.2.17 Inhibition of Glutathione S-Transferases

Natural products and dyes were used to study the effect of the compound on CDNB activity against GSTE6 and GSTE7. Various concentration ranges of natural products and dyes were tested to generate inhibition or stimulation curves from which IC_{50}/EC_{50} values could be determined, the IC_{50} value being the concentration required for 50 % inhibition of enzyme activity while EC_{50} value being the concentration of a compound that gives half-maximal response. The IC_{50} or EC_{50} value was determined by plotting sigmoidal concentration response curves of enzyme activity vs. log natural product or dyes concentrations using program GraphPad Prism version 6.00 for Windows, GraphPad Software, La Jolla California USA, www.graphpad.com. Each experiment was independently repeated at least 3 times.

The response value for CDNB was determined using the following assay composition (Table 3.7). Both protein sample, GSTE6 and GSTE7 was saturated under assay conditions as described in 3.2.13.1.

Table 3.7: Inhibition of glutathione s-transferase assay components

Inhibitors	Stock solution of Inhibitors (mM)	Stock solution of GSH (mM)	Stock solution of CDNB (mM)
Triphenyltin acetate	0-100	60	60
Tetradecanedioic acid	0-100	60	60
Sebacic acid	0-100	60	60
trans-chalcone	0-100	60	60
Cardiogreen	0-3	60	60
Rose Bengal	0-3	60	60
Methylene blue	0-100	60	60
Crystal violet	0-10	60	60
Phenol red	0-10	60	60
Cibacron blue	0-10	60	60

CHAPTER 4

RESULTS

4.1 DNA Extraction

The *gste*6 and *gste*7 is an epsilon class GST gene contains no intron. Thus, DNA instead of RNA was extracted from *Drosophila melanogaster*. The concentration of DNA extracted was quantified using the absorbance readings of the nanodrop (Thermo Scientific). Absorbance was read at 260 nm and 280 nm. An A_{260} of 1.0 corresponds to a concentration of 50 µg/mL for DNA. Purity of nucleotide can be evaluated by ratio of $Absorbance_{260nm}/Absorbance_{280nm}$ as a range of 0.5 to 1 is considered pure DNA.

4.2 Polymerase Chain Reaction (PCR)

PCR reaction was performed according to the conditions mentioned in material and methods section. Gene sequence for *gste*6 and *gste*7 was obtained from http://flybase.org/. Primers were designed and used to amplify the gene. Amino acids of protein, gene sequence and primer sequences used are as below:

Figure 4.1 shows amino acids of protein and gene sequence of *gste*6 with respective primers for TOPO and restriction enzyme cloning. Both the start codon (ATG) and stop codon (TAG) is in bold case in the beginning and ending of the gene sequence. The forward primer (pink) and reverse primer (green) without stop codon was used in TOPO cloning reaction. The forward primer (blue) includes the restriction site for *Nde1* (underlined) and aligned at the beginning of the sequence while the reverse primer (purple) includes the restriction site for *EcoR1* (underlined) and aligned at the ending was used in restriction enzyme cloning reaction.

222 Amino acids

MVKLTLYGLDPSPPVRAVKLTLAALNLTYEYVNVDIVARAQLSPEYLEKNPQHTVPTL
EDDGHYIWDSHAIIAYLVSKYADSDALYPKDPLKRAVVDQRLHFESGVVFANGIRSISK
SVLFQGQTKVPKERYDAIIEIYDFVETFLKGQDYIAGNQLTIADFSLVSSVASLEAFVAL
DTTKYPRIGAWIKKLEQLPYYEEANGKGVRQLVAIFKKTNFTFEA

Theoretical pI/MW: 5.84/ 25,014.6 Da

669 bp Gene and primers

5'-**ATG** GTG AAA TTG ACT TTA TAC G -3'

5' GGAATTC CAT**ATG** gtgaaattgactttatac 3'

5'**ATG****GTGAAATTGACTTTATACG**GTTTGGACCCCAGTCCCCCAGTTCGCGCTGTT
AAGCTTACTTTGGCCGCTCTAAACCTAACCTACGAATATGTAAACGTTGACATTGTG
GCTCGTGCCCAACTTTCACCGGAATATCTGGAGAAGAATCCACAGCATACGGTGCC
CACCCTGGAGGATGACGGTCACTACATCTGGGATTCGCATGCCATTATTGCCTATTT
GGTCTCGAAATATGCCGATTCCGATGCCCTATACCCGAAAGATCCTCTCAAGCGGG
CTGTTGTGGATCAGCGGCTGCACTTTGAATCCGGAGTGGTCTTTGCCAATGGCATAA
GGAGCATATCGAAGTCAGTGCTCTTCCAGGGACAGACGAAAGTACCCAAGGAGCG
ATACGATGCCATTATCGAGATCTACGATTTTGTGGAAACTTTTCTCAAGGGACAGG
ATTACATTGCTGGCAATCAACTGACCATTGCGGATTTCAGTCTCGTTTCATCGGTGG
CCTCCCTTGAGGCCTTCGTGGCCTTGGATACGACTAAGTATCCCAGGATCGGTGCTT
GGATCAAAAAGCTGGAACAGCTTCCATACTACGAGGAAGCCAATGGCAAGGGCGT
CCGCCAGTTGGTGGCCATTTTCAAGAA**GACCAATTTCACATTCGAAGCA**TGA 3'

5'-TGC TTC GAA TGT GAA ATT GGT C- 3

5' CG GAATTC **tca**tgcttcgaatgtgaa 3

Figure 4.1: Amino acids of protein and gene sequence of *gste*6 aligned with forward and reverse primers of TOPO cloning and restriction enzyme cloning respectively

Figure 4.2 shows amino acids of protein and gene sequence of *gste*7 with respective primers for TOPO and restriction enzyme cloning. Both the start codon (ATG) and stop codon (TAG) is in bold case in the beginning and ending of the gene sequence. The forward primer (pink) and reverse primer (green) without stop codon was used in TOPO cloning reaction. The forward primer (blue) includes the restriction site for *Nde1* (underlined) and aligned at the beginning of the sequence while the reverse primer (purple) includes the restriction site for *Xho1* (underlined) and aligned at the ending was used in restriction enzyme cloning reaction.

223 Amino acids

MPKLILYGLEASPPVRAVKLTLAALEVPYEFVEVNTRAKENFSEEFLKKNPQHTVPTLE
DDGHYIWDSHAIIAYLVSKYGKTDSLYPKDLLQRAVVDQRLHFESGVIFANALRSITKP
LFAGKQTMIPKERYDAIIEVYDFLEKFLAGNDYVAGNQLTIADFSIISTVSSLEVFVKVD
TTKYPRIAAWFKRLQKLPYYEEANGNGARTFESFIREYNFTFASN

Theoretical pI/MW: 6.12/ 25,510.1 Da

672 bp Gene and primers

5'-**ATG** CCC AAA TTG ATA CTG TAC G-3'

5' GGAATTC CAT**ATG** cccaaattgatactgtac 3'

5'ATG**CCCAAATTGATACTGTACG**GCTTGGAGGCAAGTCCACCAGTTCGTGCCGT
CAAATTGACCTTGGCTGCCCTGGAGGTTCCCTACGAATTCGTGGAGGTAAACACTC
GGGCCAAGGAAAACTTCTCTGAGGAGTTTCTGAAGAAGAATCCACAGCACACGGT
GCCCACGTTGGAGGACGATGGACATTATATCTGGGACTCACATGCCATTATTGCCT
ATCTGGTGTCCAAATACGGCAAAACGGACAGTCTCTATCCGAAAGATCTCCTCCAG
CGTGCTGTCGTGGATCAGCGATTGCATTTCGAGTCCGGAGTGATCTTCGCTAATGC
ACTGAGAAGCATTACCAAGCCACTTTTCGCCGGTAAGCAAACGATGATTCCCAAG
GAGCGTTACGATGCGATTATTGAGGTCTATGACTTCCTGGAGAAATTCCTTGCTGG
AAATGACTACGTCGCCGGCAATCAGCTTACGATTGCCGACTTTAGTATCATATCAA
CTGTGTCCTCGTTGGAGGTCTTCGTAAAGGTGGACACGACCAAATATCCTCGGATA
GCTGCATGGTTCAAGAGACTCCAAAAGCTGCCCTACTACGAGGAGGCCAACGGCA
ATGGTGCTCGTACATTTGAGTCCTTCATCAGAGAGTA**TAATTTCACTTTCGCATC
GAAT**TAA 3'

5'-ATT CGA TGC GAA AGT GAA ATT A- 3'

5' CCG CTCGAG **tta**attcgatgcgaaagt 3'

Figure 4.2: Amino acids of protein and gene sequence of *gste7* aligned with forward and reverse primers of TOPO cloning and restriction enzyme cloning respectively

4.2.1 PCR Gel Image for TOPO Cloning

Figure 4.3 above shows the gel image of amplified *gste*6 gene, a single band in between 500 bp and 750 bp (lane 3) whereas no band was observed on lane 2 which was the negative control where everything added was similar except template was replaced with distilled water.

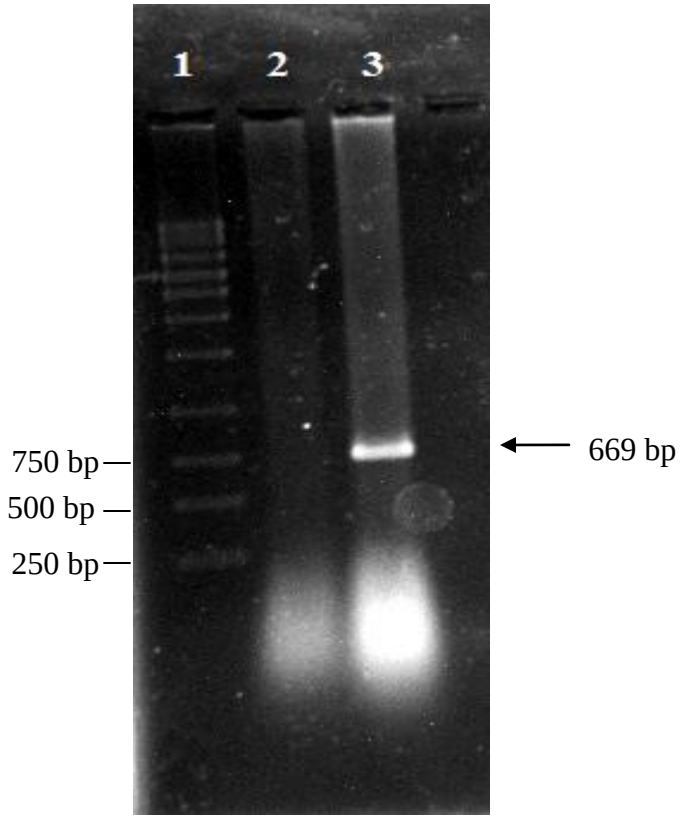

Figure 4.3: The *gste*6 amplicon image on 1% (w/v) agarose gel electrophoresis. Lane 1: 1 kb DNA ladder; Lane 2: Control with distilled water and Lane 3: PCR product of *gste*6

Figure 4.4 above shows the gel image of amplified *gste*7 gene, a single band in between 500 bp and 750 bp (lane 3) whereas no band was observed on lane 2 which was the negative control where everything added was similar except template was replaced with distilled water.

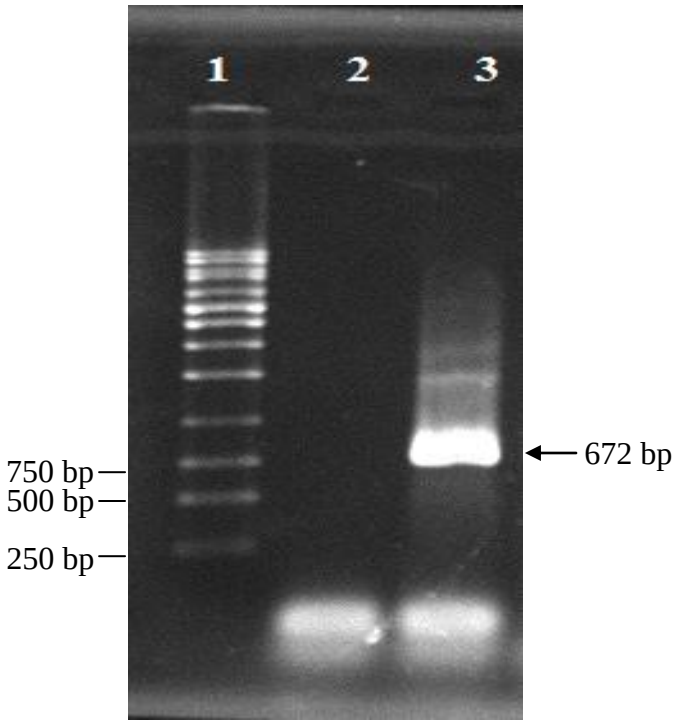

Figure 4.4: The *gste*7 amplicon image on 1% (w/v) agarose gel electrophoresis. Lane 1: 1 kb DNA ladder; Lane 2: Control with distilled water and Lane 3: PCR product of *gste7*

4.2.2 PCR Gel Image for Restriction Enzyme Cloning

Figure 4.5 above shows the gel image of amplified *gste*6 and *gste*7 gene, a single band in between 500 bp and 750 bp (lane 2 and lane 3) whereas no band was observed on lane 4 and lane 5 which was the negative control where everything added was similar except template was replaced with nucleases free water.

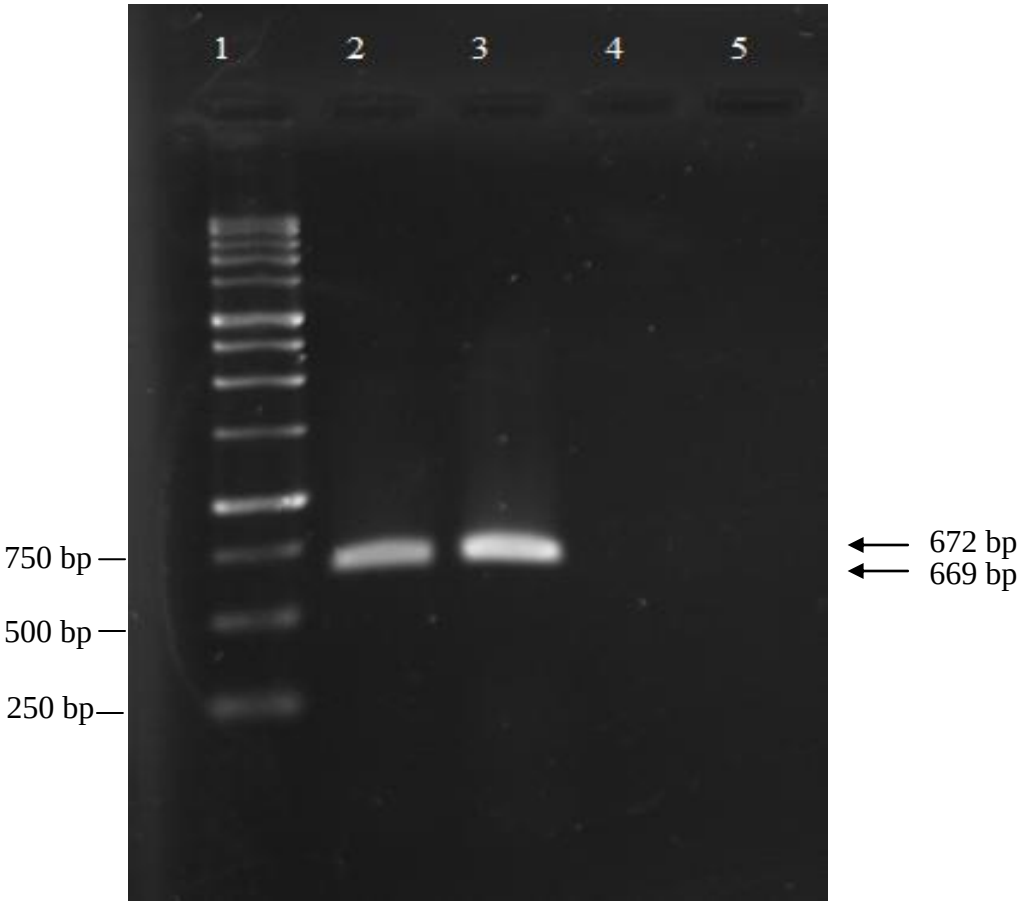

Figure 4.5: The *gste*6 and *gste*7 amplicon image on 1% (w/v) agarose gel electrophoresis. Lane 1: 1 kb DNA ladder; Lane 2: PCR product of *gste*6; Lane 3: PCR product of *gste*7; Lane 4: Control of *gste*6 with nucleases free water and Lane 5: Control of *gste*7 with nucleases free water

4.3 Cloning of the PCR product

4.3.1 TOPO Cloning

pBAD/TOPO® ThioFusion™ Expression Kit (Invitrogen) was used as it provides a highly efficient, 5-minute, one-step cloning strategy ("TOPO® Cloning") for the direct insertion of Taq polymerase-amplified PCR products into a plasmid vector for soluble and simplified protein purification in *E.coli*. Taq polymerase which has a non-template-dependent terminal transferase activity adds a single deoxyadenosine (A) to the 3´ ends of PCR products. The linearized vector supplied in the kit has single; overhanging 3´ deoxythymidine (T) residues therefore allows PCR inserts to ligate efficiently with the vector. Figure 3.1 shows the features of pBAD/Thio-TOPO® and the point of insertion of the PCR product.

4.3.1.1 Positive Clone Analysis

The positive clone analysis for *gste*6 done using Trx Forward and pBAD Reverse sequencing primers as PCR primers resulting in either with absence of bands or bands at incorrect size (gel image not shown), therefore clones that give positive results from plasmid purification analysis and PCR analyzed using the purified plasmid as template was sent out for full sequencing.

4.3.1.2 Plasmid Purification of *gste6*

Figure 4.6 shows 7 random colonies were picked from the transformation plate of *gste*6 gene. The clones were cultured in LB broth containing 100 µg/mL ampicillin at final concentration. Plasmid was purified from all 7 cultures and was loaded into 1% (w/v) agarose gel. Figure shows the gel image of purified plasmids from 7 random colonies, only clones at lane 4, 5 and 8 at expected correct size where the band was in the range of 5000 bp to 6000 bp. The size of a ligated plasmid was expected at the range of 6000 bp.

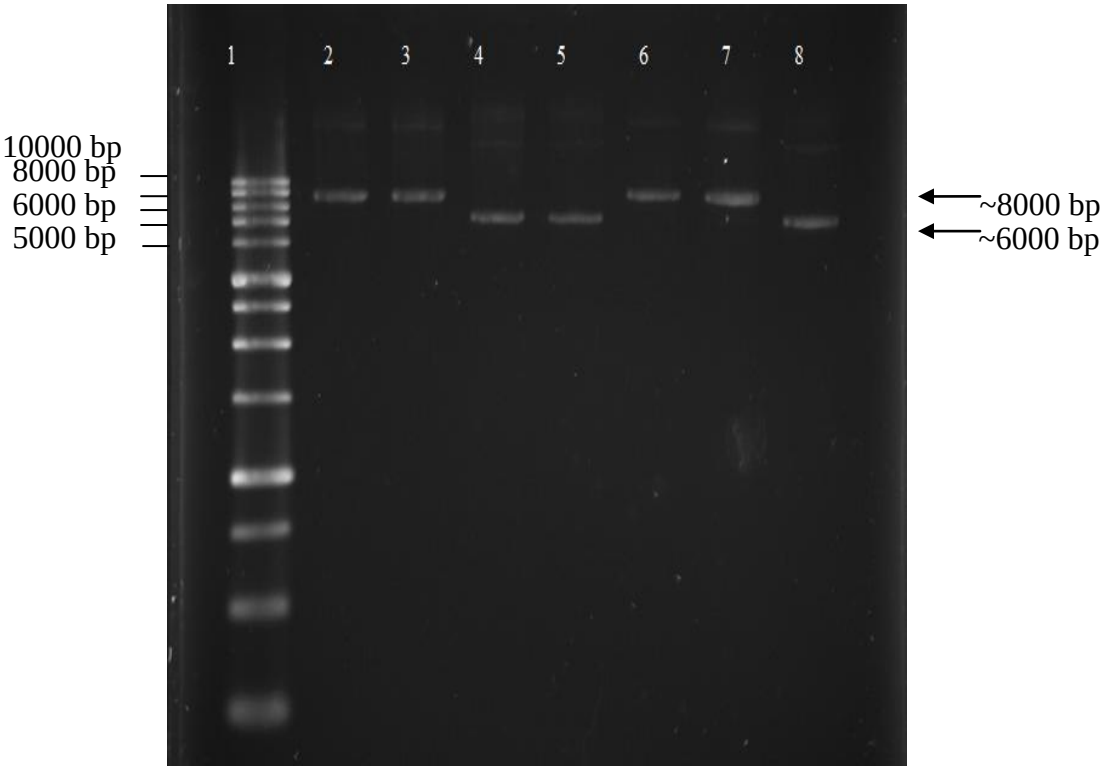

Figure 4.6: Purified plasmids of *gste*6 from 7 random colonies image on 1% (w/v) agarose gel electrophoresis. Lane 1: 1 kb DNA ladder; Lane 2-8: Purified plasmid of *gste*6; Lane 2, 3, 6 and 7: Purified plasmid with insert at incorrect size (~8000 bp) and Lane 4, 5 and 8: Purified plasmid with insert at correct size (~6000 bp)

4.3.1.3 PCR using Plasmid as Template.

PCR was performed to further confirm that the ligated was correct for *gste*6. The purified plasmid with correct size was used as a template to perform PCR to reconfirm that the ligated product is *gste*6. It is then loaded on a 1% (w/v) agarose gel. Figure 4.7 shows 2 distinct bands only on lane 2 with upper band between the ranges of 5000 bp-6000 bp and lower band at between 500 bp -750 bp proved that the ligated product was *gste*6.

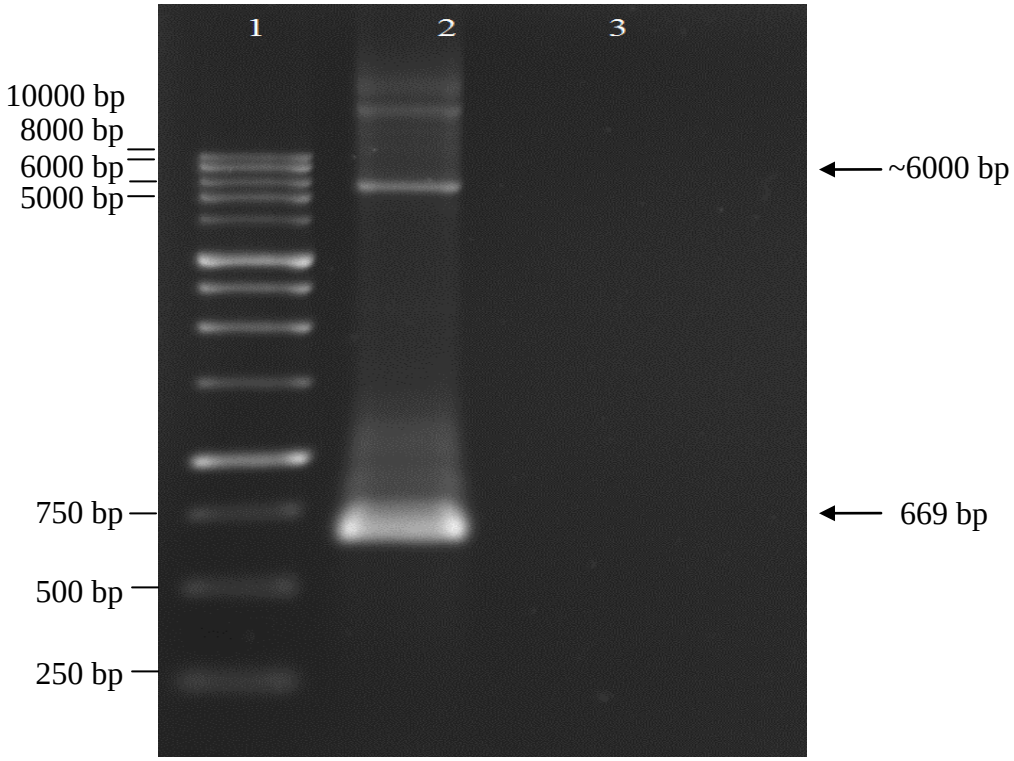

Figure 4.7: PCR performed using extracted *gste*6 plasmid as template image on 1% (w/v) agarose gel electrophoresis. Lane 1: 1 kb DNA ladder; Lane 2: PCR with plasmid DNA as template and Lane 3: PCR without template replaced with distilled water

4.3.1.4 Sequencing Results

The purified plasmids containing TOPO *gste*6 gene was sent for sequencing to First Base Laboratories for identification. Results obtained were analyzed using Basic Local Alignment Search Tool (BLAST) from http://blast.ncbi.nlm.nih.gov/. Figure 4.8 shows the BLAST search tool results that revealed only 75% similarity with the *Drosophila melanogaster* chromosome 2R, complete sequence which denotes the glutathione S-transferase, E6 (Figure 4.9). Thus, TOPO cloning method was not used to clone *gste7*.

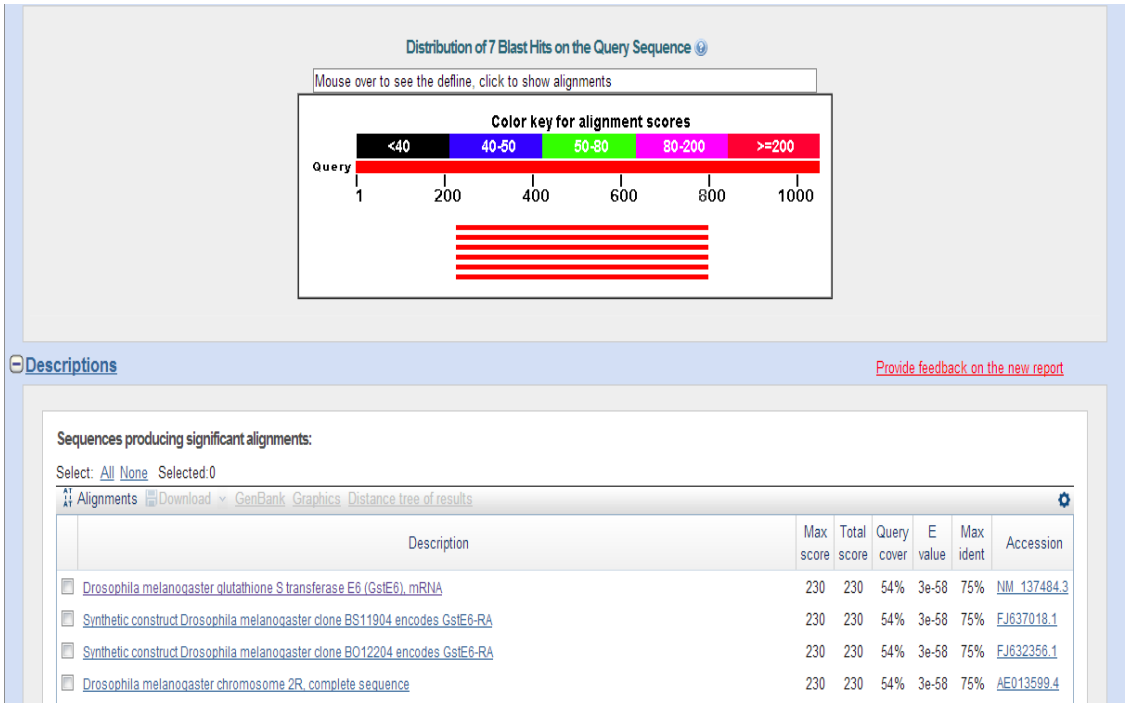

Figure 4.8: Blast search tool results of the recombinant *gste*6 (http://blast.ncbi.nlm.nih.gov/)

Figure 4.9: Expansion of Sequence ID: AE013599.4, featuring *gste6* (http://blast.ncbi.nlm.nih.gov/)

4.3.2 Restriction Enzyme Cloning

PCR product was extracted from the agarose gel and digested with *Nde1* and *EcoR1* for *gste*6 while with *Nde1* and *Xho1* for *gste*7. The list of cutters and non-cutters (restriction enzymes) for both *gste*6 and *gste*7 gene sequence was obtained from www.restrictionmapper.org. It was then matched with the cutters and non-cutters of pET-30a (+). The cloning vector used was pET-30a (+), and digested with the same restriction enzymes. The restriction sites for *Nde1*, *EcoR1* and *Xho1* were located at the multiple cloning sites of the pET-30a (+) plasmid DNA as shown in Figure 3.2.

4.3.2.1 PCR Products and pET-30a (+) Vector Enzyme Digestion

The purified PCR product of *gste*6, *gste*7 gene and pET-30a (+) vector was then subjected to double digest. *Nde1* and *EcoR1* for *gste*6 while with *Nde1* and *Xho1* for *gste*7. The digested product was loaded into 1% (w/v) agarose gel. Figure 4.10 shows the gel image of the digested product. There were 3 bands at lane 2, 3 and 4 at the range of 5000 bp-6000 bp in size which indicates the undigested and digested pET-30a (+) vector. Typically, uncut vector (supercoiled) will appear to migrate differently (in distance) in comparison to the same vector when linearized (digested). The band at lane 5 and 6 was noticed in between 700 bp and 1000 bp in size which was the digested *gste*6 and *gste*7 PCR product.

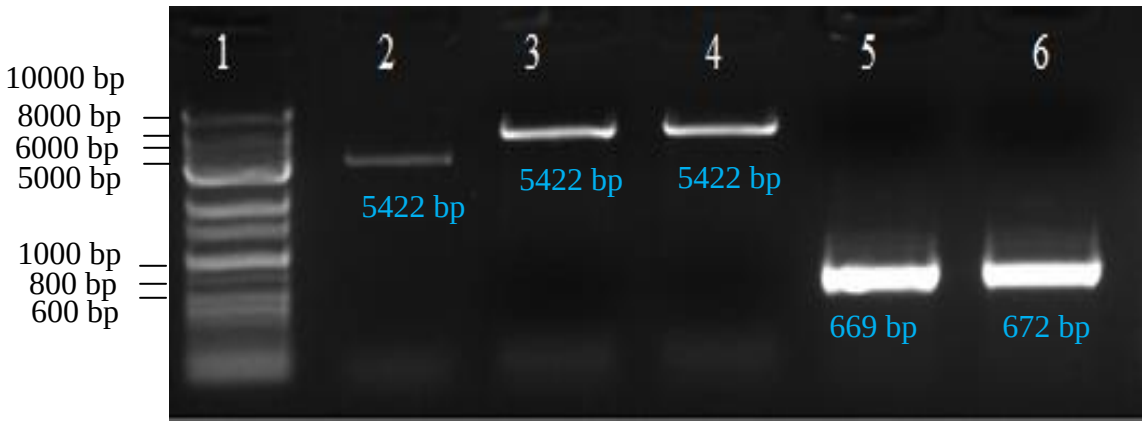

Figure 4.10: Digested and undigested pET-30a (+) vector and PCR products of *gste*6 and *gste*7 image on 1% (w/v) agarose gel electrophoresis. Lane 1: 1 kb DNA ladder; Lane 2: pET30a (+) uncut; Lane 3: pET30a (+) *EcoRI*, *NdeI* digestion; Lane 4: pET30a (+) *NdeI*, *XhoI* digestion; Lane 5: *gste*6 *EcoRI*, *NdeI* digestion and Lane 6: *gste*7 *NdeI*, *XhoI* digestion

4.3.2.2 Ligation and Transformation with *E.coli* BL21 (DE3) pLysS

Double digested with *Nde1* and *EcoR1* PCR product of *gste*6 and vector was ligated while double digested with *Nde1* and *Xho1* PCR product of *gste*7 and vector was ligated respectively. The ligation mixture was loaded into 1% (w/v) agarose gel to obtain purified ligated product. Gel image showed very faint band of ligated product respectively (gel image not shown), thus the ligation mixture was directly used for transformation with *E.coli* BL21 (DE3) pLysS on LB agar plate containing 30 µg/mL kanamycin.

4.3.2.3 Plasmid Purification

4.3.2.3.1 Plasmid Purification of *gste*6

Six random colonies were picked from the transformation plate of *gste*6 gene. The clones were cultured in LB broth containing 30 µg/mL kanamycin. Plasmid was purified from all 6 cultures and was loaded into 1% (w/v) agarose gel. Figure 4.11 shows the gel image of purified plasmids from 6 random colonies all at correct expected size where the band was in the range of 5000 bp to 6000 bp. The size of a ligated plasmid was expected at the range of 6000 bp.

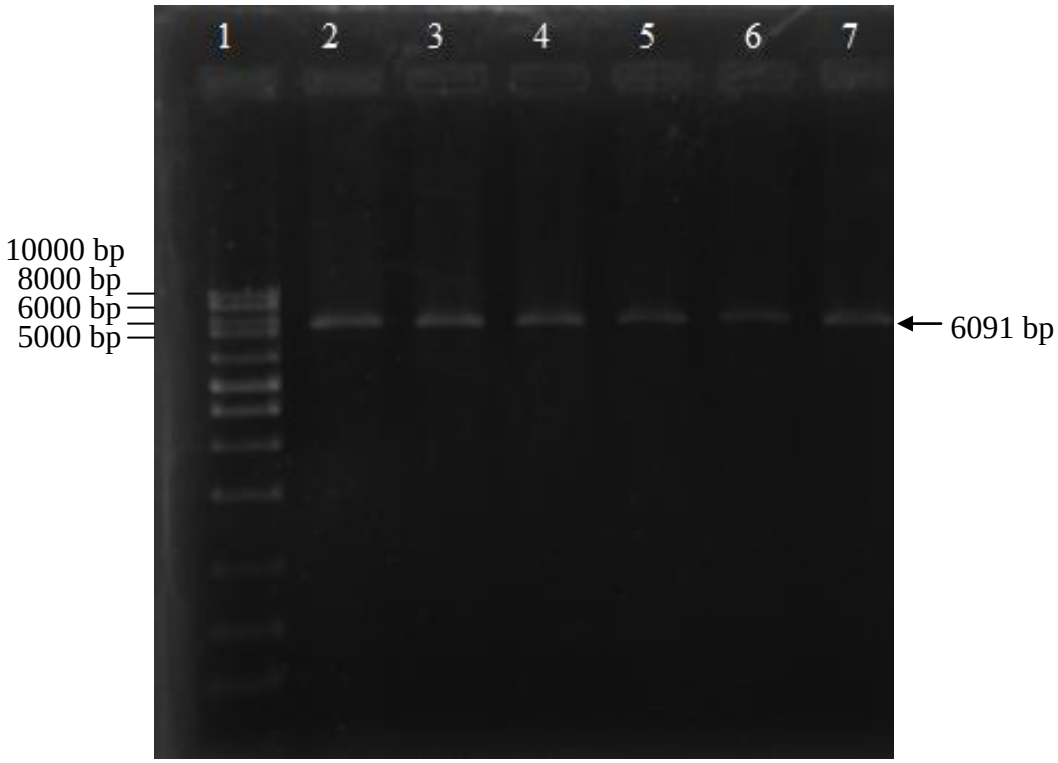

Figure 4.11: Purified plasmids of *gste*6 from 6 random colonies image on 1% agarose gel electrophoresis. Lane 1: 1 kb DNA ladder and Lane 2-7: Purified plasmid of *gste*6

4.3.2.3.2 Plasmid Purification of *gste*7

Six random colonies were picked from the transformation plate of *gste*7 gene. The clones were cultured in LB broth containing 30 µg/mL kanamycin. Plasmid was purified from all 7 cultures and was loaded into 1% (w/v) agarose gel. Figure 4.12 shows the gel image of purified plasmids from 7 random colonies all at correct expected size where the band was in the range of 5000 bp to 6000 bp. The size of a ligated plasmid was expected at the range of 6000 bp.

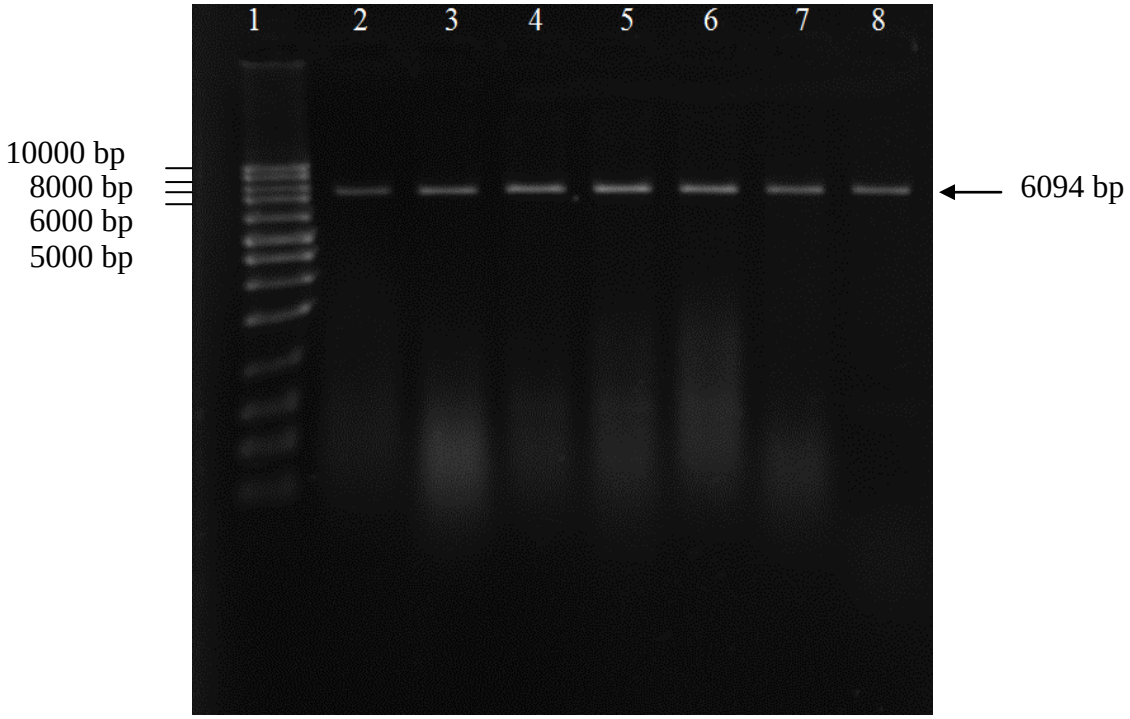

Figure 4.12: Purified plasmids of *gste*7 from 7 random colonies image on 1% (w/v) agarose gel electrophoresis. Lane 1: 1 kb DNA ladder and Lane 2-8: Purified plasmid of *gste*7

4.3.2.4 PCR using Plasmid as Template.

PCR was performed to further confirm that the ligation product was correct for *gste*6. The purified plasmid with correct size was used as a template to perform PCR to reconfirm that the ligated product is *gste*6. It is then loaded on 1% (w/v) agarose gel. Figure 4.13 shows bands on lane 2 between the ranges of 500 bp -750 bp proved that the ligated product was *gste*6.

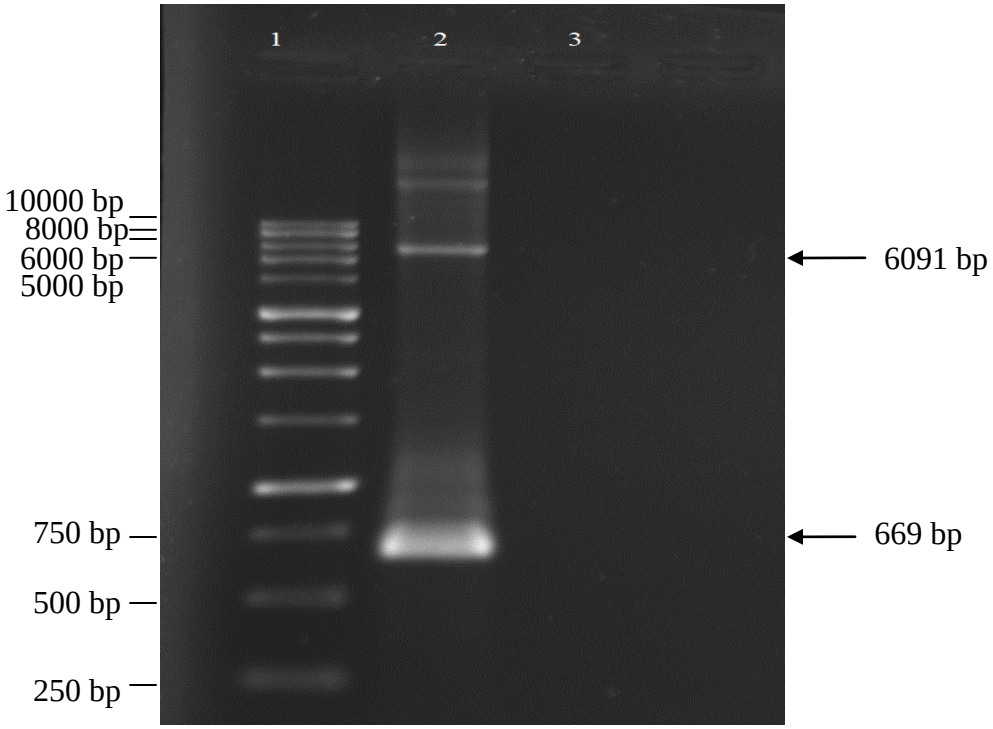

Figure 4.13: PCR performed using extracted *gste*6 plasmid as template image on 1% (w/v) agarose gel electrophoresis. Lane 1: 1 kb DNA ladder; Lane 2: PCR with plasmid DNA as template and Lane 3: PCR without template replaced with nuclease free water

PCR was performed to further confirm that the ligation product was correct for *gste*7. The purified plasmid with correct size was used as a template to perform PCR to reconfirm that the ligated product is *gste*7. It is then loaded on a 1% (w/v) agarose gel. Figure 4.14 shows 2 distinct bands on lane 2 with upper band between the ranges of 5000 bp- 6000 bp and lower band at between 500 bp -750 bp proved that the ligated product was *gste7*.

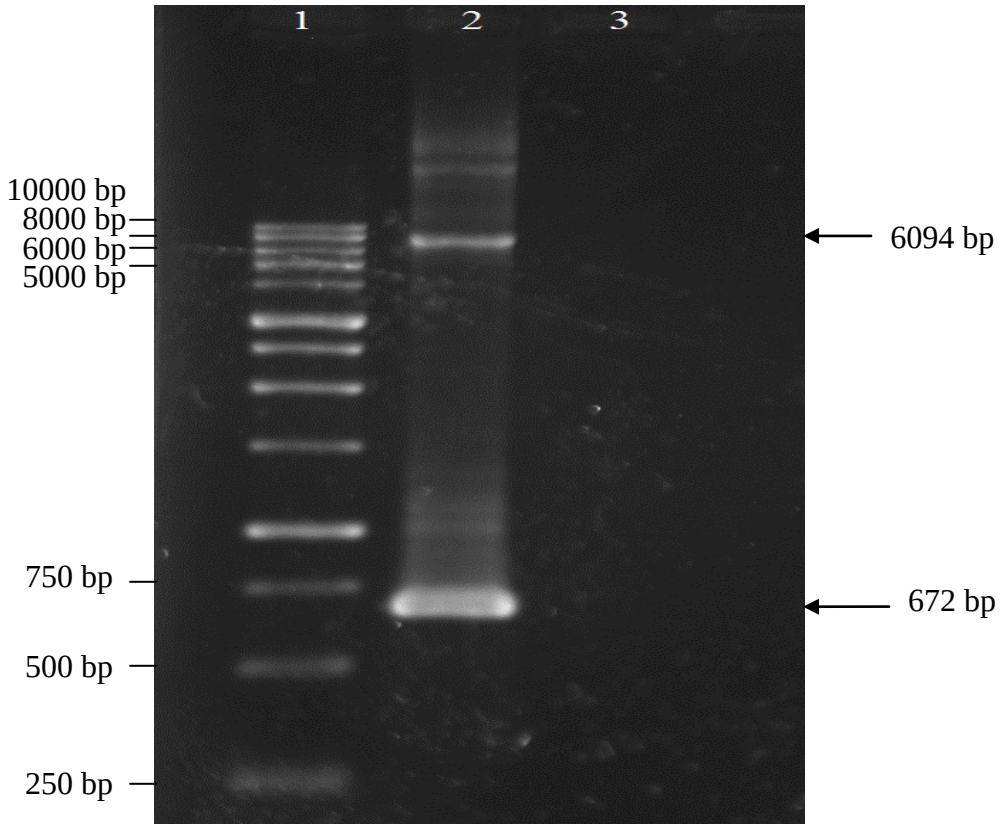

Figure 4.14: PCR performed using extracted *gste7* plasmid as template image on 1% (w/v) agarose gel electrophoresis. Lane 1: 1 kb DNA ladder; Lane 2: PCR with plasmid DNA as template and Lane 3: PCR without template replaced with nucleases free water

.

4.3.2.5 Sequencing Results

The purified plasmid containing *gste*6 and *gste*7 gene were sent for sequencing to COSMO GENETECH CO., LTD for full sequencing and identification. Results obtained were analyzed using Basic Local Alignment Search Tool (BLAST) from http://blast.ncbi.nlm.nih.gov/. Figure 4.15 and Figure 4.17 respectively shows the BLAST search tool results that revealed only 99% similarity with the *Drosophila melanogaster* chromosome 2R, complete sequence which denotes the glutathione S-transferase, E6 and E7 respectively (Figure 4.16 and Figure 4.18).

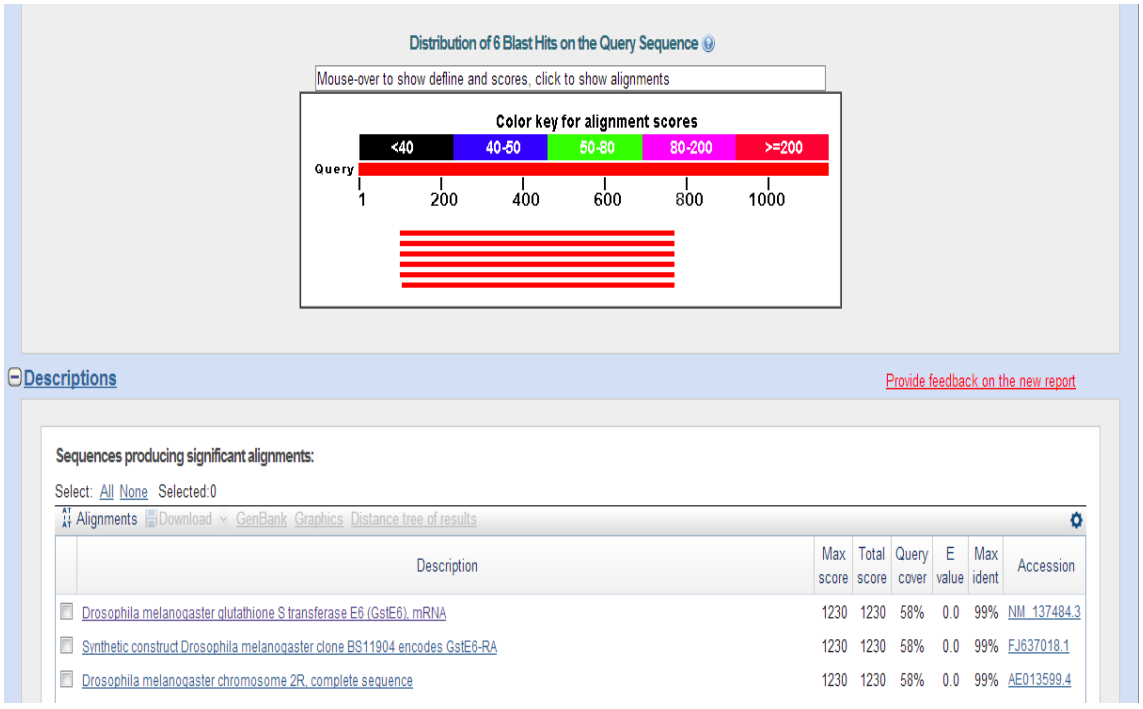

Figure 4.15: Blast search tool results of the recombinant *gste*6 (http://blast.ncbi.nlm.nih.gov/)

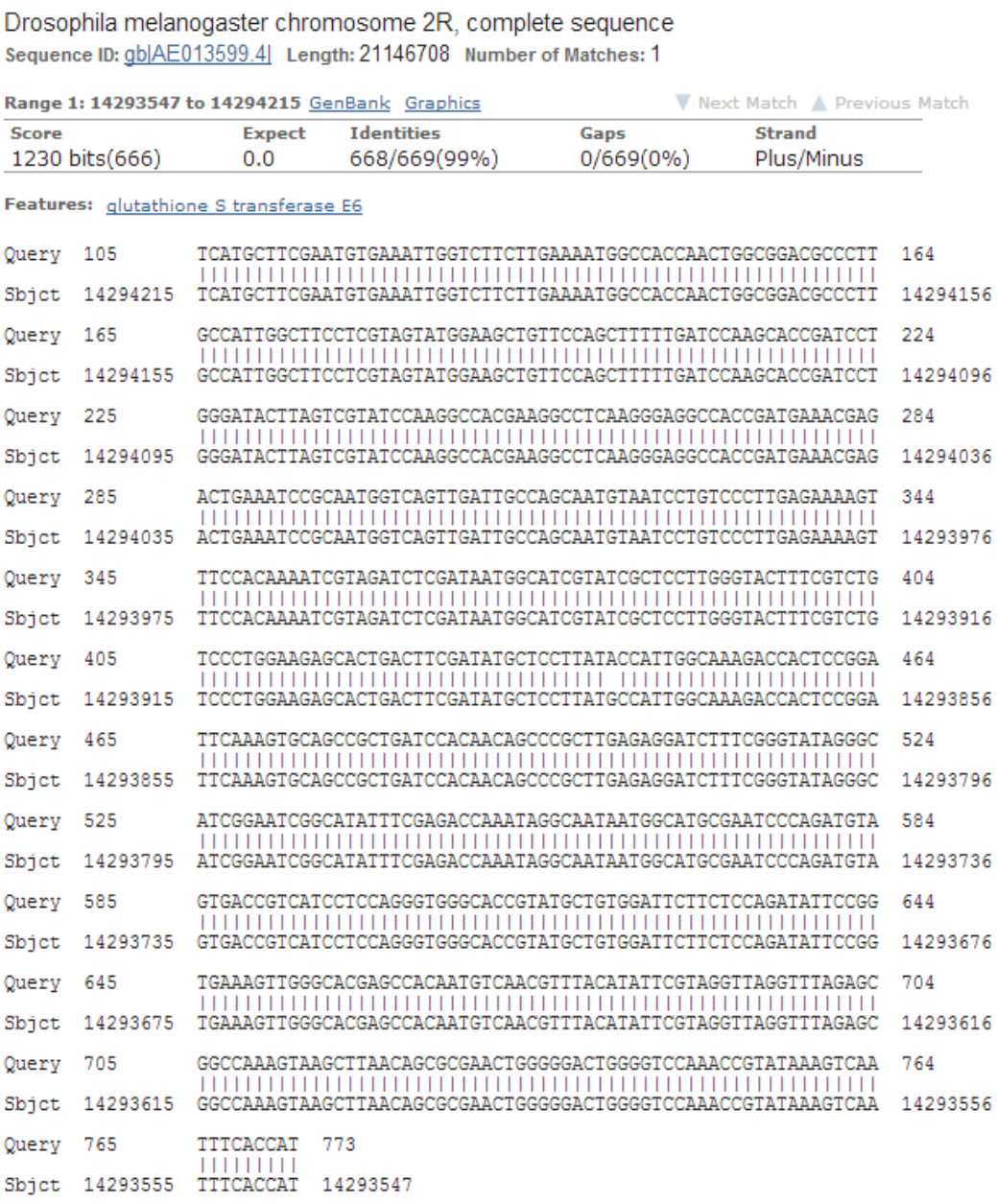

Figure 4.16: Expansion of Sequence ID: AE013599.4, featuring *gste*6 http://blast.ncbi.nlm.nih.gov/)

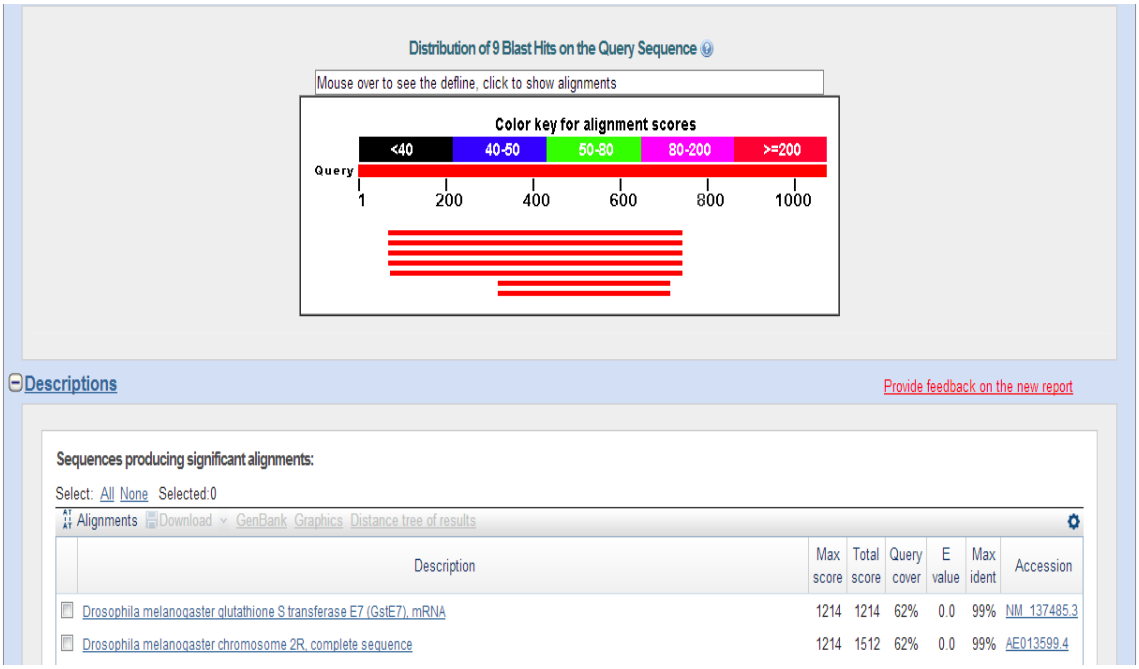

Figure 4.17: Blast search tool results of the recombinant *gste7* http://blast.ncbi.nlm.nih.gov/)

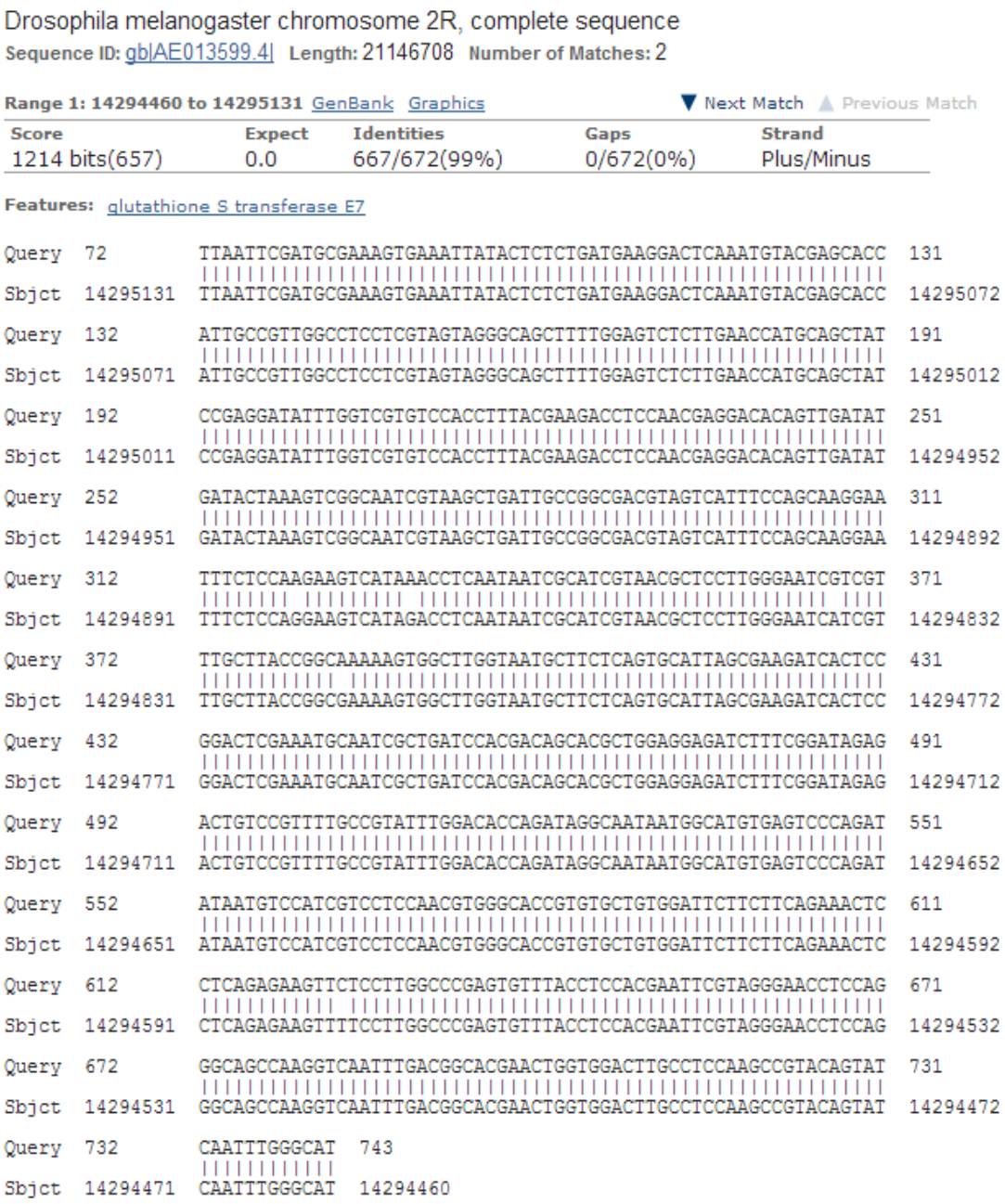

Figure 4.18: Expansion of Sequence ID: AE013599.4, featuring *gste*7 http://blast.ncbi.nlm.nih.gov/)

4.3.2.6 Silent Mutation on Extracted Genome

The PCR products of *gste*6 and *gste*7 amplified was sequenced. The results showed there was silent mutation on base at position 439 in *gste*6 gene resulted change of the amino acid sequence of a protein from GGC to GGT which both encodes for glycine (Figure 4.19).

Silent mutation at position 223,463,481,517 and 527 in *gste*7 gene which all resulted changes of the amino acid sequence of a protein but do not result in radically different properties of the changed amino acids. Silent mutation at position 223 resulted change in amino acid sequence from GAA to GAG which both encodes for glutamic acid. Silent mutation at position 463 resulted change in amino acid sequence from TTC to TTT which both encodes for phenylalanine. Silent mutation at position 481 resulted change in amino acid sequence from ACC to ACG which both encodes for threonine. Silent mutation at position 517 resulted change in amino acid sequence from GTC to GTT which both encodes valine and finally silent mutation at position 527 resulted changes in amino acid sequence from CTG to TTG which both encodes leucine (Figure 4.20).

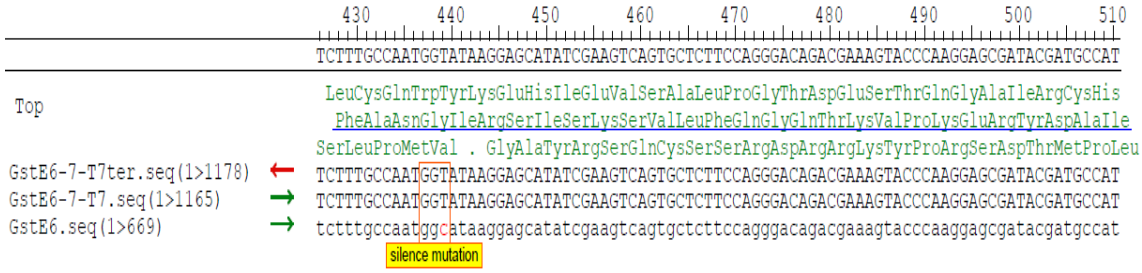

Figure 4.19: Silent mutation on bases at position 439 of *gste*6 gene

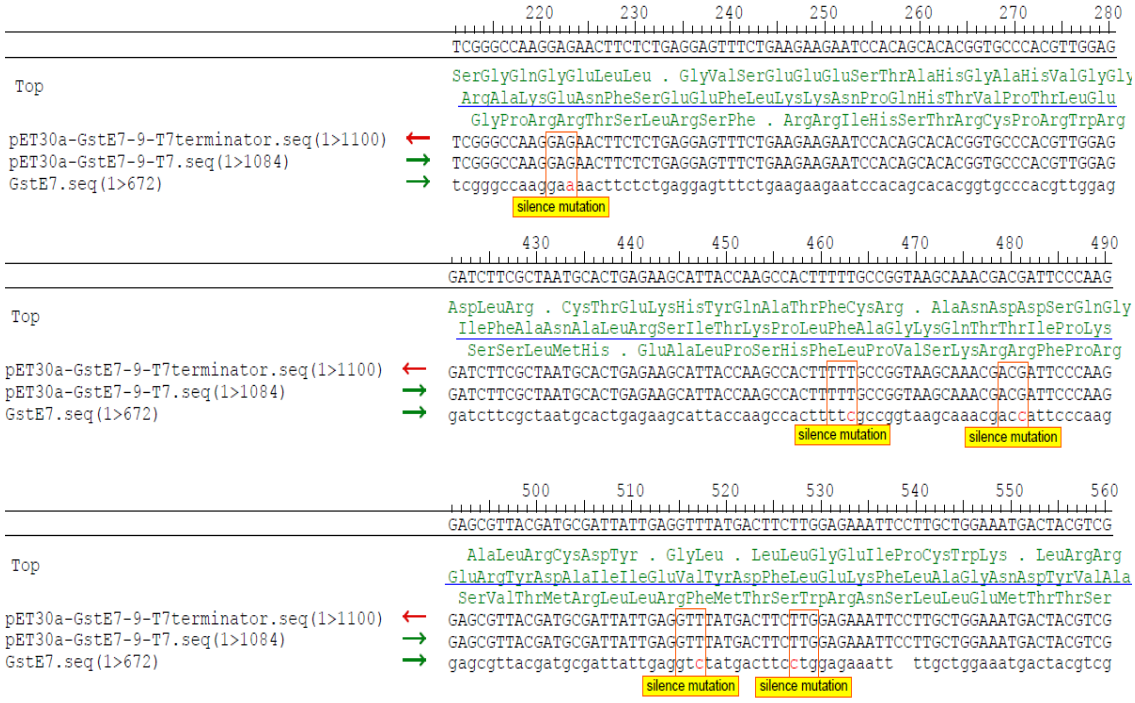

Figure 4.20: Silent mutation on bases at position 223, 463, 481, 517 and 527 of *gste*7 gene

4.4 Purification of Recombinant Enzyme

The recombinant GSTE6 and GSTE7 proteins were purified using multiple matrices. A total of three columns were used in order to purify GSTE6 GST and GSTE7 GST respectively. Eluted protein was concentrated using Vivaspin 20: MW10000 (Sartorius stedim) at 6000 rpm for 15-30 minutes depending on the volume and purity of the protein and was analyzed on 12% (w/v) SDS-PAGE stained with Coomasie Brilliant Blue G250.

4.4.1 Purification of Recombinant of GSTE6

4.4.1.1 GSTrap™ HP with 10 mM GSH at pH 7.4

Figure 4.21 shows the SDS-Page gel image purified using GSTrap™ HP. The protein was eluted with 10 mM of reduced glutathione (GSH) in phosphate buffer at pH 7.4. Purification resulted in some amount of desired protein was eluted out as unbound protein (lane 3 and lane 4). The unbound protein had high level of activity against CDNB. The bound protein was eluted out with 100% of 10 mM GSH. The concentrated protein sample resulted in 2 lighter bands at lane 5 and shows little activity against CDNB.

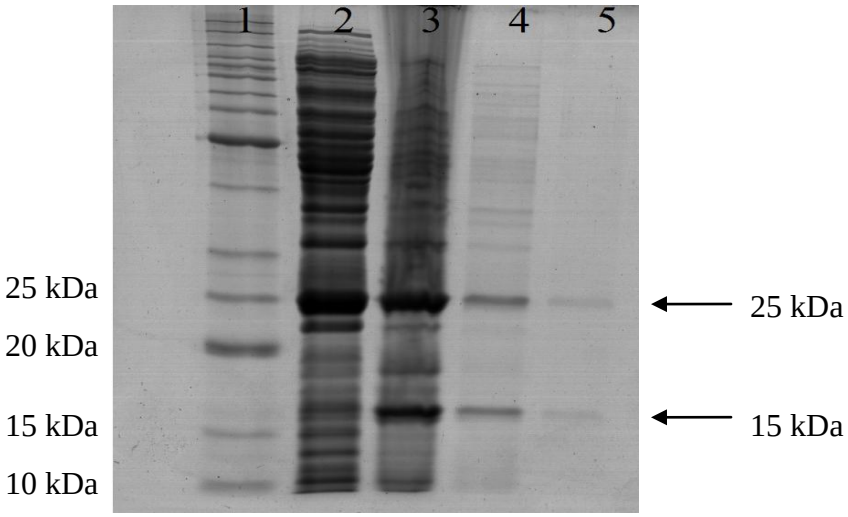

Figure 4.21: SDS-PAGE of purification of GSTE6 using Glutathione Sepharose. Lane 1: Protein Ladder; Lane 2: Bacteria crude lysate; Lane 3: First 10 mL Flow through fraction (void); Lane 4: Second 10 mL Flow through fraction (void) and Lane 4: Elution with 10 mM GSH at pH 7.4

4.4.1.2 HiTrap Q HP™ with 1 M NaCl at pH 7.4

Figure 4.22 shows the SDS-Page gel image purified using HiTrap Q Sepharose matrix. The protein was eluted with 1 mM of sodium chloride salt at pH 7.4. Purification resulted in larger amount of desired protein was eluted out as unbound protein at lane 3. The unbound protein had high level of activity against CDNB. The bound protein was eluted out with 100% of 1 mM sodium chloride salt. The concentrated protein sample resulted in multiple non-specific bands at lane 4 and shows little activity against CDNB.

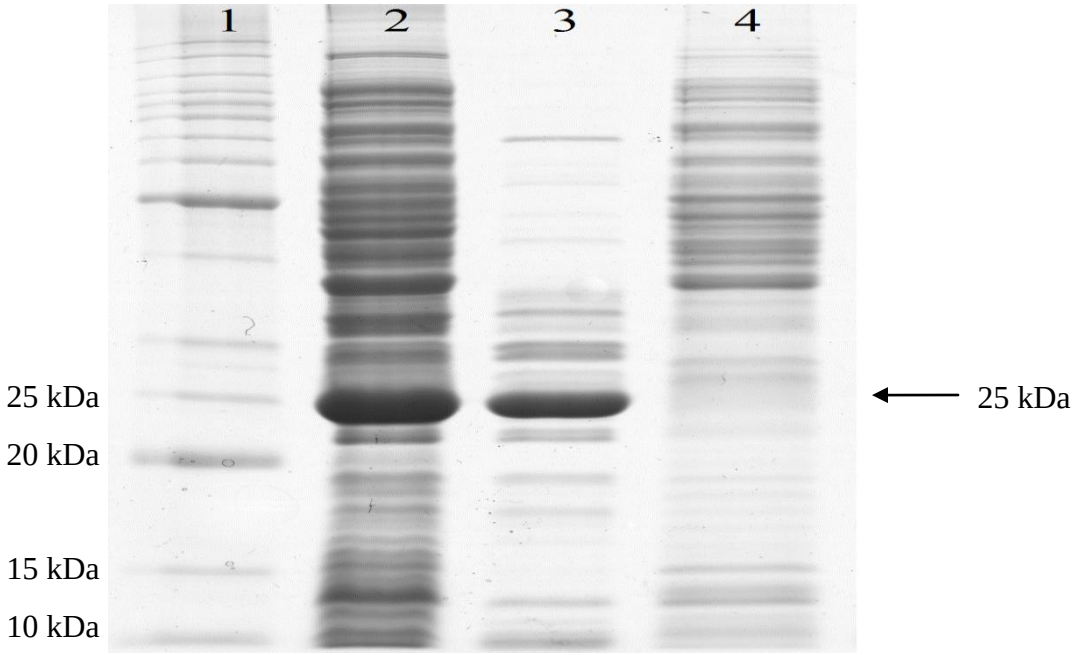

Figure 4.22: SDS-PAGE of purification of GSTE6 using Q Sepharose. Lane 1: Protein Ladder; Lane 2: Bacteria crude lysate; Lane 3: Flow through fraction (void) and Lane 4: Elution with 1 M NaCl at pH 7.4

4.4.1.3 HiTrap™ Q HP followed by BSP-SG with 2 mM BSP at pH 7.4

Figure 4.23 shows the SDS-Page gel image purified using HiTrap Q Sepharose matrix followed by Bromosulfophthalein-GSH matrix. The unbound protein eluted out from HiTrap Q Sepharose matrix (lane 3) was subjected to purification using Bromosulfophthalein-GSH matrix. The flow through from HiTrap Q Sepharose matrix was injected into the Bromosulfophthalein-GSH matrix. The column was washed with 1 M of sodium chloride, pH 7.4 to remove any non-specific protein binding (lane 6). The desired protein was eluted with 2 mM BSP in phosphate buffer at pH 7.4. The concentrated protein sample resulted in one prominent thick band at approximately 25 kDa with few non-specific bands at lane 7 and shows high activity against CDNB.

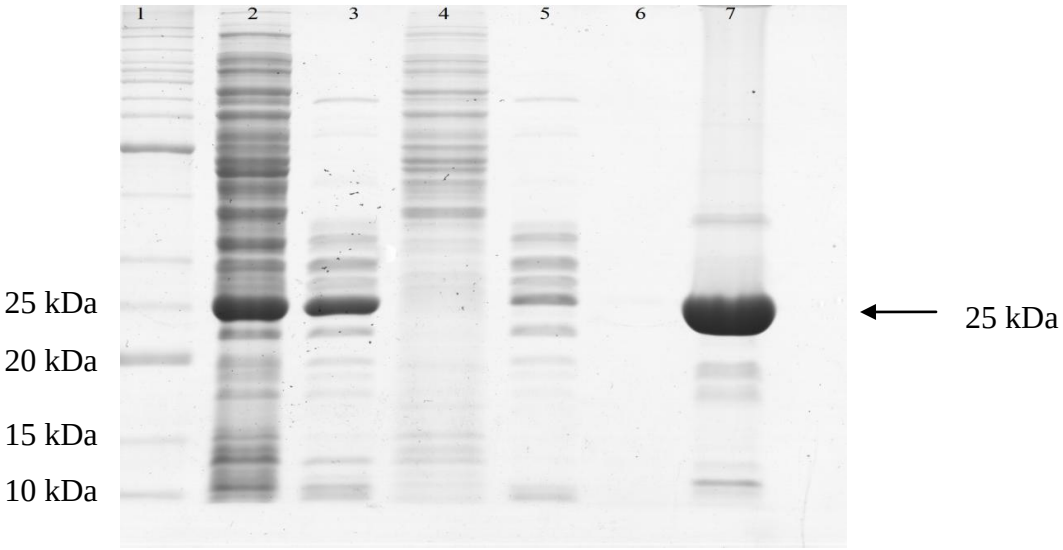

Figure 4.23: SDS-PAGE of purification of GSTE6 using BSP-SG. Lane 1: Protein Ladder; Lane 2: Bacteria crude lysate; Lane 3: Flow through fraction of HiTrap™ Q HP (void); Lane 4: Elution with 1 M NaCl at pH 7.4; Lane 5: Flow through fraction of BSP-SG (void); Lane 6: Washing with 1 M NaCl at pH 7.4 and Lane 7: Elution with 2 mM BSP at pH 7.4

4.4.2 Purification of Recombinant of GSTE7

4.4.2.1 HiTrap Q HP™ with 1 M NaCl at pH 7.4

Figure 4.24 shows the SDS-Page gel image purified using HiTrap Q Sepharose matrix. The protein was eluted with 1 M of sodium chloride salt at pH 7.4. Purification resulted in larger amount of desired protein was eluted out as unbound protein at lane 3. The unbound protein had high level of activity against CDNB. The bound protein was eluted out with 100% of 1 M sodium chloride salt. The concentrated protein sample resulted in multiple non-specific bands at lane 4 and shows little activity against CDNB.

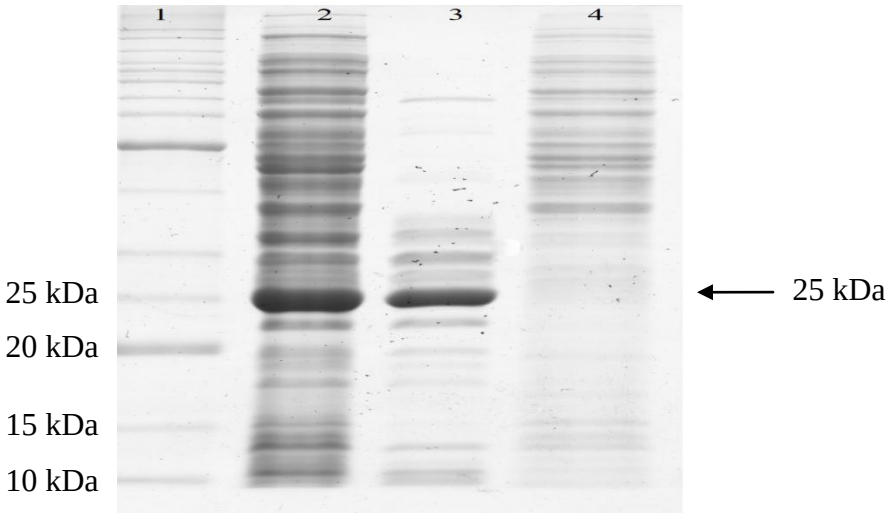

Figure 4.24: SDS-PAGE of purification of GSTE7 using Q Sepharose. Lane 1: Protein Ladder; Lane 2: Bacteria crude lysate; Lane 3: Flow through fraction (void) and Lane 4: Elution with 1 M NaCl at pH 7.4

4.4.2.2 HiTrap™ CM FF with 1 M NaCl at pH 7.4

Figure 4.25 shows the SDS-Page gel image purified using HiTrap CM Sepharose matrix. The protein was eluted with 1 mM of sodium chloride salt at pH 7.4. Purification resulted in larger amount of desired protein was eluted out as unbound protein at lane 3. The unbound protein had high level of activity against CDNB. The bound protein was eluted out with 100% of 1 M sodium chloride salt. The concentrated protein sample resulted in no bands at lane 4 and no activity was detected against CDNB.

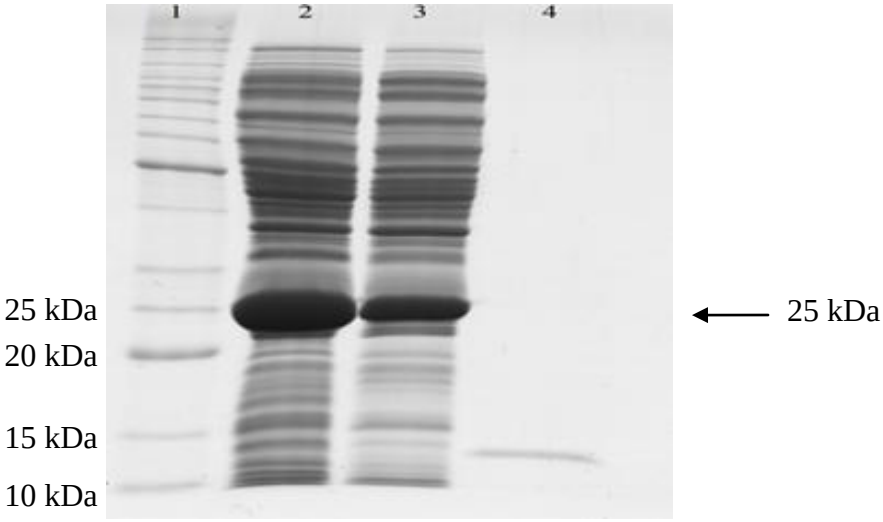

Figure 4.25: SDS-PAGE of purification of GSTE7 using CM Sepharose. Lane 1: Protein Ladder; Lane 2: Bacteria crude lysate; Lane 3: Flow through fraction (void) and Lane 4: Elution with 1 M NaCl at pH 7.4

4.4.2.3 HiTrap™ Q HP followed by BSP-SG with 2 mM BSP at pH 7.4

Figure 4.26 shows the SDS-Page gel image purified using HiTrap Q Sepharose matrix followed by Bromosulfophthalein-GSH matrix. The unbound protein eluted out from HiTrap Q Sepharose matrix (lane 3) was subjected to purification using Bromosulfophthalein-GSH matrix. The flow through from HiTrap Q Sepharose matrix was injected into the Bromosulfophthalein-GSH matrix. The column was washed with 1 M of sodium chloride, pH 7.4 to remove any non-specific protein binding (lane 6). The desired protein was eluted with 2 mM BSP in phosphate buffer at pH 7.4. The concentrated protein sample resulted in one prominent thick band at approximately 25 kDa with few non-specific bands at lane 7 and shows high activity against CDNB.

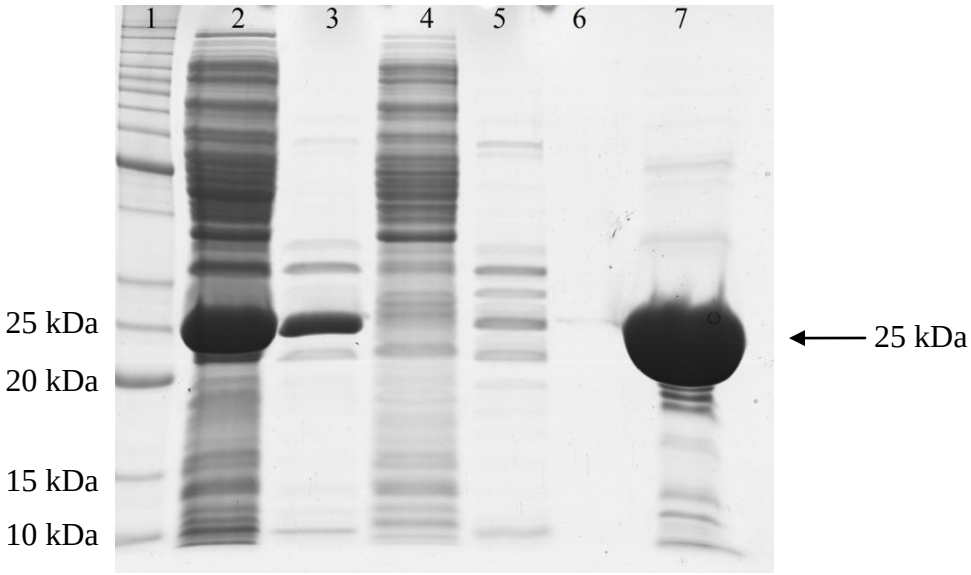

Figure 4.26: SDS-PAGE of purification of GSTE7 using BSP-SG. Lane 1: Protein Ladder; Lane 2: Bacteria crude lysate; Lane 3: Flow through fraction of HiTrap™ Q HP (void); Lane 4: Elution with 1 M NaCl at pH 7.4; Lane 5: Flow through fraction of BSP-SG (void); Lane 6: Washing with 1 M NaCl at pH 7.4 and Lane 7: Elution with 2 mM BSP at pH 7.4

4.4.2.4 Optimized HiTrap™ Q HP followed by BSP-SG with 2 mM BSP at pH 7.4

Figure 4.27 shows the optimized SDS-Page gel image of GSTE6 and GSTE7 purified using HiTrap Q Sepharose matrix followed by Bromosulfophthalein-GSH matrix. The unbound protein eluted out from HiTrap Q Sepharose matrix was subjected to purification using Bromosulfophthalein-GSH matrix. The flow through from HiTrap Q Sepharose matrix was injected into the Bromosulfophthalein-GSH matrix. The column was washed with 1 M of sodium chloride at pH 7.4 to remove any non-specific protein binding. The desired protein was eluted with 2 mM BSP in phosphate buffer at pH 7.4. An example of the purification spectrum using Bromosulfophthalein-GSH matrix showed in Appendix E. The eluted sample was concentrated with using Vivaspin 20: MW10000. The concentrated sample was diluted 1:4 with sample buffer. The gel image shows distinct band at lane 2 and lane 3 at approximately 25 kDa.

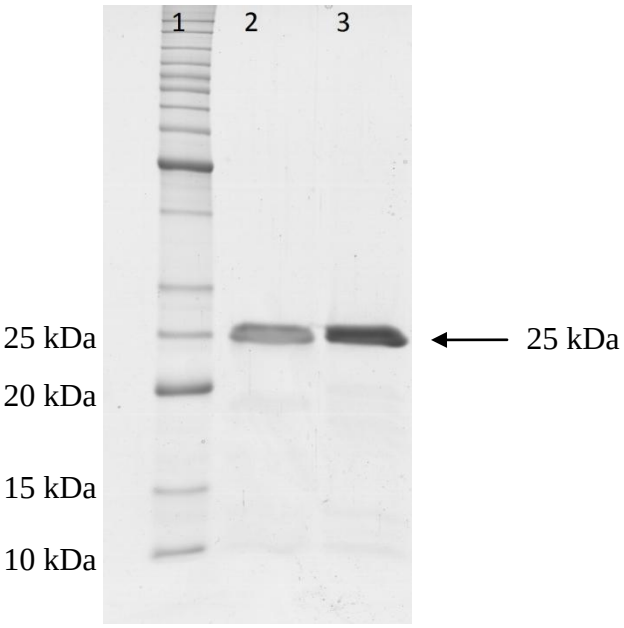

Figure 4.27: Optimized SDS-PAGE of purification of GSTE6 and GSTE7 using BSP-SG. Lane 1: Protein Ladder; Lane 2: Diluted elution of purified GSTE6 with 2 mM BSP at pH 7.4 and Lane 3: Diluted elution of purified GSTE7 with 2 mM BSP at pH 7.4.

4.5 Substrate Specificities

The purified recombinant protein of GSTE6 and GSTE7 respectively was used to determine the substrate specificities against substrates as listed in the Table 4.1 below. The results data shows both recombinant proteins active towards CDNB, DCNB and *p*-NBC only. No activity was detected against *trans*-Hex-2-enal, Hexa-2,4-dienal, *trans*-Oct-2-enal, *trans*-4-Phenyl-butene-2-one,trans, *trans*,*trans*-Hepta-2,4-dienal, Ethacrynic acid, bromosulfophthalein, cumene hydroperoxide and hydrogen peroxide. For recombinant protein of GSTE6, CDNB (80.67±4.43 nmol/mL/mg) was the best substrate followed by DCNB (18.11±1.04 nmol/mL/mg) and finally *p*-NBC (3.67±0.58 nmol/mL/mg) but as for the recombinant protein of GSTE7 CDNB (740.33±15.04 nmol/mL/mg) was the best substrate followed by *p*-NBC (249.67±9.61 nmol/mL/mg) and lastly DCNB (37.05±2.11 nmol/mL/mg).

Table 4.1: Substrates specificity of recombinant GSTE6 and GSTE7

Substrates	Specific activity (nmol/mL/mg)	
	GSTE6	GSTE7
1-Chloro-2, 4-dinitrobenzene (CDNB)	80.67±4.43	740.33±15.04
1, 2-Dichloro-4-nitrobenzene (DCNB)	18.11±1.04	37.05±2.11
trans-Hex-2-enal	ND	ND
Hexa-2, 4-dienal	ND	ND
trans-Oct-2-enal	ND	ND
trans-4-Phenyl-butene-2-one	ND	ND
trans, trans-Hepta-2, 4-dienal	ND	ND
Ethacrynic acid	ND	ND
p-Nitrobenzyl chloride (*p*-NBC)	3.67±0.58	249.67±9.61
Bromosulfophthalein (BSP)	ND	ND
Cumene hydrogen peroxide	ND	ND
Hydrogen peroxide	ND	ND

Means±SD of three experiments, each with triplicate determinations. *ND denotes not detected.

4.6 Kinetic Parameters of GSTE6 and GSTE7

To measure the activity of recombinant protein of GSTE6 and GSTE7 respectively, CDNB, DCNB and *p*-NBC was used as a substrate. The conversion of CDNB, DCNB and *p*-NBC to glutathione substrate conjugate was measured according to 3.2.13.1, 3.2.13.2 and 3.2.13.3 respectively. Different substrate range was used for each substrate accordingly for kinetic analysis. Michaelis-Menten kinetic analysis was then used to determine the affinity of the substrate (K_m) and the catalytic rate ($K_{cat)}$ for each recombinant protein. The plot was formed using the Michaelis-Menten rate equation. It shows the quantitative relationship between the initial velocity (V_0), the maximum velocity (V_{max}), and the initial substrate concentration [S]. All these points are related through Michaelis constant K_m, which is equal to V_0= ½ V_{max}. A large K_m means that a high concentration of substrate was needed to achieve V_{max} and a small one required a small amount of substrate and it has high affinity for the substrate (strong binding). K_{cat} is the maximum number of substrate molecules converted to product on a single enzyme molecule per second ("turnover number"). The K_{cat}/ K_m ratio describes the overall enzyme efficiency. High K_{cat}/ K_m ratio indicates that the product turnover rate is higher than the substrate concentration, which means it is an efficient enzyme. Some of the Michaelis Menten plot generated using GraphPad Prism showed Appendix F.

Recombinant GSTE6 enzyme had a V_{max} = 0.52±0.024 nmol/min, K_m = 0.024±0.001 mM, K_{cat} = 0.13 min^{-1} and K_{cat}/ K_m = 5.25 $min^{-1}mM^{-1}$ for CDNB. For DCNB, it had a V_{max} = 0.029±0.008 nmol/min, K_m = 0.17±0.001 mM, K_{cat} = 0.007 min^{-1} and K_{cat}/ K_m = 0.042 $min^{-1}mM^{-1}$. As for *p*-NBC the enzyme had V_{max} = 0.21±0.013 nmol/min, K_m = 0.28±0.005 mM, K_{cat} = 0.051 min^{-1} and K_{cat}/ K_m = 0.18 $min^{-1}mM^{-1}$.

Recombinant GSTE7 enzyme had a V_{max} = 0.83±0.028 nmol/min, K_m = 0.14±0.009 mM, K_{cat} = 0.086 min^{-1} and K_{cat}/ K_m = 0.62 $min^{-1}mM^{-1}$ for CDNB. For DCNB, it had a V_{max} = 0.30±0.033 nmol/min, K_m = 0.42±0.002 mM, K_{cat} = 0.043 min^{-1} and K_{cat}/ K_m = 0.10 $min^{-1}mM^{-1}$. As for *p*-NBC the enzyme had V_{max} = 1.31±0.051 nmol/min, K_m = 0.060±0.002 mM, K_{cat} = 0.14 min^{-1} and K_{cat}/ K_m = 2.25 $min^{-1}mM^{-1}$.

The comparison of the initial-rate enzyme kinetics between GSTE6 and GSTE7 enzyme for CDNB showed that GSTE6 have enzyme higher affinity, catalytic efficiency and catalytic rate. As for DCNB, GSTE7 has higher catalytic rate and catalytic efficiency with similar enzyme affinity. Finally for *p*-NBC, GSTE7 has higher enzyme affinity, catalytic rate and catalytic efficiency compared to GSTE6.

Table 4.2: Kinetics parameters of recombinant GSTE6 and GSTE7

Parameters	CDNB		DCNB		*p*-NBC	
	GSTE6	GSTE7	GSTE6	GSTE7	GSTE6	GSTE7
V_{max} (µmol/min)	0.52±0.024	0.83±0.028	0.029±0.008	0.30±0.033	0.21±0.013	1.31±0.051
K_m (mM)	0.024±0.001	0.14±0.009	0.17±0.001	0.42±0.002	0.28±0.005	0.060±0.002
K_{cat} (min^{-1})	0.13	0.086	0.007	0.043	0.051	0.14
K_{cat}/K_m ($min^{-1}mM^{-1}$)	5.25	0.62	0.042	0.10	0.18	2.25

GSTs were characterized for kinetic parameters using CDNB, DCNB and *p*-NBC as substrates. The data are mean ± standard error of at least three independent experiments.

4.7 Secondary Structure Analysis by Circular Dichroism (CD)

The CD spectra of the recombinant protein of GSTE6 and GSTE7 were scanned from 190 to 250 nm at a concentration of 0.2 mg/mL for both GSTE6 and GSTE7 respectively. The spectra profiles are shown in Figure 4.28. Both recombinant proteins were active towards CDNB conjugation, has similarities in the CD spectra as well measurable enzymatic activities suggest that the recombinant GST were properly folded. The spectra profile indicates that the both recombinant protein is an alpha helix rich protein. The CD profile shows difference in peak positions and peak intensities between recombinant protein GSTE6 and GSTE7.

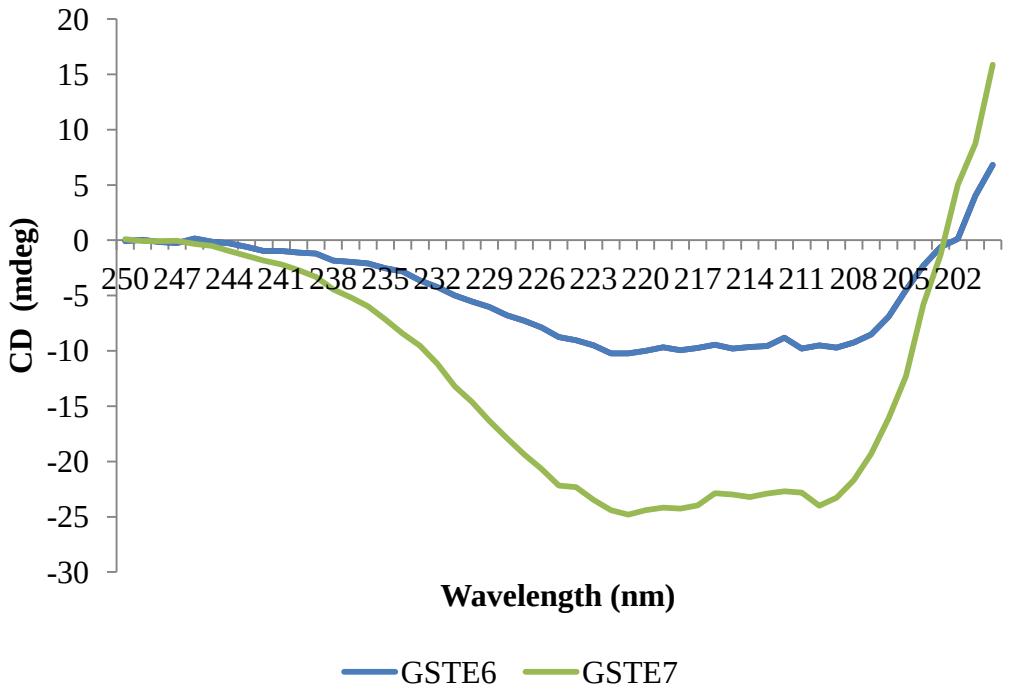

Figure 4.28: Circular dichroism spectra of the recombinant GSTE6 and GSTE7

4.8 Thin Layer Chromatography of Pesticides

Figure 4.29 shows conjugate reaction product of glutathione (GSH) and CDNB (positive control) with purified GSTE6 and GSTE7 enzyme respectively. Independent chromatographic analysis of purified GSTE6 and GSTE7 containing glutathione mixed with pesticides temophos, malathion, DDT, fenthion, fenitrothion, permethrin, bromophos, chlorpyrifos, clodinafop-Propargyl, fenoxaprop-ethyl, propoxur, isoproturon and methyl parathion respectively showed negative results with absence of conjugation reactions.

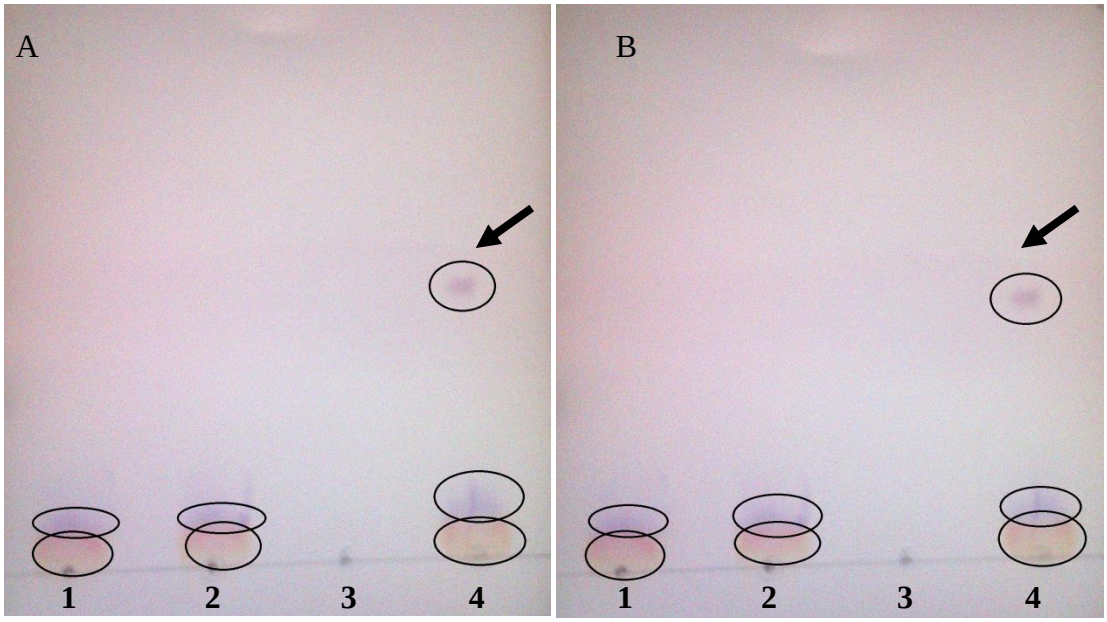

Figure 4.29: Chromatographic analysis of purified GSTE6 (A) and GSTE7 (B) containing glutathione plus with 1-chloro-2, 4,-dinitrobenzene (CDNB) as co-substrates. Lane 1: GSH, CDNB and Buffer A; Lane 2: Sample, GSH and Buffer A; Lane 3: Sample, CDNB and Buffer A and Lane 4: Sample, CDNB, GSH and Buffer A. Conjugate reaction products using co-substrates CDNB are indicated by arrows.

4.9 Effect of Natural Products and Dyes on GSTE6 and GSTE7 Enzyme

The effect of the natural products and dyes towards GSTE6 and GSTE7 using the CDNB conjugation assay was studies and the data are tabulated in Table 4.3. To measure the effect of natural products and dyes on recombinant protein of GSTE6 and GSTE7 respectively, triphenyltin acetate, tetradecanedioic acid, sebacic acid, *trans*-chalcone, cardiogreen, crystal violet, methylene blue, rose bengal, phenol red and cibacron blue was used. Different substrate range was used for each compound accordingly for kinetic analysis. Nonlinear regression analysis using log (concentration) response curves analysis was then used to determine the IC_{50} or EC_{50} for each recombinant protein. Some of the non-linear regression plot generated using the GraphPad prism showed in Appendix G and Appendix H.

By this experiment, the strength of inhibition was rose bengal > cardiogreen > phenol red > crystal violet > tetradecanedioic acid > methylene blue > cibacron blue > *trans*-chalcone for GSTE6 and rose bengal > cardiogreen > phenol red > crystal violet > cibacron blue > tetradecanedioic acid for GSTE7. For both GSTE6 and GSTE7, triphenyltin acetate results in endpoint saturation with smallest amount. No measurable activity was detected. Sebacic acid in the other hand does not impose any effect on the CDNB activity. For GSTE6, rose bengal, cardio green and phenol red dyes exhibited effectively inhibition resulting in IC_{50} ranging from 3-7 nM while crystal violet, tetradecanedioic acid, methylene blue, cibacron blue and trans- chalcone inhibited with IC_{50} ranging from 30-90 nM.

For GSTE7, rose bengal and cardiogreen dyes exhibited effectively inhibition resulting in IC_{50} ranging from 1-9 nM while phenol red, crystal violet, cibacron blue and tetradecanedioic acid inhibited with IC_{50} ranging from 30-500 nM. Interestingly, methylene blue and *trans*-chalcone showed to stimulate GSTE7 activity towards CDNB with EC_{50} ranging from $1 \times 10^5 – 3 \times 10^5$ nM. The statistical value had goodness of fit R^2 value above 95%.

Table 4.3: Effect of selected compounds on recombinant GSTE6 and GSTE7

Compound	Compound concentration range (mM)	GSTE6 IC_{50} (nM)	GSTE7 IC_{50} (nM)	EC_{50} (nM)
Triphenyltin acetate	0-100	NA	NA	
Tetradecanedioic acid	0-100	57.82	588.71	
Sebacic acid	0-100	NE	NE	
trans-chalcone	0-100	86.79		2.958×10^5
Cardiogreen	0-3	4.21	9.22	
Crystal Violet	0-10	32.24	50.59	
Methylene Blue	0-100	76.66		1.747×10^5
Rose Bengal	0-3	3.68	1.07	
Phenol Red	0-10	7.29	30.36	
Cibacron blue	0-10	82.64	210.56	

The data are mean value of at least three independent experiments. The statistical value had goodness of fit R^2 value above 95%.
*NA denotes not activity. *NE denotes not effect.

4.10 DNA and Protein Analysis

The *Drosophila* GST genes are located on chromosome 2, 3 and X. Figure 4.30 showed location of Epsilon class GSTs on chromosome 2R in *Drosophila melanogaster*. The *gste*1 to *gste*10 genes form a tight cluster whereas the remaining Epsilon genes are dispersed along the chromosome.

The alignment of the Epsilon class GSTs protein sequences of *Drosophila* with *Musca domestica* Epsilon class 6A and 6B is shown in Figure 4.31. All Epsilon class proteins of *Drosophila* together with Epsilon class GST of *Musca Domestica* could be brought into close alignment with few exceptional namely GSTE10 and GSTE14 being the most divergent sequence while GSTE12 variant A being the most convergent. The identities of all pairs of the Epsilon-class sequences of *Drosophila* and *Musca domestica* Epsilon class 6A and 6B are presented in Figure 4.32. GSTE6 were closely identical with GSTE5 (75%) while GSTE7 were closely identical to GSTE8 (71%). GSTE6 and GSTE7 were 69% identical. In comparison with *Musca domestica* Epsilon class 6A and 6B, GSTE6 identical 62% and 59% respectively while GSTE7 identical 61% respectively. Both GSTE6 and GSTE7 show more less 40% identity with other *Drosophila* Epsilon class proteins.

Figure 4.33 showed GSTE6 interaction with GSTE7, GSTE5 and Hsp 23 (Heat shock protein) (Giot *et al.*, 2003; Guruharsha *et al.*, 2011). Interestingly, GSTE8 also shows interaction with Hsp 23, Hsp22, Hsp 27, Hsc70Cb and Hsp68. It also showed to be interacting with Ref (2) p. GSTE6 strongly co-expressed with GSTE7, GSTE8, GSTE5, GSTE3, GSTE9 and GSTD1 while GSTE7 strongly co-expressed with GSTE6, GSTE8, GSTE3 and GSTE9 (Jensen *et al*., 2009).

Figure 4.34 showed predicted functional partners in various organisms. GSTE6 and GSTE7 showed 100% conserved in *Drosophila* genus and almost 30- 50% conserved in *Aedes aegyti, Culex quinquefasciatus, Anopheles gambiae, Nasonia vitripennis, Apis mellifera, Tribolium castaneum, Pediculus humanus and Ixodes scapularis.* The genes showed less than 20% conserved in other organism ranging from bacteria to Achaea.

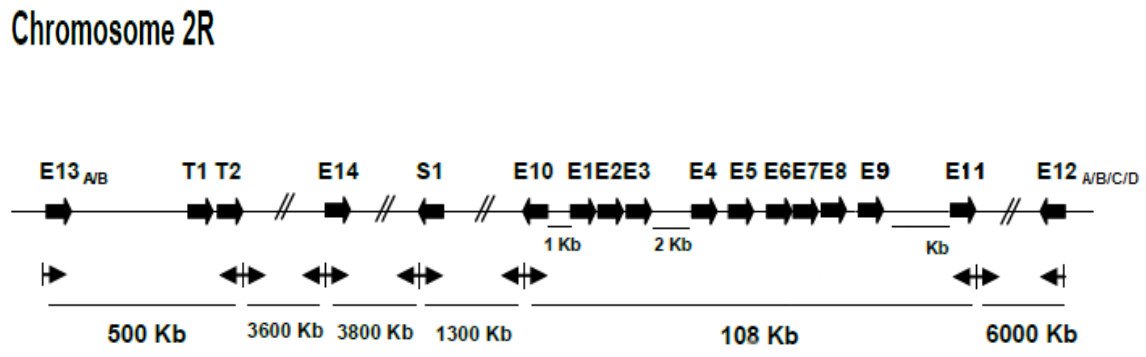

Two genes are alternatively spliced (indicated by subscript letters). The genes are shown as arrows indicating direction of transcription

Figure 4.30: Epsilon class *Drosophila* GST genes are located on chromosomes 2R (Adapted from Saisawang *et al.*, 2011).

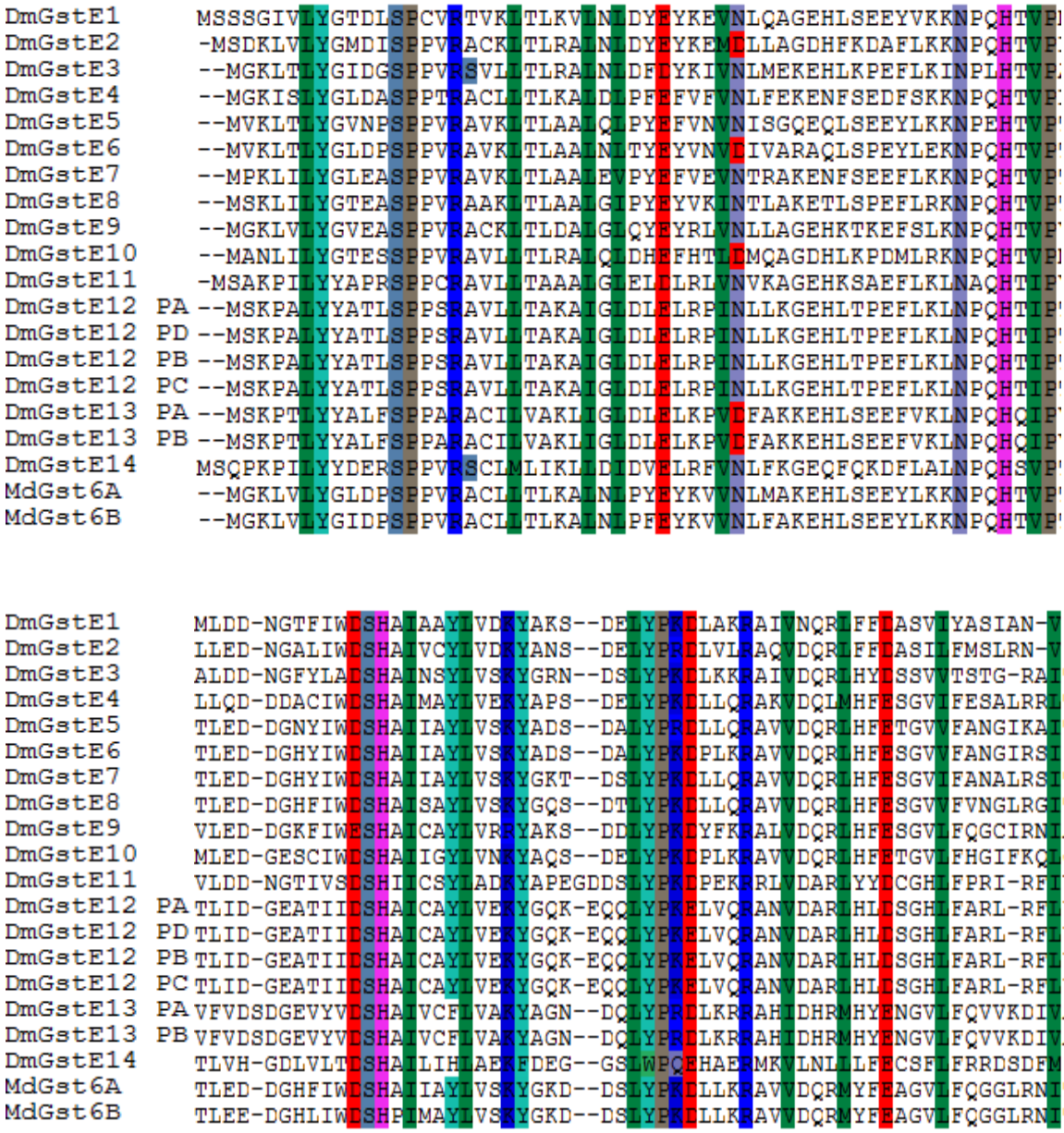
DmGstE1 MSSSGIVLYGTDLSPCVRTVKLTLKVLNLDYEYKEVNLQAGEHLSEEYVKKNPQHTVP
DmGstE2 -MSDKLVLYGMDISPPVRACKLTLRALNLDYEYKEMDLLAGDHFKDAFLKKNPQHTVP
DmGstE3 --MGKLTLYGIDGSPPVRSVLLTLRALNLDFDYKIVNLMEKEHLKPEFLKINPLHTVP
DmGstE4 --MGKISLYGLDASPPTRACLLTLKALDLPFEFVFVNLFEKENFSEDFSKKNPQHTVP
DmGstE5 --MVKLTLYGVNPSPPVRAVKLTLAALQLPYEFVNVNISGQEQLSEEYLKKNPEHTVP
DmGstE6 --MVKLTLYGLDPSPPVRAVKLTLAALNLTYEYVNVDIVARAQLSPEYLEKNPQHTVP
DmGstE7 --MPKLILYGLEASPPVRAVKLTLAALEVPYEFVEVNTRAKENFSEEFLKKNPQHTVP
DmGstE8 --MSKLILYGTEASPPVRAAKLTLAALGIPYEYVKINTLAKETLSPEFLRKNPQHTVP
DmGstE9 --MGKLVLYGVEASPPVRACKLTLDALGLQYEYRLVNLLAGEHKTKEFSLKNPQHTVP
DmGstE10 --MANLILYGTESSPPVRAVLLTLRALQLDHEFHTLDMQAGDHLKPDMLRKNPQHTVP
DmGstE11 -MSAKPILYYAPRSPPCRAVLLTAAALGLELDLRLVNVKAGEHKSAEFLKLNAQHTIP
DmGstE12 PA --MSKPALYYATLSPPSRAVLLTAKAIGLDLELRPINLLKGEHLTPEFLKLNPQHTIP
DmGstE12 PD --MSKPALYYATLSPPSRAVLLTAKAIGLDLELRPINLLKGEHLTPEFLKLNPQHTIP
DmGstE12 PB --MSKPALYYATLSPPSRAVLLTAKAIGLDLELRPINLLKGEHLTPEFLKLNPQHTIP
DmGstE12 PC --MSKPALYYATLSPPSRAVLLTAKAIGLDLELRPINLLKGEHLTPEFLKLNPQHTIP
DmGstE13 PA --MSKPTLYYALFSPPARACILVAKLIGLDLELKPVDFAKKEHLSEEFVKLNPQHQIP
DmGstE13 PB --MSKPTLYYALFSPPARACILVAKLIGLDLELKPVDFAKKEHLSEEFVKLNPQHQIP
DmGstE14 MSQPKPILYYDERSPPVRSCLMLIKLLDIDVELRFVNLFKGEQFQKDFLALNPQHSVP
MdGst6A --MGKLVLYGLDPSPPVRACLLTLKALNLPYEYKVVNLMAKEHLSEEYLKKNPQHTVP
MdGst6B --MGKLVLYGIDPSPPVRACLLTLKALNLPFEYKVVNLFAKEHLSEEYLKKNPQHTVP

DmGstE1 MLDD-NGTFIWDSHAIAAYLVDKYAKS--DELYPKDLAKRAIVNQRLFFDASVIYASIAN-V
DmGstE2 LLED-NGALIWDSHAIVCYLVDKYANS--DELYPRDLVLRAQVDQRLFFDASILFMSLRN-V
DmGstE3 ALDD-NGFYLADSHAINSYLVSKYGRN--DSLYPKDLKKRAIVDQRLHYDSSVVTSTG-RAI
DmGstE4 LLQD-DDACIWDSHAIMAYLVEKYAPS--DELYPKDLLQRAKVDQLMHFESGVIFESALRRL
DmGstE5 TLED-DGNYIWDSHAIIAYLVSKYADS--DALYPRDLLQRAVVDQRLHFETGVVFANGIKAI
DmGstE6 TLED-DGHYIWDSHAIIAYLVSKYADS--DALYPKDLPLKRAVVDQRLHFESGVVFANGIRSI
DmGstE7 TLED-DGHYIWDSHAIIAYLVSKYGKT--DSLYPKDLLQRAVVDQRLHFESGVIFANALRSI
DmGstE8 TLED-DGHFIWDSHAISAYLVSKYGQS--DTLYPKDLLQRAVVDQRLHFESGVVFVNGLRGI
DmGstE9 VLED-DGKFIWESHAICAYLVRKYAKS--DDLYPKDLYFKRALVDQRLHFESGVLFQGCIRNL
DmGstE10 MLED-GESCIWDSHAIIGYLVNKYAQS--DELYPKDLPLKRAVVDQRLHFETGVLFHGIFKQL
DmGstE11 VLDD-NGTIVSDSHIICSYLADKYAPEGDDSLYPKDLPEKRLVDARLYYDCGHLFPRI-RFI
DmGstE12 PA TLID-GEATIIDSHAICAYLVEKYGQK-EQQLYPKELVQRANVDARLHLDSGHLFARL-RFL
DmGstE12 PD TLID-GEATIIDSHAICAYLVEKYGQK-EQQLYPKELVQRANVDARLHLDSGHLFARL-RFL
DmGstE12 PB TLID-GEATIIDSHAICAYLVEKYGQK-EQQLYPKELVQRANVDARLHLDSGHLFARL-RFL
DmGstE12 PC TLID-GEATIIDSHAICAYLVEKYGQK-EQQLYPKELVQRANVDARLHLDSGHLFARL-RFL
DmGstE13 PA VFVDSDGEVYVDSHAIVCFLVAKYAGN--DQLYPRDLKRRAHIDHRMHYENGVLFQVVKDIV
DmGstE13 PB VFVDSDGEVYVDSHAIVCFLVAKYAGN--DQLYPRDLKRRAHIDHRMHYENGVLFQVVKDIV
DmGstE14 TLVH-GDLVLTDSHAILIHLAEKFDEG--GSLWPQERHAEFMKVLNLLLFECSFLFRRDSDFM
MdGst6A TLED-DGHFIWDSHAIIAYLVSKYGKD--DSLYPKDLLKRAVVDQRMYFEAGVLFQGGLRNI
MdGst6B TLEE-DGHLIWDSHPIMAYLVSKYGKD--DSLYPKDLLKRAVVDQRMYFEAGVLFQGGLRNI

GSTE12 with four variant while GSTE13 with two variant. Sequences were aligned using CLUSTAL W (BioEdit version 7.2.0 software). Identical amino acids with 100% threshold (as defined by the BLOSUM62 matrix) are shaded in different colours each representing different amino acids.

Figure 4.31: Complete amino acid alignment of *Drosophila* Epsilon class GSTs and *Musca domestica* 6A and 6B.

	DmGstE1	DmGstE2	DmGstE3	DmGstE4	DmGstE5	DmGstE6	DmGstE7	DmGstE8	DmGstE9	DmGstE10
DmGstE1	ID	0.540	0.453	0.466	0.462	0.462	0.466	0.448	0.466	0.438
DmGstE2	0.540	ID	0.434	0.466	0.461	0.470	0.477	0.439	0.457	0.468
DmGstE3	0.453	0.434	ID	0.500	0.495	0.490	0.533	0.518	0.457	0.437
DmGstE4	0.466	0.466	0.500	ID	0.576	0.554	0.614	0.581	0.477	0.433
DmGstE5	0.462	0.461	0.495	0.576	ID	0.747	0.695	0.711	0.490	0.454
DmGstE6	0.462	0.470	0.490	0.554	0.747	ID	0.690	0.698	0.509	0.466
DmGstE7	0.466	0.477	0.533	0.614	0.695	0.690	ID	0.708	0.511	0.491
DmGstE8	0.448	0.439	0.518	0.581	0.711	0.698	0.708	ID	0.495	0.450
DmGstE9	0.466	0.457	0.457	0.477	0.490	0.509	0.511	0.495	ID	0.462
DmGstE10	0.438	0.468	0.437	0.433	0.454	0.466	0.491	0.450	0.462	ID
DmGstE11	0.383	0.389	0.408	0.358	0.389	0.398	0.402	0.384	0.420	0.390
DmGstE12A	0.384	0.408	0.402	0.417	0.376	0.394	0.406	0.408	0.414	0.377
DmGstE12D	0.402	0.422	0.421	0.437	0.406	0.424	0.428	0.428	0.441	0.406
DmGstE12B	0.402	0.422	0.421	0.437	0.406	0.424	0.428	0.428	0.441	0.406
DmGstE12C	0.402	0.422	0.421	0.437	0.406	0.424	0.428	0.428	0.441	0.406
DmGstE13A	0.331	0.342	0.339	0.370	0.365	0.334	0.370	0.343	0.343	0.351
DmGstE13B	0.331	0.342	0.339	0.370	0.365	0.334	0.370	0.343	0.343	0.351
DmGstE14	0.256	0.256	0.256	0.311	0.247	0.256	0.294	0.260	0.252	0.274
MdGst6A	0.511	0.484	0.563	0.599	0.608	0.621	0.614	0.599	0.585	0.466
MdGst6B	0.488	0.479	0.558	0.590	0.594	0.599	0.605	0.585	0.572	0.466

	DmGstE11	DmGstE12A	DmGstE12D	DmGstE12B	DmGstE12C	DmGstE13A	DmGstE13B	DmGstE14	MdGst6A	MdGst6B
DmGstE1	0.383	0.384	0.402	0.402	0.402	0.331	0.33	0.256	0.511	0.488
DmGstE2	0.389	0.408	0.422	0.422	0.422	0.342	0.342	0.256	0.484	0.479
DmGstE3	0.408	0.402	0.421	0.421	0.421	0.339	0.339	0.256	0.563	0.558
DmGstE4	0.358	0.417	0.437	0.437	0.437	0.370	0.370	0.311	0.599	0.590
DmGstE5	0.389	0.376	0.406	0.406	0.406	0.365	0.365	0.247	0.608	0.594
DmGstE6	0.398	0.394	0.424	0.424	0.424	0.334	0.334	0.256	0.621	0.599
DmGstE7	0.402	0.406	0.428	0.428	0.428	0.370	0.370	0.294	0.614	0.605
DmGstE8	0.384	0.408	0.428	0.428	0.428	0.343	0.343	0.260	0.599	0.585
DmGstE9	0.420	0.414	0.441	0.441	0.441	0.343	0.343	0.252	0.585	0.572
DmGstE10	0.390	0.377	0.406	0.406	0.406	0.351	0.351	0.274	0.466	0.466
DmGstE11	ID	0.448	0.488	0.488	0.488	0.356	0.356	0.309	0.407	0.407
DmGstE12A	0.448	ID	0.896	0.896	0.896	0.346	0.346	0.276	0.488	0.426
DmGstE12D	0.488	0.896	ID	1.000	1.000	0.381	0.381	0.276	0.477	0.455
DmGstE12B	0.488	0.896	1.000	ID	1.000	0.381	0.381	0.276	0.477	0.455
DmGstE12C	0.488	0.896	1.000	1.000	ID	0.381	0.381	0.276	0.477	0.455
DmGstE13A	0.356	0.346	0.381	0.381	0.381	ID	1.000	0.272	0.374	0.361
DmGstE13B	0.356	0.346	0.381	0.381	0.381	1.000	ID	0.272	0.374	0.361
DmGstE14	0.309	0.276	0.276	0.276	0.276	0.272	0.272	ID	0.307	0.294
MdGst6A	0.407	0.448	0.477	0.477	0.477	0.374	0.374	0.307	ID	0.909
MdGst6B	0.407	0.426	0.455	0.455	0.455	0.361	0.361	0.294	0.909	ID

Box in green indicated percentage amino acid identities between GSTE6 and GSTE7. Box in blue indicated highest percentage amino acid identities with respect to GSTE6 and GSTE7 respectively. Sequences identities matrix was prepared using BioEdit version 7.2.0 software.

Figure 4.32: Matrix table of percentage amino acid identities for the sequences aligned of *Drosophila* Epsilon class GSTs and *Musca domestica* 6A and 6B.

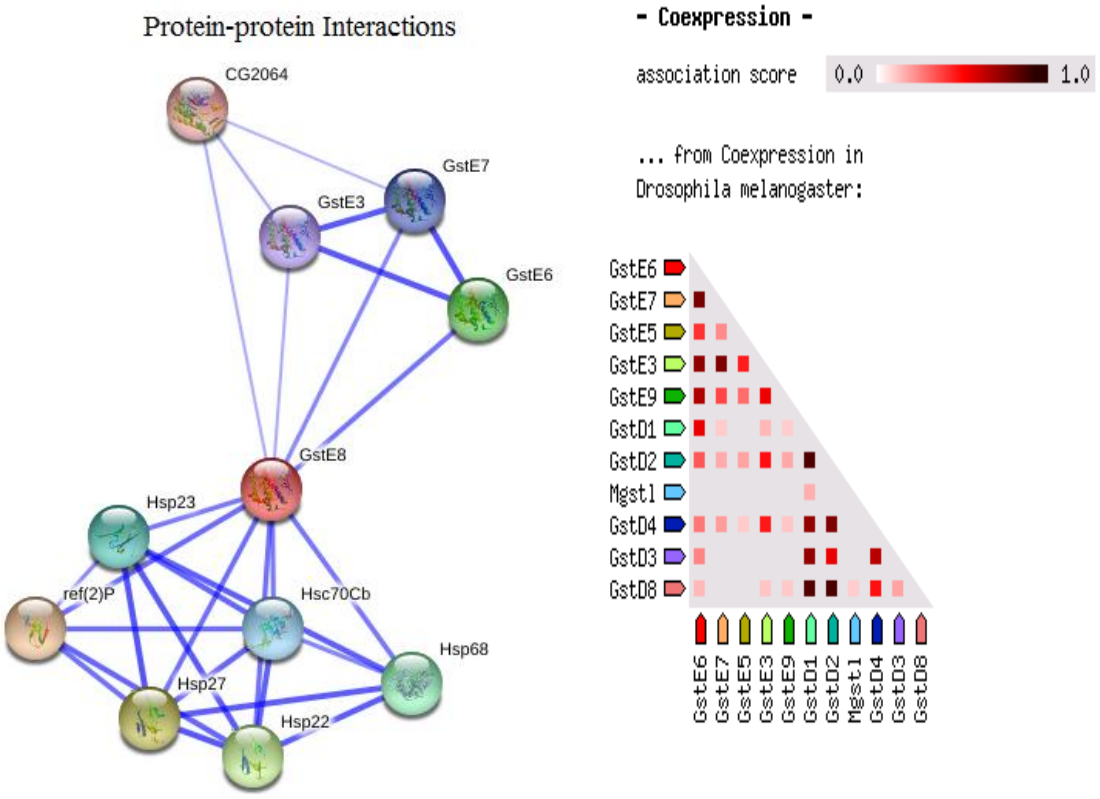

Figure 4.33: Predicted protein interactions and co-expression association score among closely related class of GST proteins using STRING 9.05 database from http://string-db.org/ (Jensen *et al.*, 2009) supported by Giot *et al*., (2003) and Guruharsha *et al*., (2011).

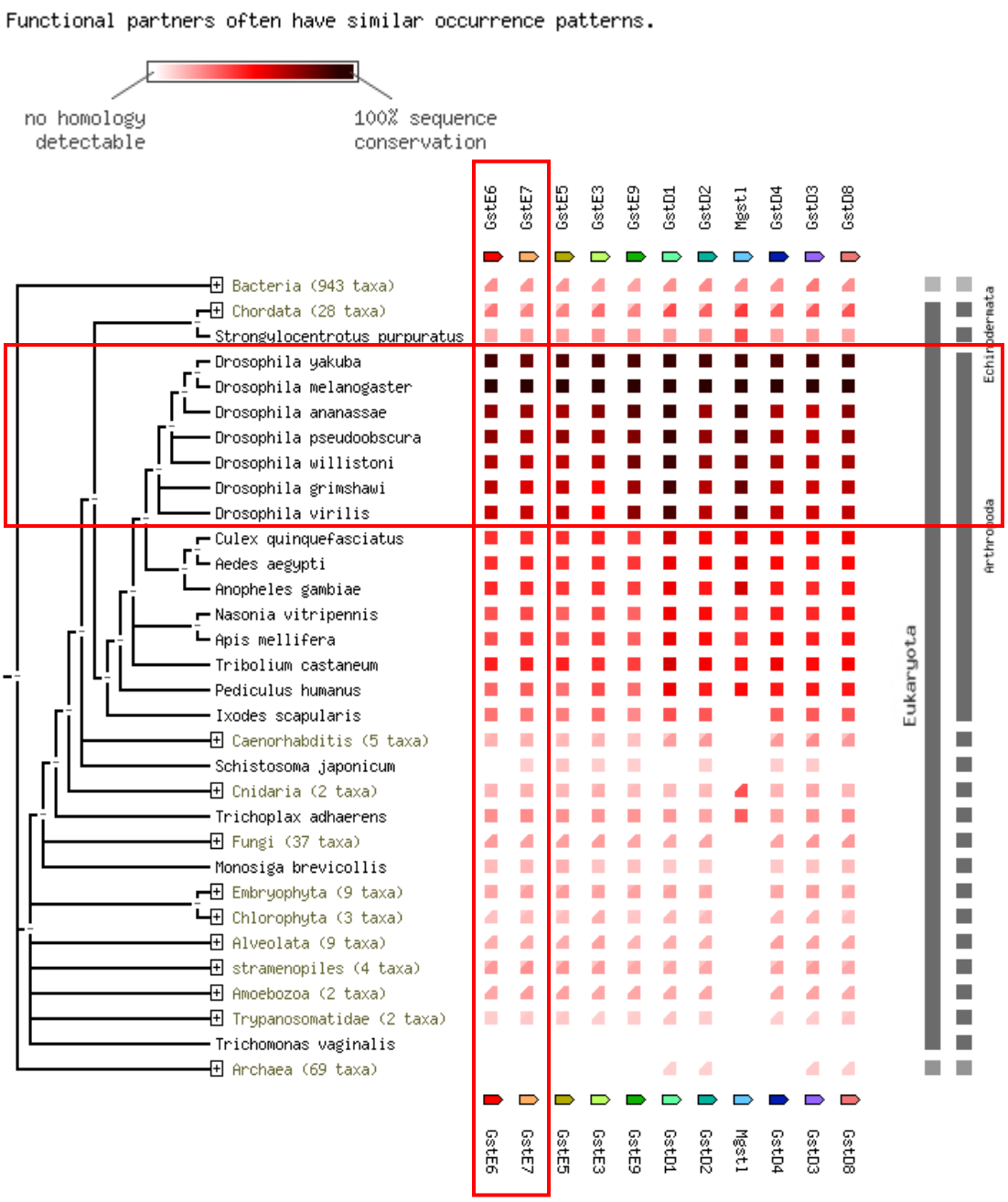

Figure 4.34: Predicted functional partners in various organisms using STRING 9.05 database from http://string-db.org/ (Jensen *et al.*, 2009).

CHAPTER 5

DISCUSSION

5.1 DNA and Protein Bioinformatics

The *Drosophila* GST genes are located on chromosome 2, 3 and X. Saisawang *et al.,* (2011) reported existence of additional four Epsilon class protein denoted GSTE11-GSTE14 besides ten Epsilon members that has been previously reported by Sawicki *et al.,* (2003). Saisawang *et al.,* (2011) analysis reported *gste1* to *gste10 genes* form a tight cluster whereas the remaining Epsilon genes are dispersed along the chromosome (Figure 4.30). It has been previously reported that the coding sequences of the Epsilon class GSTs contain no introns (Sawicki *et al.*, 2003) and they can be conceptually translated. The alignment of the Epsilon class GSTs protein sequences of *Drosophila* with *Musca domestica* Epsilon class 6A and 6B is shown in Figure 4.31. All Epsilon class proteins of *Drosophila* together with Epsilon class GST of *Musca Domestica* could be brought into close alignment with few exceptional namely GSTE10 and GSTE14 being the most divergent sequence because of a C-terminal extension of approximately 16 and 7 amino acids respectively while GSTE12 variant A with approximately 24 amino acids truncated. The identities of all pairs of the Epsilon-class amino acid sequences of *Drosophila* and *Musca domestica* Epsilon class 6A and 6B are presented in Figure 4.32. GSTE6 are closely identical with GSTE5 (75%) while GSTE7 were closely identical to GSTE8 (71%). GSTE6 and GSTE7 were 83% similar and 69% identical. In comparison with *Musca domestica* Epsilon class 6A and 6B, GSTE6 79% and 77% similar and also 62% and 59% identical respectively while GSTE7 77% similar and also 61% identical respectively. Both GSTE6 and GSTE7 shows lesser than 40% identity with other *Drosophila* Epsilon class proteins. The sequence

homology within the clusters, together with the physical proximity of all Epsilon genes on chromosome 2 (Figure 4.30), suggests that the cluster was probably formed by repeated duplication events without subsequent rearrangement of an Epsilon ancestral gene (Sawicki *et al.*, 2003)

5.2 Phylogenetics of Epsilon Class GSTs

Phylogenies studies done by Friedman, (2011) proved by evidence that Delta and Epsilon subclasses share a common branch and not with other subclasses. Examination of Delta-Epsilon taxonomic distribution suggested Delta class older in origin than Epsilon class GSTs. Freidman, (2011) also suggested that the Epsilon-GSTs evolved from the Delta subclass. This event took place between the times when Hymenoptera and Coleoptera was originated as a lineage. Therefore, both genes were present in all *Drosophila* genuses and distributed in organism ranging from bacteria, eukaryotes to Achaea (Figure 4.34).

5.3 Cloning and Expression of *Drosophila melanogaster* Epsilon class E6 and E7

Saisawang *et al.*, (2011) demonstrates that every isoform of GSTs appears to be expressed in the late embryonic stages of *Drosophila melanogaster*. The occurrence that GSTs genes are expressed in embryos implies differential gene regulation. It suggests that those GST isoforms may have various functions other than detoxification. In general, GST expression occurs in response to a variety of environmental stimuli, in a tissue or developmental-specific manner.

In this study, *gste6* and *gste7* which express in adult *Drosophila melanogaster* genome (Table 2.1) serves as template was amplified by the conventional polymerase chain reaction due to absence of introns in the coding sequences (Sawicki *et al*., 2003). The term intron

refers to both the DNA sequence within a gene and the corresponding sequence in RNA transcripts which will be removed by RNA splicing while the final RNA product of a gene is being generated. It also known as a non-coding sequences. The DNA coding sequences obtained from genome database from http://www.ncbi.nlm.nih.gov as well as the vector sequences of pBAD/Thio-TOPO (Figure 3.1) and pET-30a (+) (Figure 3.2) was studied for its number of base pairs, enzyme cutters and non-cutters enables to design suitable primers for each gene. The full-length coding sequence of GSTE6 contains 669 bp translated to give 222 amino acid while GSTE7 contains 672 bp translated to give 223 amino acids which is the same length with genome database (http://www.ncbi.nlm.nih.gov) (Figure 4.1 and Figure 4.2).

In the beginning of the project pBAD/TOPO® ThioFusion™ Expression Kit was chosen as it provides a highly efficient, 5-minute, one-step cloning strategy ("TOPO® Cloning") for the direct insertion of Taq polymerase-amplified PCR products into a plasmid vector for soluble, regulated expression and simplified protein purification in *E. coli*. The kit does not need any ligase, post-PCR procedures, or PCR primers containing specific sequences (described in pBAD/TOPO® ThioFusion™ Expression Kit user manual) (http://www.lifetechnologies.com/order/catalog/product/K37001) and it was been widely used for cloning and expression of many genes (Moulis *et al.*, 2006; Fabre *et al.*, 2005; Koukiekolo *et al.*, 2005; Cheng *et al.*, 2005; Que Xuchu *et al.*, 2002). The primers were designed according to the manufacturer's instructions. The forward PCR primer was designed to ensure that protein is in frame with the N-terminal leader peptide in order clone in frame with thioredoxin as HP-thioredoxin acts as a translation leader to facilitate high-level expression and in some cases, solubility. The reverse PCR primer was designed to remove the native stop codon in the gene of interest and preserve the reading frame through

the C-terminal tag in order to include the V5 epitope and polyhistidine region to assist with purification procedure. The polymerase chain reaction was successful and as a starter the *gste*6 and *gste*7 gene was able to be amplified to give the PCR product in between 500 bp and 750 bp (Figure 4.3 and Figure 4.4).

The PCR product for TOPO cloning was ligated into pBAD/Thio-TOPO®, and transformed the recombinant vector into chemically competent TOP10 One Shot® *E. coli* on LB- ampicillin plate. The recombinant genes were successfully cloned and purified. Figure 4.6 showed the gel image of purified plasmids of *gste*6. The sequencing result of plasmid at correct size obtained was analyzed using Basic Local Alignment Search Tool (BLAST). Figure 4.8 showed the BLAST search tool results that revealed only 75% similarity with the *Drosophila melanogaster* chromosome 2R, complete sequence which denotes the glutathione S-transferase, E6 (Figure 4.8 and Figure 4.9). Repeated attempt to clone the gene using pBAD/Thio-TOPO® was no success. Therefore, restriction enzyme cloning method was employed to use vector pET-30a (+).

pET-30a (+) expression vector was chosen as it was used previous work in cloning and expression of *Drosophila melanogaster* delta and Epsilon class GSTs (Sawicki *et al.,* 2003). The primers for restriction enzyme cloning initially was designed to include *Nde1* and *EcoR1* for *gste*6 while *Nde1* and *Xho1* for *gste*7 because it includes 6X Histidine tagging to the gene of interest which will assist with purification procedure. The polymerase chain reaction was successful and the genes were able to be amplified to give the PCR product in between 500 bp and 750 bp in size (Figure 4.5).

The PCR product for restriction enzyme cloning was ligated pET-30a (+) and transformed the recombinant vector into chemically competent *E.coli* BL21 (DE3) pLysS and BL21

Star™ (DE3) pLysS *E. coli* on LB-kanamycin plate. Chemically competent *E.coli* BL21 (DE3) pLysS was chosen as it was widely used to express GST recombinants (Saisawang *et al.*, 2011; Wongtrakul *et al.*, 2010; Lumjuan *et al.*, 2005; Sawicki *et al*., 2003) and only chemically competent *E.coli* BL21 (DE3) pLysS successfully transformed both genes. The recombinant genes were successfully cloned and purified. Figure 4.11 and Figure 4.12 showed the gel image of purified plasmids of both *gste*6 and *gste*7. The sequencing result of plasmid at correct size obtained was analyzed using Basic Local Alignment Search Tool (BLAST). Figure 4.15 and Figure 4.17 showed the BLAST search tool results that revealed 99% similarity with the *Drosophila melanogaster* chromosome 2R, complete sequence which denotes the glutathione S-transferase, E6 and E7 respectively (Figure 4.16 and Figure 4.18). Sequencing results obtained for the PCR products (Figure 4.19) showed the recombinant protein contained one amino acid changes from the wild type at position 439 in *gste*6 gene resulted change of the amino acid sequence of a protein from GGC to GGT which both encodes for glycine and found to be single base changes from pyrimidine changed to be pyrimidine. Amino acid changes at position 223,463,481,517 and 527 in *gste*7 all resulted change of the amino acid sequence of a protein but do not result in radically different properties of the changed amino acids (Figure 4.20) as it was single base changes such as purine changed to be purine and pyrimidine changed to be purine. Unfortunately, the change between purine and pyrimidine suggests an error of recombinant cloning. However, it was not clear that this single mutation affect any catalytic function of the enzyme. Amino acid changes within these enzymes were caused from either purine changed to be purine or pyrimidine changed to be pyrimidine that causes variation of similar nucleotide are a common incident that can be performed by expression host. Interestingly, this implies the *E. coli* BL21 (DE3) pLysS expression host may prefer

those amino acid variations or it may be a real isoform occurring in the *Drosophila* cells.

5.4 Protein Purification of *Drosophila melanogaster* Epsilon Class E6 and E7

The recombinant GSTE6 and GSTE7 were tried to be purified using multiple matrices. A total three columns were used in order to purify GSTE6 and GSTE7 respectively which include GSTrap™ HP, HiTrap Q HP, HiTrap™ CM FF and Bromosulfophthalein-GSH matrix (Table 3.5). Purification with HiTrap Q Sepharose matrix showed that almost all desired protein were eluted out as unbound protein therefore, the unbound proteins were purified using BSP/GSH-agarose matrix. The proteins were highly expressed and isolated using BSP/GSH-agarose matrix which has been shown to capture a number of Epsilon-class GSTs from *D.melanogaster* (Alias and Clark, 2007; Alias and Clark, 2010). Both isoforms were heterologously expressed and purified to apparent high homogeneity. Both were expressed as soluble forms and expressed differently under the same conditions. High expression levels were observed with both clones. The subunit size of GSTE6 and GSTE7 are predicted to be 25.015 kDa and 25.51 kDa respectively based on their amino acid compositions. Sodium dodecyl sulfate-polyacrylamide gel electrophoresis (SDS-PAGE) of purified enzymes was approximately 25 kDA respectively which corresponds to the calculated molecular mass (Figure 4.27) and were in agreement with data previously reported by Saisawang *et al.*, (2011).

5.5 Biochemical Characterization of *Drosophila melanogaster* Epsilon class E6 and E7

In the present study, substrate specificity of these isozymes were determined using 12 model substrates belonging to halogenated compounds, α, β-unsaturated carbonyl compounds, peroxide and organic compound. *trans*-Hex-2-enal, a plant derived green leaf aldehyde was known to stimulate olfactory system (Rogers *et al*., 1999). *trans*-Oct-2-enal, *trans*-Hex-2-enal, Hexa-2, 4-dienal, *trans, trans*-hepta-2, 4-dienal are toxic α, β-unsaturated carbonyl allelochemicals are commonly presented in corn, wheat, and oats (Yu, 2002). Peroxides such as hydrogen peroxides and organic hydroperoxide such as cumene hydroperoxide generates cytotoxic product during microsomal lipid peroxidation which causes membrane destruction and DNA damage (Yu, 2002). Table 4.1 showed that the pattern of specific activity toward these substrates was almost similar between GSTE6 and GSTE7. Both isozymes only react towards CDNB, DCNB and *p*-NBC. Among those tested, CDNB was the best substrate for both genes with 80.67±4.43 and 740.33±15.04 nmol/mL/mg respectively followed by DCNB 18.11±1.04 nmol/mL/mg and *p*-NBC 3.67±0.58 nmol/mL/mg for GSTE6 while *p*-NBC 249.67±9.61 nmol/mL/mg followed by DCNB 37.05±2.11 nmol/mL/mg for GSTE7. Wongtrakul *et al.*, (2010) and Wang *et al.*, (1991) reported that only Epsilon class GSTs able to accept and react with DCNB supports our data. It was suggested that the detoxification capability of GSTs against insecticides is correlated to its catalytic activity with DCNB rather than CDNB (Wei *et al.*, 2001).

The different properties of these two enzymes were further exemplified by a comparison of the kinetic properties (Table 4.2). The comparison of the initial-rate enzyme kinetics between GSTE6 and GSTE7 enzyme for CDNB showed that GSTE6 have higher affinity (K_m = 0.024 ± 0.001 mM for GSTE6 and K_m = 0.14 ± 0.009 mM for GSTE7), catalytic

efficiency (K_{cat}/ K_m = 5.25 $min^{-1}mM^{-1}$ for GSTE6 and K_{cat}/ K_m = 0.62 $min^{-1}mM^{-1}$ for GSTE7) and catalytic rate (K_{cat} = 0.13 min^{-1} for GSTE6 and K_{cat} = 0.086 min^{-1} for GSTE7). As for DCNB, GSTE7 has higher catalytic rate (K_{cat} = 0.007 min^{-1} for GSTE6 and K_{cat} = 0.043 min^{-1} for GSTE7) and catalytic efficiency (K_{cat}/ K_m = 0.042 $min^{-1}mM^{-1}$ for GSTE6 and K_{cat}/ K_m = 0.10 $min^{-1}mM^{-1}$ for GSTE7) with similar enzyme affinity (K_m = 0.17 ± 0.001 mM for GSTE6 and K_m = 0.42 ± 0.002 mM for GSTE7). Finally for *p*-NBC, GSTE7 has higher enzyme affinity, catalytic rate and catalytic efficiency (K_m = 0.060 ± 0.002 mM, K_{cat} = 0.14 min^{-1} and K_{cat}/ K_m = 2.25 $min^{-1}mM^{-1}$) compared to GSTE6 (K_m = 0.28 ± 0.005 mM, K_{cat} = 0.051 min^{-1} and K_{cat}/ K_m = 0.18 $min^{-1}mM^{-1}$). GSTE6 is a more efficient enzyme at turning over CDNB supported by pervious study done by Saisawang *et al.*, (2003) while GSTE7 is a more efficient enzyme at turning over DCNB and *p*-NBC.

The CD profiles are shown in Figure 4.28. Similarities in the CD spectra between GSTE6 and GSTE7 as well as their measurable substrate specificity activities in vivo and in vitro strongly suggest that the recombinants GST Es are properly folded. The profiles of their CD spectra indicated that the secondary structures of these recombinant GSTs have high α-helical contents. The CD profiles also revealed substantial differences in peak positions and peak intensities between GSTE6 and GSTE7. GSTE6 seems to be less stable than GSTE7. These differences indicated that GSTE6 and GSTE7 have considerable variations in their secondary structural organization. Such variations in structure may form the basis of differences in their corresponding substrate specificities and in catalytic efficiency (Tang and Tu, 1994) although both originated from same cluster and located next to each other on the genomic DNA (Figure 4.30). Thin layer chromatography of insecticides showed the isozymes do not able to conjugate 12 tested insecticides (Figure 4.29). Temophos, malathion, DDT, fenthion, fenitrothion, permethrin, bromophos, chlorpyrifos, clodinafop-

Propargyl, fenoxaprop-ethyl, propoxur, isoproturon and methly parathion were used in this test. Temophos, malathion, DDT, fenthion, fenitrothion, permethrin, bromophos, chlorpyrifos, propoxur, isoproturon and methly parathion are known as insecticides from family of either organophosphate or organochloride while clodinafop- Propargyl and fenoxaprop-ethyl are known as herbicides widely used in agricultural work. The test suggests both recombinant GSTE6 and GSTE7 does not react or involves in detoxification of insecticides and herbicides.

The effect of few natural products and dyes on the recombinant isozymes was tabulated in Table 4.3. By this experiment, the strength of inhibition is rose bengal > cardiogreen > phenol red > crystal violet > tetradecanedioic acid > methylene blue > cibacron blue > *trans*-chalcone for GSTE6 and rose bengal > cardiogreen > phenol red > crystal violet > cibacron blue > tetradecanedioic acid for GSTE7. Phenol red, cardio green and rose bengal dyes exhibited effectively inhibition resulting in IC50 ranging from 3-7 nM on GSTE6 and as for GSTE7 cardio green and rose bengal dyes exhibited effectively inhibition resulting in IC_{50} ranging from 1-9 nM. Interestingly, *trans*-chalcone and methylene blue showed to stimulate GSTE6 activity towards CDNB with EC_{50} ranging from 1×10^5- 3×10^5 nM. The potency of xanthene food dye, rose bengal being the most effective inhibitors among the rest with IC_{50} of 0.003 and 0.001 µM on GSTE6 and GSTE7 respectively has been observed in earlier experiment with Drug-Metabolizing Enzymes namely cytochrome P_{450} and UDP-glucuronosyltransferase, where IC_{50} on micromolar inhibitor level were determined (21.2 and 15 µM) respectively (Mizutani, 2008). Another study by Uesugi *et al.*, (2006) also reported rose bengal strongly inhibited human UDP-glucuronosyltransferase (UGT1A6) activity with IC_{50} of 0.015 mM. The author added phenyl-xanthene dyes, such as rose bengal (RB) are known as light-enhancing reagents

(catalytic light reaction) by the generation of $^1O_2$ a superoxide anion on the dyes. Chalcone are open chain flavonoids that are widely biosynthesized in plants. A study by Batovska and Todorova, (2010) revealed the pharmacological properties of natural and synthetic chalcones as antioxidant, cytotoxic, anticancer, antimicrobial, antiprotozoal, antiulcer, antihistaminic and anti-inflammatory activities but mechanism of action of *trans*-chalcone as an inhibitor to GSTE6 while as a stimulator for GSTE7 is remaining unclear. Studies done using methylene blue showed methylene blue inhibits the ability of the purified Hsp90/Hsp70-based chaperone machinery to enable ligand binding by the glucocorticoid receptor (Wang *et al*., 2010) and acts as nitric oxide synthase inhibitor (Mayer *et al.*, 1993). Armstrong, (1997) reported that, certain haloalka (e) nes including ethylene bromide and methylene chloride forms a highly reactive episulfonium ion intermediates that catalyze GST activation reactions. But, its action as an inhibitor to GSTE6 while as a stimulator for GSTE7 is remaining unclear. Basic triphenylmethane dyes such as crystal violet have been shown to inhibit glutathione S-transferases from both insect sources (Balabaskaran and Smith, 1970) and from rat liver (Debnam *et al.*, 1993). The mode of inhibition of crystal violet appeared to involve competition by the free dye with the electrophilic substrate (Glanville and Clark, 1997).

The inhibition of glutathione transferase can have both positive and negative effects. As for the negative site, the inhibition of the enzyme may lead to toxic consequences because it causes the detoxification activity of the enzyme to be decreased. Incapable to detoxify the electrophilic compound harms the DNA, proteins and lipids hence results in various diseases such as cancers and neurodeganative disorders. On the positive site, inhibition of the detoxification enzyme prevents resistance problems occurs in cancer therapy as the

compounds can be used to inhibit GST activity and also developed as adjuvant in cancer treatment (Rachel *et al*., 2003).

5.6 Role of *Drosophila melanogaster* Epsilon class E6 and E7

Protein interaction studies done by Giot *et al.*, (2003) and Guruharsha *et al.*, (2011) reported that GSTE6 showed interaction with GSTE7, GSTE5 and Hsp 23 (Heat shock protein). Interestingly, GSTE8 also showed interaction with Hsp 23. The studies indicated GSTE8 mainly interacts with heat shock proteins, heat shock factors, heat shock cognates and those proteins known to be a stress inducible protein such as Hsp22, Hsp 27, Hsc70Cb and Hsp68. It also involved in folding and unfolding of other functional proteins. It also showed to be interacting with Ref (2) p that associates with pre-mRNA 3' end processing complex that eventually associated with mRNA maturation. GSTE6 strongly co-expressed with GSTE7, GSTE8, GSTE5, GSTE3, GSTE9 and GSTD1 while GSTE7 strongly co-expressed with GSTE6, GSTE8, GSTE3 and GSTE9 (Jensen *et al.*, 2009) (Figure 4.33). These give insights of possible role of a selective protein to be the key regulator of sets of genes.

The role of GSTE6 and GSTE7 enzyme in detoxification process remains unclear. Literature review above reported that Epsilon class GSTs involved in detoxification process but current findings does not show any promising evidence its involvement in detoxification. According to studies done by Yang *et al.*, (2007), *gste*6 found abundant in hindgut while *gste*7 found abundant in Malpighian tubules. A comprehensive microarray-based atlas of adult gene expression in multiple *Drosophila* tissues available (http://flyatlas.org) reported that, *gste*6 expressed in adult crop, midgut, tubule, hindgut, ovary and larval hindgut while *gste*7 expressed in adult crop, midgut, tubule, hindgut,

virgin spermatheca and larval midgut, hindgut and fat body. Drnevich *et al.*, (2004) in his study reported that, *gste*6 together *gste*5, *gste*1 and *gste*8 and few other genes were expressed thus play a role in male reproductive fitness and success. Li *et al*., (2008) has identified the potential DNA transcription factor binding motifs (TFBMs) of cytochrome P450s, GSTs and carboxylesterases expressed in the *Drosophila melanogaster* third instar larval midguts. *gste*6 reported to have GRE-like, Fox-like, NF-kappaB-like and E47-like TFBMs while *gste*7 reported to have GRE-like and E47-like TFBMs. The four mentioned TFBMs are known to have mammalian function and were observed to be linked to the oxidative stress response (Li *et al.*, 2008). The author reported GSTE6 and GSTE7 enzyme responded different levels of dietary hydrogen peroxide. However, the author concluded that there is no solid evidence to prove if some or all of the potential TFBMs are functional or response of the midgut-associated GSTs to the oxidative stress, dietary H_2O_2. They may simply be associated with these genes with limited or no role in response to this oxidative stressor. *gste*7 gene in another study appeared to be involved in activation of survival program through immune deficiency (IMD) pathway as it reported expressed in strongly infected airway epithelium of *Drosophila melanogaster* (Wagner, *et al*., 2009). IMD pathway is appearing to be the only functional NF-kappaB activating pathway in epithelial cells. Exposure of *Drosophila* to toxins evokes coordinated response by the Malpighian tubules, involving both alterations in detoxification pathways as well as enhanced transport through DHR96, the *Drosophila* ortholog of the vertebrate PXR/CAR family of nuclear receptors (Chahine and Donnell, 2010).

In the other hand, studies by Willoughby *et al.*, (2006) stated that in insects either two distinct receptors have evolved the ability to regulate a very similar set of genes. More than one receptor pathway exists to regulate similar sets of genes. This suggests the possibilities

of induction of *gste*6 and *gste*7 together with other genes. Apart from that, basal expression and induction was detected in the key metabolic tissues, namely sections of the midgut, and the malpighian tubules. However, difference in the expression of both *gste*6 and *gste*7 gene and its inability to detoxify possibly due to cis-regulatory elements controlling the expression of genes may not be acting independently whereby the substrate models may be acting solely to increase the transcriptional output of the tissue-specific modules (Willoughby *et al*., 2006) and the fact that these two genes are found sequentially on the chromosome may support a model of coordinated regulation (Lumjuan *et al*., 2011).

5.7 Future Studies

The results presented in this thesis have shown that it may not be possible to unravel the complex functions of the *Drosophila melanogaster* Epsilon class E6 and E7 enzyme in its contribution to either insecticide resistance or oxidative stress. However, what is needed is to carry out these experiments on larger numbers of field strains or using the laboratory susceptible and resistant strains and correlates GSTE6 and GSTE7 enzymes with resistance using other various insecticides and other xenobiotics as substrates besides used in this project. Apart from that, more physiological putative substrates needed to be tested in order to study its physiological role in details. In addition, structure elucidation based on X-ray crystallography of these genes will shed light on their special structural features. Determination of the three dimensional structure of both genes allows to determine either the genes plays a role in detoxification process or it only recognizes a much narrower group of electrophilic compounds. There is still a considerable need for future research in relation to the findings presented in this thesis on how GST-mediated resistance is either coordinately regulated to involve different members from multiple groups of glutathione transferases or it acts independently.

CHAPTER 6

CONCLUSION

Drosophila melanogaster Epsilon class E6 and E7 gene was successfully cloned, purified and biochemically characterized. The recombinant proteins were readily purified using the combination of both anionic chromatography and BSP-GSH affinity column. Although both genes have significant identity in amino acid sequence conservation which indicates they are in the same class, each enzyme displayed unique biochemical characteristics. This suggests that different residue in the enzyme active site plays a role in enzymatic specificity of each isoform.

Besides that, availability of both genes in database allows cloning of individual gene for determination of its physiological function with various substrates. The data shows both isoforms specifically conjugate common substrates such as CDNB, DCBN and *p*-NBC with different catalytic activity. This gives us insights of physiological function network of each gene in *Drosophila* cells differ tremendously. However, the recombinant proteins do not show any promising results neither with physiological substrates nor with pesticides doubts the possibility of involvement in either as detoxification process or prevents oxidative stress in the cells. It was suggested that the detoxification capability of GSTs against insecticides is correlated to its catalytic activity with DCNB rather than CDNB thus the recombinant proteins may only be involved in normal defense mechanism in cells.

In addition, the recombinant proteins showed to be inhibited significantly by naturally occurring product and various dyes suggest it can help to inhibit the detoxification activity of the GST isoenzymes in cancerous cells as a whole with exceptional to GSTE7 which found to be stimulated by *trans*-chalcone and methylene blue. Moreover, stimulation of

only GSTE7 activity upon addition of methylene blue dye and *trans*-chalcone influences us to concern the possible cause that could lead to this difference. Moreover, future findings needed to be included on how GST-mediated resistance is either coordinately regulated to involve different members from multiple groups of glutathione s-transferases or it acts independently.

REFERENCES

Alias, Z. and Clark, A.G. (2010). Adult *Drosophila melanogaster* glutathione S-transferases: Effects of acute treatment with methyl parathion. Pesticide Biochemistry and Physiology. 98: 94-98.

Alias, Z. and Clark, A.G. (2007). Studies on the glutathione S-transferase proteome of adult *Drosophila melanogaster*. Responsiveness to chemical challenge. Proteomics. 7: 3618-3628.

Anne, M.H. (2013). Glutathione Chemical Structure. Retrieved from http://chemistry.about.com/od/factsstructures/ig/Chemical-Structures---G/Glutathione.htm.

Armstrong, R.N. (1997). Glutathione S-transferases: reaction mechanism, structure, and function. Chemical Research in Toxicology. 4:131–140.

Armstrong, R. (2012). Bridging projects: Glutathione transferase (GST) superfamily. Retrieved on 8th March 2013 from http://enzymefunction.org/about/bridging-projects/gst-superfamily.

Atkinson, H.J. and Babbitt, P.C. (2009). Glutathione S- transferases Are Structural and Functional Outliers in the Thioredoxin Fold. Biochemistry. 48: 46.

Balabaskaran, S. and Smith, J.N. (1970). The inhibition of 1, 1, 1-trichloro-2, 2-bis-(p-chlorophenyl) ethane (DDT) dehydrochlorinase and glutathione S-aryltransferase in grass-grub and housefly preparations. Biochemical Journal. 117: 989–996.

Batovska, D.I. and Todorova, I.T. (2010). Trends in Utilization of the Pharmacological Potential of Chalcones. Current Clinical Pharmacology. 5: 1-29.

Beall, C., Fyrberg, C., Song, S. and Fyrberg, E. (1992). Isolation of a *Drosophila* gene encoding glutathione S-transferase. Biochemical Genetics. 30: 515-527.

Booth, J., Boyland, E. and Sims, P. (1961). An enzyme from rat liver catalyzing conjugations with glutathione. Biochemical Journal. 79: 516-524.

Boyland, E. and Chasseaud, L.F. (1969). The role of glutathione and glutathione S transferases in mercapturic acid biosynthesis. Advance Enzymology. 32:173.

Bradford, M.M. (1979). A rapid and sensitive method for the quantitation of the microgram quantities of protein utilizing the principle of protein-dye binding. Journal of Analytical Biochemistry. 72: 248-254.

Brophy, P.M, Southan, C. and Barrett, J. (1989). Glutathione S- transferases in the tapeworm *Moniezia expansa*. Biochemical Journal. 262: 939.

Chahine, S. and O'Donnell, M. (2010). Interactions between detoxification mechanisms and excretion in Malpighian tubules of *Drosophila melanogaster*. The Journal of Experimental Biology. 214: 462-468.

Charoensilp, G., Vararattanavech, A., Leelapat, P., Prapanthadara, L., & Ketterman, A.J. (2006). Characterization of *Anopheles dirus* glutathione transferase Epsilon 4. Journal of Science Society of Thailand. 32: 159-165.

Chasseaud, L.F. (1979). The role of glutathione and glutathione S transferases in the metabolism of chemical carcinogens and other electrophilic agents. Advance in Cancer Research. 29:175-274.

Chelvanayagam G., Parker M.W. and Board, P.G. (2001). Fly fishing for GSTs: a unified nomenclature for mammalian and insect glutathione S- transferases. Chemico-Biological Interactions. 133: 256-260.

Che-Mendoza, A., Penilla, R.P. and Rodríguez, A.D. (2009). A review: Insecticide resistance and glutathione S-transferases in mosquitoes. African Journal of Biotechnology. 8: 1386-1397.

Cheng, B., Shukla, S., Vasunilashorn, S., Mukhopadhyay, S. and Tse-Dinh, Y.C. (2005). Bacterial cell killing mediated by topoisomerase I DNA cleavage activity. Journal of Biological Chemistry. 280: 38489-38495.

Clark, A.G., Smith, J.N. and Speir, T.W. (1973) Cross specificity in some vertebrate and insect glutathione-transferases with methyl parathion (dimethyl-p-nitrophenyl phosphorothionate), 1-chloro-2, 4-dinitrobenzene and S-crotonyl-N-acetylcysteamine as substrates. Biochemical Journal. 135: 385-392.

Clark, A.G. (1989). The comparative enzymology of the glutathione S-transferases from non-vertebrate organisms. Comparative Biochemistry and Physiology. 92: 419-446.

Coles, B. and Ketterer, B. (1990). The role of glutathione and glutathione S-transferases in chemical carcinogenesis. Biochemistry and Molecular Biology. 25: 47-70.

Combes, B. and Stakelum, G. S. (1961) A liver enzyme that conjugates sulfobromophthalein sodium with glutathione. Journal of Clinical Investigation. 40: 981-988.

Danielson, U. H. and Mannervik, B. (1985). Kinetic independence of the subunits of cytosolic glutathione S-transferases from the rat. Journal of Biochemistry. 231: 263-267.

Debnam, P., Glanville, S. and Clark, A.G. (1993). Inhibition of glutathione S-transferases from rat liver by basic triphenylmethane dyes. Biochemical Pharmacology. 45: 1227-1233.

Deng, H., Huang, Y., Feng, Q., and Zheng, S. (2009). Two epsilon glutathione S-transferase cDNAs from the common cutworm, *Spodoptera litura*: Characterization and developmental and induced expression by insecticides. Journal of Insect Physiology. 55: 1174–1183.

Ding, Y., Ortelli, F., Rossiter, L.C., Hemingway, J., Ranson, H. (2003). The *Anopheles gambiae* glutathione transferase supergene family: annotation, phylogeny and expression profiles. BMC Genomics. 4: 35–50.

Dirr, H., Reinemer, P. and Huber, R. (1994). X-ray crystal structure of cytosolic glutathione S- transferases: Implication for protein architecture, substrate recognition and catalytic function. European Journal of Biochemistry. 220: 645-661.

Drnevich, J.M., Reedy, M.M., Ruedi, E.A., Rodriguez-Zas, S. and Hughes, K.A. (2004). Quantitative evolutionary genomics: differential gene expression and male reproductive success in *Drosophila melanogaster*. Proceedings of the Royal Society B: Biological Sciences. 271: 2267–2273.

Edward, R., Dixon, D.P and Walbot, V. (2000). Plant glutathione S-transferases: Enzymes with multiple functions in sickness and health. Trends Plant Science. 5:193-198

Enayati, A.A., Ranson, H., and Hemingway, J. (2005). Mini Review: Insects glutathione S-transferases and insecticide resistance. Journal of Insect Molecular Biology. 14: 3-8.

Fabre, E., Bozonnet, S., Arcache, A., Willemot, R.M., Vignon, M., Monsan, P. and Remaud-Simeon M. (2005). Role of the two catalytic domains of DSR-E dextransucrase and their involvement in the formation of highly alpha-1, 2 branched dextran. Journal of Bacteriology. 187: 296-303.

Fournier, D., Bride, J.M., Poirie, M., Berge, J.B. and Plapp, F.W. (1992) Insect glutathione S-transferases: Biochemical characteristics of the major forms from houseflies susceptible and resistant to insecticides. Journal of Biological Chemistry. 267: 1840-1845.

Friedman, R. (2011). Genomic organization of the glutathione S-transferase family in insects. Molecular Phylogenetics and Evolution. 61: 924–932.

Frova, C. (2006). Glutathione S- transferases in the genomics era: New insights and perspectives. Biomolecular Engineering. 23: 149–169.

Fukami, J.I. (1984). Metabolism of several insecticides by glutathione S-transferase. International Encyclopedia of Pharmacology and Therapeutics. 113: 223-264.

Geiger, P. (2002). *Drosophila Melanogaster*. An Introduction to *Drosophila melanogaster*. Retrieved from http://biology.arizona.edu/sciconn/lessons2/lessons.html.

Giot *et al*. (2003). A Protein Interaction Map of *Drosophila melanogaster*. Science Express. 302: 1727-1736. DOI:10.1126/science.1090289.

Glanville, S.D. and Clark, A.G. (1997). Inhibition of human glutathione s-transferases by basic triphenylmethane dyes. Journal of Life Sciences. 60: 1535-1544.

Guruharsha *et al*. (2011). A Protein Complex Network of *Drosophila melanogaster*. Cell. 147: 690-703.

Habig, W.H., Pabst, M.J. and Jakoby, W.B. (1974). Glutathione S-transferases: the first enzymatic step in mercapturic acid formation. Journal of Biological Chemistry. 249: 7130.

Hayes, J. D. and Pulford, D. J. (1995). The glutathione S-transferase supergene family: regulation of GST and the contribution of the isoenzymes to cancer chemoprotection and drug resistance. Critical Reviews in Biochemistry and Molecular Biology. 30: 445-600.

Hayes J.D., Flanagan, J.U., and Jowsey, I.R. (2005). Glutathione transferase. Annual Review of Pharmacology and Toxicology. 45: 51-88.

Hemingway, J., Hawkes, N.J., McCarroll, L. and Ranson, H. (2004). The molecular basis of insecticide resistance in mosquitoes. Insect Biochemistry and Molecular Biology. 34: 653-665.

Hunaiti, A.A., Elbetiha, A.M., Obeidat, A.M., and Owais, M.W. (1995). Development studies on *Drosophila melanogaster* Glutathione S Transferases and its induction by oxidaizolone. Insect Biochemistry and Molecular Biology. 25: 1115-1119.

Jakobsson, P. J., Morgenstern, R., Mancini, J., Ford-Hutchinson, A. and Persson, B. (1999) Common structural features of MAPEG-a widespread superfamily of membrane associated proteins with highly divergent functions in eicosanoid and glutathione metabolism. Protein Science. 8: 689-692.

Jensen *et al*. (2009). STRING 8- A global view on proteins and their functional interactions in 630 organisms. Nucleic Acids Research. 37. Doi:10.1093/nar/gkn760.

Koukiekolo, R., Cho, H.Y., Kosugi, A., Inui, M., Yukawa, H. and Doi, R.H. (2005). Degradation of corn fiber by *Clostridium cellulovorans* cellulases and hemicellulases and contribution of scaffolding protein CbpA. Applied and Environmental Microbiology. 71: 3504-3511.

Ketterer, B. (1986). Detoxification reactions of glutathione and glutathione S- transferases. Xenobiotica. 16: 957-973.

Ketterman, A. J., Saisawang, C. and Wongsantichon, J. (2011). Insect glutathione S-transferases. Drug Metabolism Review. 43: 253-265.

Kim, J., Suh, H., Kim, S., Kim, K., Ahn, C. and Yim, J. (2006) Identification and characteristics of the structural gene for the *Drosophila* eye colour mutant sepia, encoding PDA synthase, a member of the Omega class glutathione S-transferases. Biochemical Journal. 398: 451-460.

Krohne-Ehrich, G., Schirmer, R. H. and Untucht-Grau, R. (1977) Glutathione reductase from human erythrocytes. Isolation of the enzyme and sequence analysis of the redox-active peptide. Europen Journal of Biochemistry. 80: 65-71

Li, H.M., Buczkowski, G., Mittapalli, O., Xie, J., Wu, J., Westerman, R., Schemerhorn, B.L., Murdock, L.L. and Pittendrigh, B.R. (2008). Transcriptomic profiles of *Drosophila melanogaster* third instar larval midgut and responses to oxidative stress. Journal of Insect Molecular Biology. 17: 325–339.

Lumjuan, N., McCarroll, L., Prapanthadara, L.A., Hemingway, J. and Ranson, H. (2005) Elevated activity of an Epsilon class glutathione transferase confers DDT resistance in the dengue vector, *Aedes aegypti*. Insect Biochemistry and Molecular Biology. 35: 861-871.

Lumjuan, N., Stevenson, B.J., Prapanthadara, L.A., Somboon, P., Brophy, P.M., Loftus, B.J., Severson, D.W. and Ranson, H. (2007). The *Aedes aegypti* glutathione transferase family. Insect Biochemistry and Molecular Biology. 37: 1026-1035.

Lumjuan, N., Rajatileka, S., Changsom, D., Wicheer, J., Leelapat, P., Prapanthadara, L., *et al.* (2011). The role of the *Aedes aegypti* Epsilon glutathione S- transferases in conferring resistance to DDT and pyrethroid insecticides. Insect Biochemistry and Molecular Biology. 41: 203-209.

Mannervik, B. (1985). The isoenzymes of glutathione transferase. Advance Enzymology Related Areas Molecular Biology. 57: 357-417.

Mannervik, B. and Danielson, U.H. (1988). Glutathione S- transferases—structure and catalytic activity. CRC Critical Review in Biochemistry. 23: 283-337.

Mannervik, B., Board, P.G., Hayes, J.D., Listowsky, I., and Pearson, W.R. (2005). Nomenclature for Mammalian Soluble Glutathione S- transferases. Methods in Enzymology. 401.

Mayer, B., Brunner, F., and Schmidt, K. (1993). Inhibition of nitric oxide synthesis by methylene blue. Biochemical Pharmacology Journal. 26: 367-374.

Meister, A. (1988) Glutathione metabolism and its selective modification. Journal of Biological Chemistry. 263: 17205-17208

Mizutani, T. (2009). Toxicity of Xanthene Food Dyes by Inhibition of Human Drug-Metabolizing Enzymes in a Noncompetitive Manner. Journal of Environmental and Public Health. 1-9. Doi:10.1155/2009/953952.

Morgenstern, R., Guthenberg, C. and DePierre, J. W. (1982) Microsomal glutathione S-transferase. Purification, initial characterization and demonstration that it is not identical to the cytosolic glutathione S-transferases A, B, C. European Journal of Biochemistry. 128: 243-248.

Moulis, C., Joucla, G., Harrison, D., Fabre, E., Potocki-Veronese, G., Monsan, P. and Remaud-Simeon, M. (2006). Understanding the polymerization mechanism of glycoside-hydrolase family 70 glucansucrases. Journal of Biological Chemistry. 281: 31254-31267.

Niranjan, R.B.P, Prasad, G.B. and Raghavendra, K. (2011). In silico characterization and comparative genomic analysis of the *Culex quinquefasciatus* glutathione S-transferase (GST) supergene family. Parasitological Research. 109: 1165-1177.

Que Xuchu, Ngo, H., Lawton, J., Mary, G., Liu, Q., Engel, J., *et al.* (2002). The cathepsin B of *Toxoplasma gondii*, toxopain-1, is critical for parasite invasion and rhoptry protein processing. Journal of Biological Chemistry. 277: 25791-25798.

Paglia, D.E. and Valentine., W.N. (1967). Studies on the quantitative and qualitative characterization of erythrocyte glutathione peroxidase. Journal of Laboratory and Clinical Medicine. 70:158-69.

Rachel, I.M.V.H, Guido, R.M.M.H, Peter, J.V.B, Jan, J.P.B, Chris T.A.E and Aalt, B. (2003). Inhibition of various glutathione S-transferase isoenzymes by RRR-α-tocopherol. Journal of Toxicology in Vitro. 17: 245–251.

Ramavati, P. (2010). Proteomic analysis of glutathione S- transferases from *Lucilia cuprina*. (Published Doctor of Philosophy‘s thesis). Victoria University of Wellington.

Ranson, H., Prapanthadara, L. and Hemingway, J. (1997). Cloning and characterization of two glutathione S-transferases from a DDT-resistant strain of *Anopheles gambiae*. Biochemical Journal. 324: 97–102.

Ranson, H., Rossiter, L., Ortelli, F., Jesen, B., Wang, X., Roth, C.W., Collins, F.H., and Hemingway, J. (2001). Identification of a novel class of insect glutathione S transferases involved in resistance to DDT in the malaria vector *Anopheles gambiae*. Biochemical Journal. 359: 295–304.

Ranson, H. and Hemingway, J. (2005) Mosquito glutathione S- transferases. Glutathione S-transferases and Gamma-Glutamyl Transpeptidases. 401: 226-238.

Rogers, M.E., Jani, M.K. and Vogt, R.G. (1999). An olfactory-specific glutathione-s-transferase in the sphinx moth *manduca sexta*. The Journal of Experimental Biology. 202: 1625–1637.

Saisawang, C., Wongsantichon, J. and Albert J. Ketterman. (2011). A preliminary characterization of the cytosolic glutathione transferase proteome from *Drosophila melanogaster*. Biochemical Journal. 442:181-90.

Sawicki, R., Singh, S.P., Mondal, A.K., Benes, H. and Zimniak, P. (2003). Cloning, expression and biochemical characterization of one Epsilon-class (GST-3) and ten Delta-class (GST-1) glutathione S-transferase from *Drosophila melanogaster*, and identification of additional nine members of the Epsilon class. Biochemical Journal. 370: 661-669.

Sheehan, D., Meade, G., Foley, V.M. and Dowd, C.A. (2001). Review article: Structure, function and evolution of glutathione S- transferases: implications for classification of non-mammalian members of an ancient enzyme superfamily. Biochemical Journal. 360: 1-16.

Sherratt, P.J., and Hayes, J.D. (2002). Glutathione S Transferases. In C. Ioannides (Eds.), Enzyme systems that metabolize drugs and other xenobiotics. (pp. 320-352). United Kingdom, UK: John Wiley & Sons Ltd.

Singh, S.P., Coronella, J.A., Benes, H., Cochrane, B.J. and Zimniak, P. (2001). Catalytic function of *Drosophila melanogaster* glutathione S-transferase GSTS1-1 (GST-2) in conjugation of lipid peroxidation end products. European Journal of Biochemistry. 268: 2912-2923.

Spector, T. (1978). Refinement of the Coomassie Blue method of protein quantization. Analytical Biochemistry. 86: 142–146.

Tang, A.H. and Tu, C.P. (1994). Biochemical characterization of *Drosophila* glutathione S transferases D1 and D21. Journal of Biological Chemistry. 269: 27876–27884.

Toung, Y.P.S., Hsieh, T.S. and Tu, C.P.D. (1990). *Drosophila* glutathione S-transferase 1-1 shares a region of sequence homology with the maize glutathione S-transferase-III. Proceedings of the National Academy of Sciences of the United States of America. 87: 31-35.

Townsend, D.M., and Tew, K.D. (2003). The role of glutathione-S-transferase in anti-cancer drug resistance. Oncogene. 22:7369–7375.

Uesugi, N., Furumiya, K and Mizutani, T. (2006). Inhibition mechanism of UDP-Glucuronosyltransferase 1A6 by xanthene food dyes. Journal of Health Science. 52: 549-557.

Wang, J.Y., McCommas, S., and Syvanen, M. (1991). Molecular cloning of a glutathione S transferase overproduced in an insecticide-resistant strain of the housefly (*Musca domestica*). Molecular Genetics and General Genetics. 227: 260–266.

Wang, Y., Qiu, L., Ranson, H., Lumjuan, N., Hemingway, J., Setzer, W.N., *et al* . (2008). Structure of an insect epsilon class glutathione S-transferase from the malaria vector *Anopheles gambiae* provides an explanation for the high DDT-detoxifying activity. Journal of Structural Biology. 164: 228–235.

Wang, A.M., Morishima, Y., Clapp, K.M., Peng, H.M., Pratt, W.B., Gestwicki, J.E., Osawa, Y., and Lieberman, A.P. (2010). Inhibition of hsp70 by methylene blue affects signaling protein. Function and ubiquitination and modulates polyglutamine protein degradation. Journal of Biological Chemistry. 21:15714-23.

Wagner, C., Isermann, K. and Roeder, T. (2009). Infection induces a survival program and local remodeling in the airway epithelium of the fly. The FASEB Journal; A Research Communication. 23: 2045-2054.

Wei, S.H., Clark, A.G., and Syvanen, M. (2001). Identification and cloning of a key insecticide metabolizing glutathione S-transferase (MdGST-6A) from a hyper insecticide resistant strain of the housefly *Musca domestica*, Insect Biochemistry and Molecular Biology. 31: 1145–1153.

Wilce, M.C.J., Board, P.G., Feil, S.C. and Parker, M.W. (1995). Crystal structure of a theta class glutathione S transferase. Embo Journal. 14: 2133-2143.

Willoughbya, L., Chunga, H., Lumba, C., Robinb, C., Batterhama, P. and Daborn, P.J. (2006). A comparison of *Drosophila melanogaster* detoxification gene induction responses for six insecticides, caffeine and Phenobarbital. Insect Biochemistry and Molecular Biology. 36: 934–942.

Wilson, T.G. (2001). Resistance of *Drosophila* to toxins. Annual Review Entomology. 46: 545-571.

Wilson, J.A. and Clark, A.G., (1996). The role of E3 esterase, glutathione S-transferases and other nonoxidative mechanisms in resistance to diazinon and other organophosphate insecticides in *Lucilia cuprina*. Pesticide Biochemistry and Physiology. 54: 85–95

Winayanuwattikun, P. and Albert, J.K. (2005). An Electron-sharing Network Involved in the Catalytic Mechanism Is Functionally Conserved in Different Glutathione Transferase Classes. The Journal of Biological Chemistry. 280: 31776–31782.

Wongtrakul, J., Pongjaroenkit, S., and Leelapat, P., Nachaiwieng, W., Prapanthadara, L.A. and Ketterman, A.J. (2010). Expression and Characterization of Three New Glutathione S- transferases, an Epsilon (AcGSTE2-2), Omega (AcGSTO1-1), and Theta (AcGSTT1-1) from *Anopheles cracens* (Diptera: *Culicidae*), a Major Thai Malaria Vector. Journal of Medical Entomology. 47: 162-171.

Yamamoto, K., Nagaoka, S., Banno, Y. and Aso, Y. (2009a). Biochemical properties of an omega-class glutathione S-transferase of the silkmoth, *Bombyx mori*. Comparative Biochemistry and Physiology. 149: 461-467.

Yamamoto, K., Shigeoka, Y., Aso, Y., Banno, Y., Kimura, M. and Nakashima, T. (2009b). Molecular and biochemical characterization of a Zeta-class glutathione S-transferase of the silkmoth. Pesticide Biochemistry and Physiology. 94: 30-35.

Yang, J., McCart, C., Woods, D. J., *et al.* (2007). A *Drosophila* systems approach to xenobiotic metabolism. Journal of Physiology Genomics. 30: 223–231.

Yu, S.J. (2002). Substrate specificity of glutathione S-transferases from the fall armyworm. Pesticide Biochemistry and Physiology. 74: 41–51

Yu, S.J. (1996). Insect glutathione S-transferases. Zoology Study. 35: 9-19.

Zhou, Z.H. and Syvanen, M. (1997). A complex glutathione transferase gene family in the housefly *Musca domestica*. Molecular and General Genetics. 256: 187-194.

APPENDICES

APPENDIX A- *Drosophila* Media Preparation

The *Drosophila* media was prepared by adding 10 g of oats, 3 g of white sugar, 6 g of brown sugar, 1 g of agar, 1.5 g of yeast into a beaker. 100 mL of tap water was poured into the beaker and heated on hot plate until it boils. The hot plate was turned off and 1.5 mL propionic and acetic acid mix (75:25) was added accordingly. The mixed media was poured into 4-5 plastic bottles. The bottles was left to cool down before transferring flies and stumped with a sponge.

APPENDIX B- Buffer, Stock and Media Solution Preparation

Eluting Buffer- 25mM Sodium Phosphate Buffer, pH 7.4

A total of 3 g of NaH_2PO_4 was dissolved in approximately 900 mL of distilled water. The pH of the solution was adjusted to 7.25 at 20ºC and the volume was made up to 1000 mL, filtered and stored 4ºC.

Buffer A- 0.1M Sodium Phosphate Buffer, pH 6.5

A total of 12 g of NaH_2PO_4 was dissolved in approximately 900 mL of distilled water. The pH of the solution was adjusted to 6.5 at 20ºC and the volume was made up to 1000 mL, filtered and stored 4ºC.

Buffer B- 0.1M Tris Buffer, pH 9.0

A total of 12.114 g of Tris base was dissolved in approximately 900 mL of distilled water. The pH of the solution was adjusted to 9.0 at 20ºC and the volume was made up to 1000 mL, filtered and stored 4ºC.

Buffer C- 0.1M Sodium Phosphate Buffer, pH 7.5

A total of 12 g of NaH_2PO_4 was dissolved in approximately 900 mL of distilled water. The pH of the solution was adjusted to 7.5 at 20ºC and the volume was made up to 1000 mL, filtered and stored 4ºC.

Buffer D- 0.25 M Sodium Phosphate Buffer, pH 7.0

A total of 30 g of NaH_2PO_4 was dissolved in approximately 900 mL of distilled water. The pH of the solution was adjusted to 7.0 at 20ºC and the volume was made up to 1000 mL, filtered and stored 4ºC.

IPTG Stock Solution (100 mM)

A total of 238.3 mg isopropyl β-D-thiogalactopyranoside was dissolved in 10 mL MΩ-cm water, filtered-sterilized and store in -20ºC.

Ampicilin Stock Solution (100 mg/mL)

A total of 5 g Ampicilin sodium salt was dissolved in 50 mL MΩ-cm water, filtered-sterilized and store in 4ºC.

Kanamycin Stock Solution (30 mg/mL)

A total of 1.5 g kanamycin monosulfate salt was dissolved in 50 mL MΩ-cm water, filtered-sterilized and store in 4ºC.

LB (Luria Bertani) agar plates (1000 mL= approx. 40 plates)

For 1000 mL, 40 g was dissolved in 950 mL distilled water. The solution was mix well and dissolved by heating with frequent agitation. The solution was sterilized in autoclave at 121ºC for 15 minutes, cooled to 45-50ºC, mixed well and dispensed into plates.

LB (Luria Bertani) Broth

For 1000 mL, 20 g was dissolved in 950 mL distilled water. The solution was mix well and dissolved by heating with frequent agitation. The solution was sterilized in autoclave at 121ºC for 15 minutes, cooled to 45-50ºC, mixed well and dispensed into 100 mL flask.

APPENDIX C- Laemmli Discontinous SDS Polyacrylamide Gel Electrophoresis

Acrylamide/Bis (30% T, 2.67% C)

A total of 146.0 g of acrylamide and 4.0 g of N, N'- methylene-bis Acrylamide was mixed in MΩ-cm water. The resulting solution was made to 500 mL, filtered and stored 4ºC

1.5M Tris-HCl, pH8.8

A total of 54.45 g of Tris base was dissolved in 60 mL MΩ-cm water and the pH was adjusted to 8.8 with HCl. The solution was made up to 300 mL with 18.3 MΩ-cm water and stored at 4ºC.

0.5M Tris-HCl, pH6.8

A total of 6 g of Tris base was dissolved in 60 mL MΩ-cm water and the pH was adjusted to 6.8 with HCl. The solution was made up to 100 mL with 18.3 MΩ-cm water and stored at 4ºC.

10% (w/v) SDS

A total of 10 g of SDS was dissolved in 50 mL MΩ-cm water with gentle shaking. The volume was made up to 100 mL.

SDS Sample Buffer

The buffer consist of 62.5 mM Tris-HCl, pH 6.8, 20% glycerol, 2% SDS and 5% β-mercaptoethanol. To prepare a buffer solution of 2 mL of 0.5 M Tris-HCl, pH 6.8, 0.4 mL glycerol, 0.4 mL 10% SDS, 0.1 mL of 0.5% (w/v) bromophenol blue and 0.75 mL of MΩ-cm water were mixed. To prepare sample in sample buffer, the sample was diluted at 1.4 ratio. The sample was heated at 95ºC for 4 minutes.

Electrophoresis (Running) buffer (1X 25mM Tris, 192 mM Glycine and 0.15 (w/v) SDS, pH 8.3).

Stock of Bio-Rad 10X Tris/ Glycine/SDS buffer was used and diluted to the final concentration according to the manufacturer instruction. Or else a running buffer was prepared by dissolving 15.1 g Tris, 5.0 g SDS and 72.1 g glycine in 5 L. The pH of the buffer was not adjusted.

Stacking Gel (0.125 M Tris-HCl, pH 6.8)

To prepare 10 mL of 4% gel: 1.33 mL 30% Acrylamide/Bis, 2.5 mL 0.5 M Tris-HCl, pH 6.8, 0.1 mL 10% SDS, 6.1 mL MΩ-cm water, 0.01 mL TEMED and 0.05 mL 10% APS was mixed gently and poured into the electrophoresis plates. All the ingredients except TEMED and APS were combined and degassed under vacuum for at least 15 minutes. The polymerization was initiated by addition of TEMED and APS followed by gentle swirling for complete mixing.

Resolving Gel (0.375 M Tris-HCl, pH 8.8)

To prepare 10 mL of 12% gel: 4.0 mL 30% Acrylamide/Bis, 2.5 mL 1.5 M Tris-HCl, pH 8.8, 0.1 mL 10% SDS, 3.35 mL MΩ-cm water, 0.005 mL TEMED and 0.05 mL 10% APS was mixed gently and poured into the electrophoresis plates. All the ingredients except TEMED and APS were combined and degassed under vacuum for at least 15 minutes. The polymerization was initiated by addition of TEMED and APS followed by gentle swirling for complete mixing.

APPENDIX D- Formulas

Catalytic activity = (ΔA x V x 1000)/ (ε x υ x Δd) (μmol/min or Units)

ΔA is absorbance change; ε is L x $mmol^{-1}$ x cm^{-1}; V is assay volume in L; υ is of sample volume; Δd in cm; t in min

Specific activity = (ΔA x V)/ (ε x υ x Δd x 1000 x C protein) (μmol/min/mg or Units/mg)

ΔA is absorbance change; ε is L x $mmol^{-1}$ x cm^{-1}; V is assay volume in L; υ is of sample volume; d in cm; t in min; C is protein concentration in mg/l)

APPENDIX E – Protein Purification Spectrum

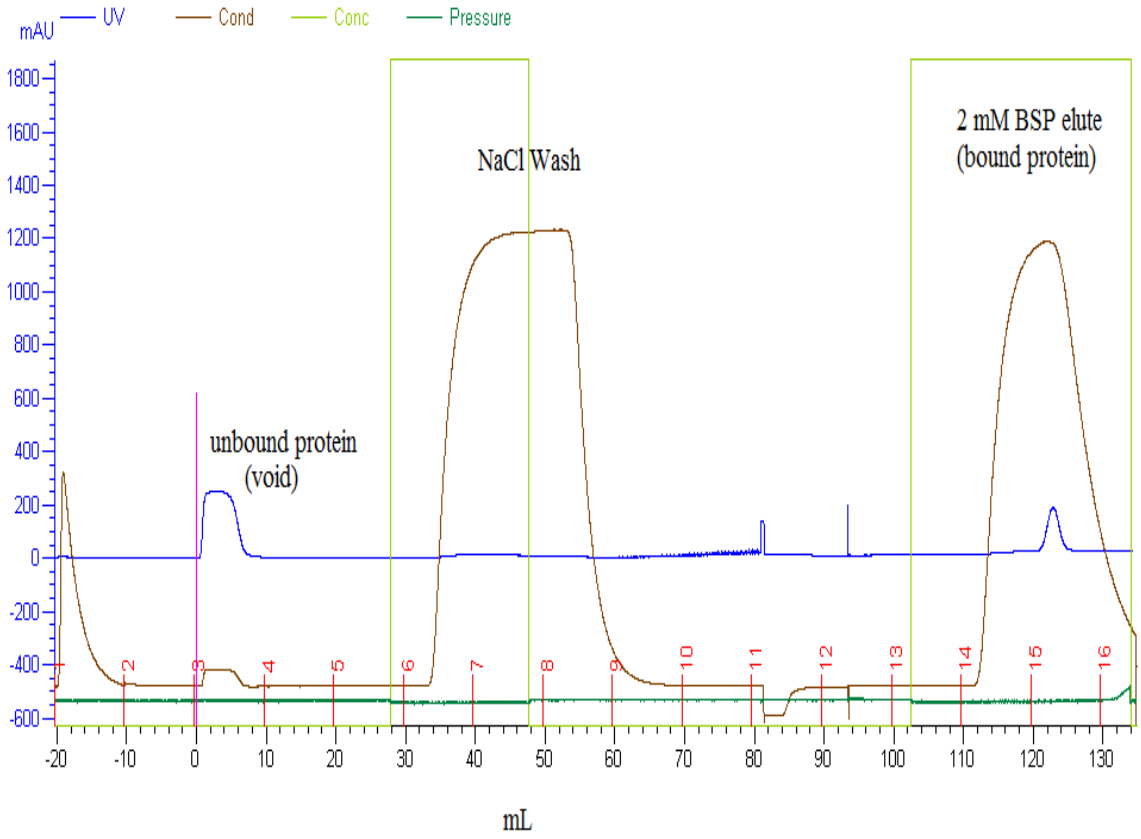

Figure E1: Purification spectrum of recombinant proteins using Bromosulfophthalein-GSH matrix.

APPENDIX F- The Effects of Substrate Concentration

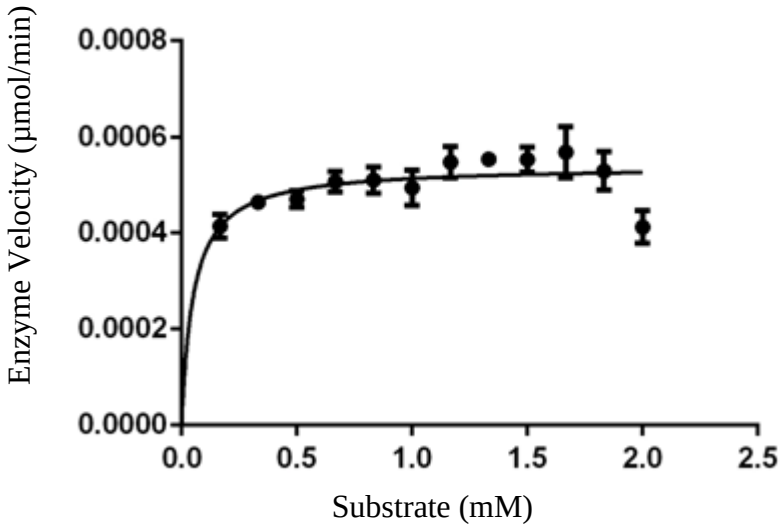

Figure F1: The Effect of Substrate (CDNB) Concentrations on GSTE6 isozyme activity. The data shown are means±SEM error bars from three independent experiments.

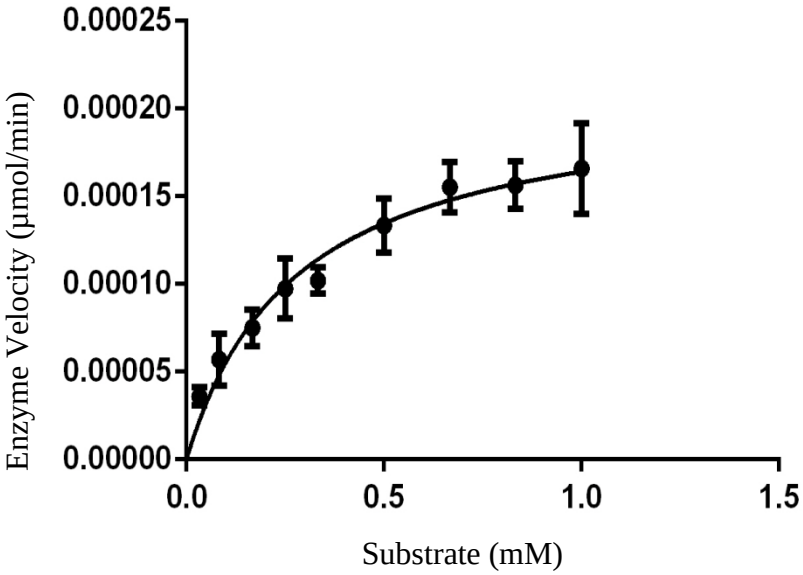

Figure F2: The Effect of Substrate (*p*-NBC) Concentrations on GSTE6 isozyme activity. The data shown are means±SEM error bars from three independent experiments.

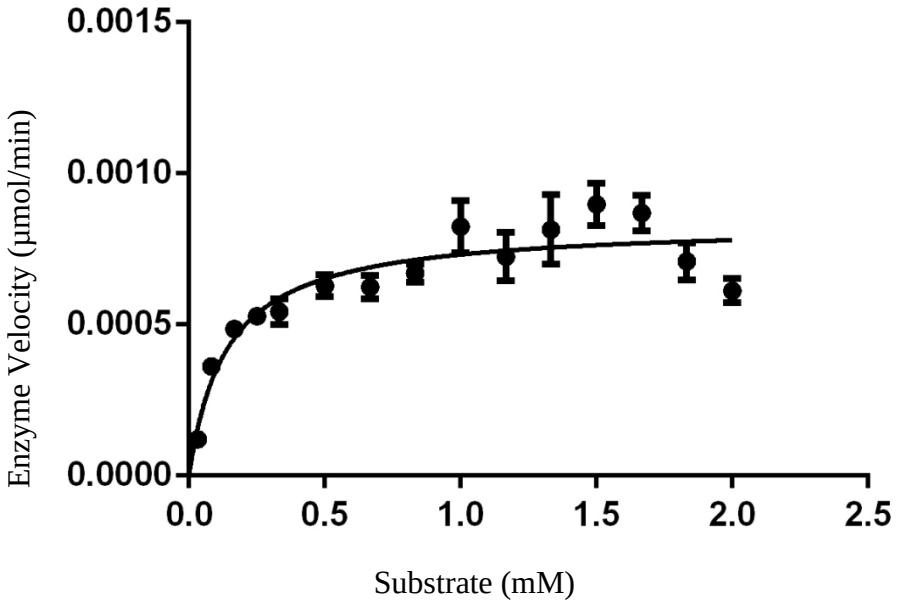

Figure F3: The Effect of Substrate (CDNB) Concentrations on GSTE7 isozyme activity. The data shown are means±SEM error bars from three independent experiments.

APPENDIX G- The Effects of Inhibitors

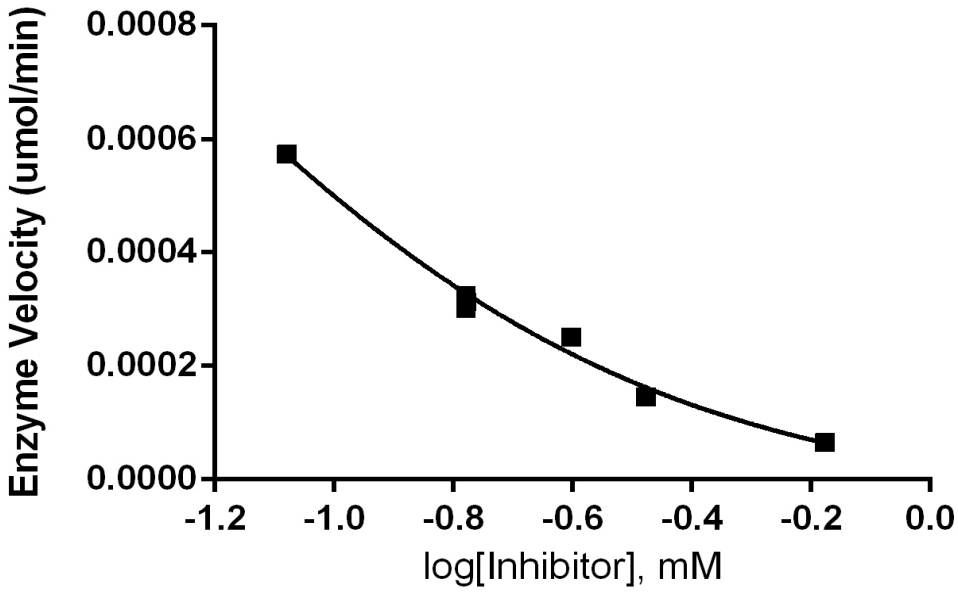

Figure G1: The Effect of Cibacron blue dye concentrations on GSTE6 CDNB isozyme activity. Data points represent average of at least three independent experiments.

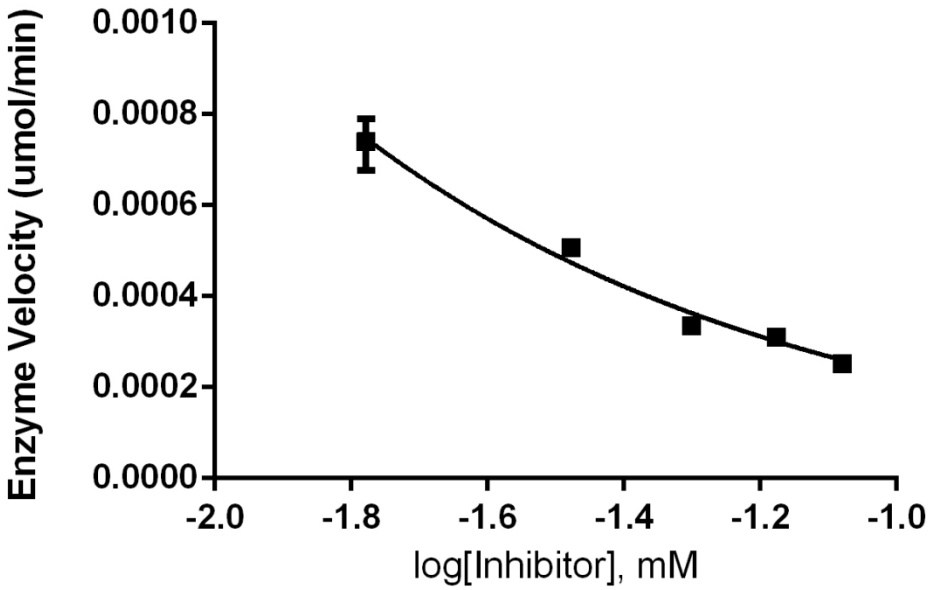

Figure G2: The Effect of Crystal Violet dye concentrations on GSTE6 CDNB isozyme activity. Data points represent average of at least three independent experiments.

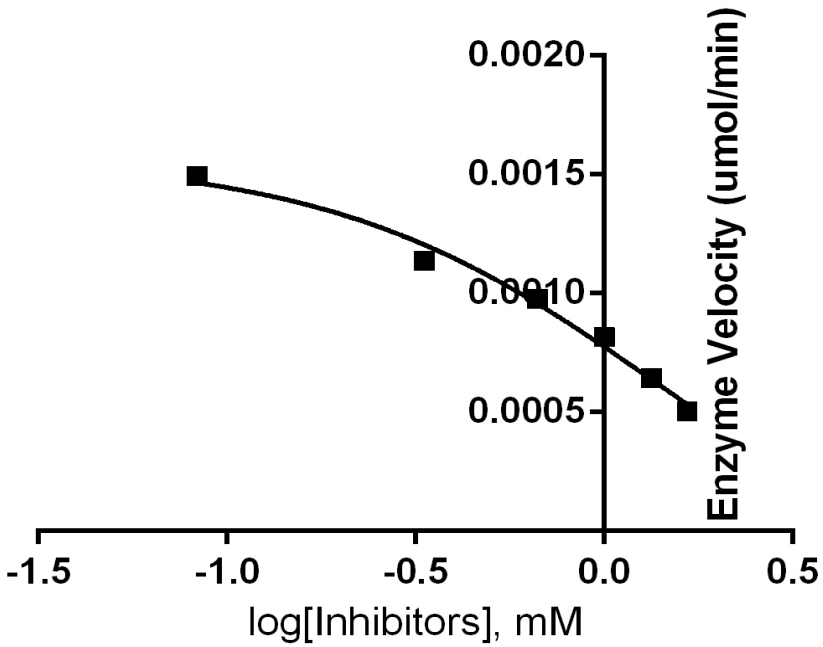

Figure G3: The Effect of Cibacron blue dye concentrations on GSTE7 CDNB isozyme activity. Data points represent average of at least three independent experiments.

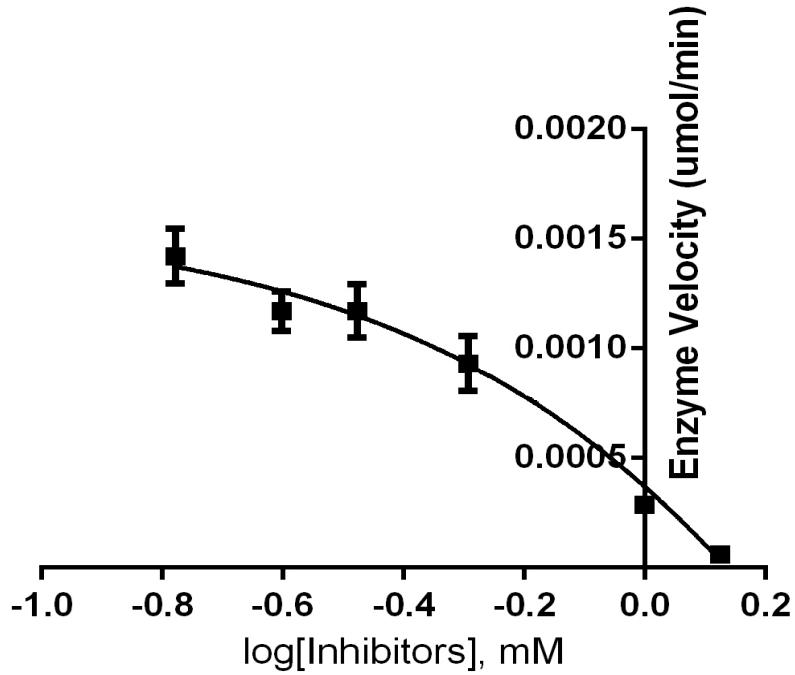

Figure G4: The Effect of Tetradecanedioic acid concentrations on GSTE7 CDNB isozyme activity. Data points represent average of at least three independent experiments.

APPENDIX H- The Effects of Agonist

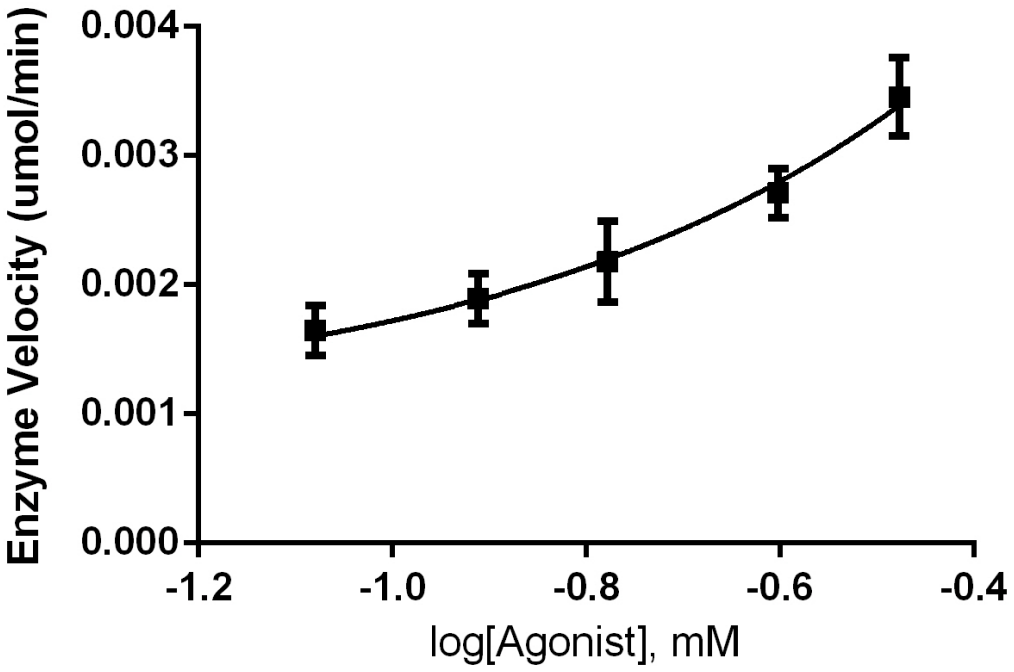

Figure H1: The Effect of *trans*-chalcone concentrations on GSTE7 CDNB isozyme activity. Data points represent average of at least three independent experiments.

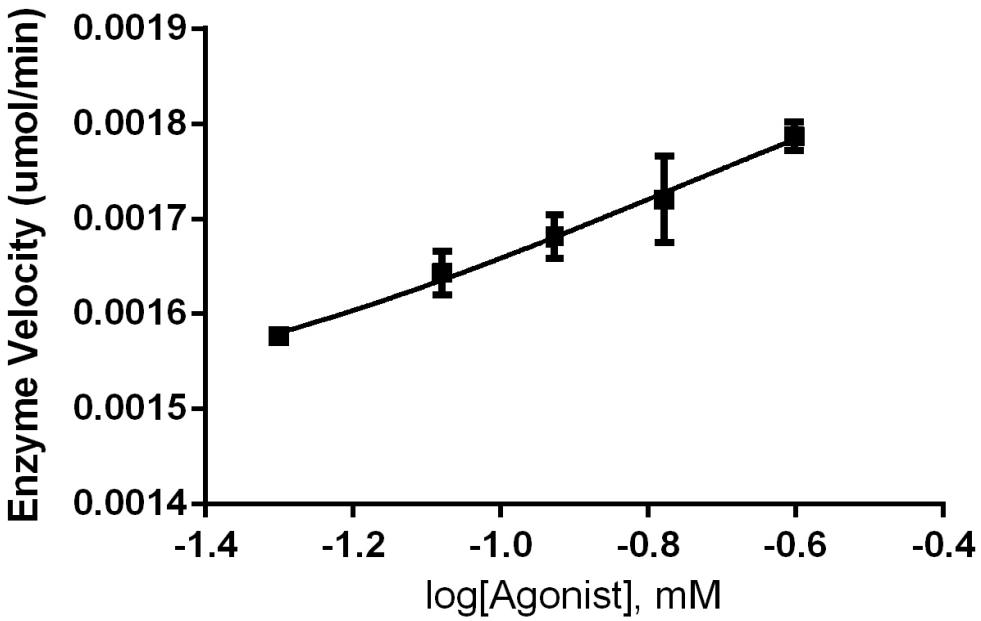

Figure H2: The Effect of Methylene Blue dye concentrations on GSTE7 CDNB isozyme activity. Data points represent average of at least three independent experiments.